Division of Pharmaceutical Technology
Faculty of Pharmacy
University of Helsinki
Finland

Automatable Microplate-Based *in vitro* Assays for Screening Intestinal Drug Transport and Metabolism

Anne Soikkeli

ACADEMIC DISSERTATION

To be presented, with the permission of the Faculty of Pharmacy of the University of Helsinki, for public examination in lecture room 1041, Viikki Biocenter 2, on 15th June 2012, at 12 noon.

Helsinki 2012

Supervisors: Professor Jouni Hirvonen
Division of Pharmaceutical Technology
Faculty of Pharmacy
University of Helsinki
Finland

Docent Moshe Finel
Centre for Drug Research
Faculty of Pharmacy
University of Helsinki
Finland

Professor Marjo Yliperttula
Division of Biopharmaceutics and Pharmacokinetics
Faculty of Pharmacy
University of Helsinki
Finland

Reviewers: Director, PhD Timo Lotta
Translational Sciences
Orion Corporation
Espoo
Finland

Professor Nico P. E. Vermeulen
Division of Molecular and Computational Toxicilogy
Department of Chemistry and Pharmaceutical Sciences
Faculty of Sciences
Vrije Universiteit Amsterdam
Netherlands

Opponent: Professor Pia Vuorela
Department of Biosciences
Division of Natural Sciences and Technology
Åbo Akademi University
Finland

ISBN 978-952-10-8060-9 (paperback)
ISBN 978-952-10-8061-6 (pdf, http://ethesis.helsinki.fi)
ISSN 1799-7372

Unigrafia
Helsinki, Finland 2012

Abstract

Automation compatibility is a prerequisite for *in vitro* transport and metabolism assays that are designed for screening large numbers of compounds at the early stages of drug discovery, in parallel with activity optimization. However, automation of more complex assays has also many benefits, even if it does not always increase the throughput of the assay directly.

In this thesis work, a new automatable high throughput screening assay was developed for detecting different compound interactions with UGT1A6, one of the human intestinal UGT enzymes. The fluorescence-based assay relies on a robust probe reaction, glucuronidation of 1-naphthol by recombinant human UGT1A6, which yields a highly fluorescent product, 1-naphthylglucuronide. Under the optimized assay conditions, the plate reader-based analysis method was able to detect a given compound interaction with the enzyme, through the probe reaction, in a comparable manner to the (cumbersome) reference HPLC-based method. The new method can analyze the interaction of many different compounds with the UGT1A6 simultaneously.

The developed assay was then used to collect data for computational model development. The effects of different compounds on the probe glucuronidation rate were used for a classification model, based on an SVM method, and for 3D-QSAR models, based on CoMFA and CoMSIA analysis. Both the models indicated physicochemical parameters and functional groups that are important for the interaction of different compounds with the UGT1A6.

Interactions of two drugs, diclofenac and indomethacin, were studied more thoroughly with the several UGT enzymes, including UGT1A6. The effect of pH on the interaction was examined in both human liver and intestinal microsomes, as well as with many individual recombinant human UGTs. The results indicated that the effects of pH were both enzyme and substrate dependent, suggesting that changes in the enzyme, probably protonation of one or more amino acid side chain, played a major role in the observed effects.

Finally, automation of three different types of cell-based assays, Caspase-Glo® 3/7, sulforhodamine B and bidirectional Caco-2 monolayer transport assays, are described in detail. Although, the bidirectional Caco-2 assay was the most challenging for automation, due to the complex assay protocol and the sensitivity of the monolayer to mechanical stress, mainly caused by pipetting, automation improved the utilization potential of the laborious method significantly.

Acknowledgements

These studies were conducted at the Division of Pharmaceutical Technology and the Centre for Drug Research, Faculty of Pharmacy, University of Helsinki, during the years 2004-2012.

These studies would not have been possible to perform without the financial support provided by Graduate School in Pharmaceutical Sciences, TEKES project e-ADME and EU-projects LIINTOP and Protein Kinase C.

I wish to express my greatest gratitude to my main supervisor Professor Jouni Hirvonen for his supervision, support and endless positive attitude during this almost-never-ending process. Without his great diplomatic skills this process would have never come to this point.

I would also like to greatly acknowledge my other supervisors Docent Moshe Finel and Professor Marjo Yliperttula. Docent Moshe Finel is thanked for giving me the possibility to join his highly respected research group and for sharing with me his wide knowledge on UGT enzymes. Professor Marjo Yliperttula is thanked for her always fresh scientific ideas, for teaching me to "read" the molecular structure and for helping me to understand the analytics.

All my co-authors, Docent Ann Marie Kaukonen, Docent Ari Tolonen, PhD Leo Ghemtio, PhD Henri Xhaard, M.Sc. Cristina Sempio, M.Sc. Hongbo Zhang, M.Sc. Mika Kurkela, M.Sc. Nenad Manevski, M.Sc. Timo Rousu, are thanked for their scientific contributions to this work. Especially, I would like to warmly thank Docent Ann Marie Kaukonen for her friendship and for guiding me to the world of science during the very first years of my studies. She also introduced me to the fascinating TECAN robot and taught me to understand its deepest thoughts. In addition to the help in the lab, Cristina is thanked for her friendship and for the unforgettable trips to Italy, during which I have had the opportunity to experience her family´s overwhelming hospitality. I would also like to thank Laboratory Technicians Sanna Sistonen and Johanna Mosorin for their valuable help in the laboratory.

Director, PhD Timo Lotta and Professor Nico P. E. Vermeulen are acknowledged for reviewing the thesis manuscript and for the constructive comments on improving it.

I feel privileged having had the possibility to work with all the great colleagues and staff at the Division of Pharmaceutical Technology during these years. The pleasant working atmosphere and continuous peer-support have helped me through the (many) difficulties I have faced during this process. Especially, I would like to thank my present and former "office room mates", who have been extremely understandable during my good and not-so-good moments (and even tolerated the smell of my horse stuff). The legendary "Johtajat", Henna, Kaisa, Sanna and Tarja, I would like to thank for their friendship, many laughs and memorable moments. Special thanks to Sanna for tutoring me in many Caco-2 –related (and not related) issues. I would also like to thank Satu for her friendship.

At least equally important during this process have been my friends, Eve, Virve, Reetta and Niina, from the high school times, Sanna ja Elli, from the years of the university studies, my dear dancing friend, Taina, and family Liuke, who have helped me during this process in many ways and taken care that I have had a life outside the work.

The lovely Finnhorse Polle has guaranteed my weekly outdoor activities throughout the last few years, and provided me a possibility to escape the busy working life for a short while every now and then.

Lisäksi haluan kiittää isääni Karia ja jo edesmennyttä äitiäni Leenaa. He ovat antaneet minun valita omat polkuni, ja tukeneet minua aina tekemissäni valinnoissa. Suurkiitokset myös pikkusiskolleni Kaisalle ymmärryksestä ja tuesta näiden vuosien aikana.

Järvenpää, May 2012

Anne Soikkeli

Contents

List of original publications

This thesis is based on the following publications, which are referred to in the text by their respective roman numerals (**I-IV**):

I Soikkeli A., Kurkela M., Hirvonen J., Yliperttula M., Finel M., 2011. Fluorescence-based high-throughput screening assay for drug interactions with UGT1A6. *ASSAY and Drug Dev Technol 9(5):495-502*

II Ghemtio L., Soikkeli A., Hirvonen J., Yliperttula M., Finel M., Xhaard H., 2012. Support Vector Machine and 3D QSAR (COMFA/CoMSIA) approaches for predicting compound interactions with UGT1A6. *Manuscript.*

III Zhang H., Soikkeli A., Tolonen A., Rousu T., Hirvonen J., Finel M., 2012. Highly variable pH effects on the interaction of diclofenac and indomethacin with human UDP-glucuronosyltransferases. *Toxicol in Vitro (in press), DOI: 10.1016/j.tiv.2012.01.005*

IV Soikkeli A., Sempio C., Kaukonen A. M., Urtti A., Hirvonen J., Yliperttula M., 2010. Feasibility evaluation of 3 automated cellular drug screening assays on a robotic workstation. *J Biomol Screen 15(1):30-41*

Abbreviations

[S]	substrate concentration
1-NG	1-naphthylglucuronide
3D-QSAR	three dimensional quantitative structure activity relationship
4-MU	4-methylumbelliferone
5-FU	5-fluorouracil
ACN	acetonitrile
ADMET	absorption, distribution, metabolism, excretion, toxicity
ADP	adenosine diphosphate
AMP	adenosine monophosphate
AS	aspiration speed
ASBT	apical sodium dependent bile acid transporter
ATP	adenosine triphosphate
ATPase	enzyme catalyzing the decomposition of ATP into ADP
AUS	area under signal
BCRP	breast cancer resistance protein
BSA	bovine serum album
Calcein-AM	acetomethoxy derivate of calcein
CDCF	5(6)-carboxy-2',7'-dichlorofluorescein
CDCFDA	diacetate ester of 5(6)-carboxy-2',7'-dichlorofluorescein
CHO	cell line derived from chinese hamster ovary
CoMFA	comparative molecular field analysis
CoMSIA	comparative molecular similarity indices analysis
COS	cell line derived from African green monkey kidney
CV_A	coefficient of variation for the assay
CYP	cytochrome P450 enzymes
DMEM	Dulbecco´s modified eagle medium
DMSO	dimethyl sulfoxide
DNA	deoxyribonucleic acid
DOX	doxorubicin
DS	dispense speed
DU-145	prostata cancer cell line
EGTA	ethylene glycol tetraacetic acid
ER	endoplasmic reticulum
FDA	Food and Drug Administration
FP	fluorescence polarization
GI%	growth inhibition percentage
GSH	glutathione
GST	glutathione S-transferase
HIM	human intestinal microsomes
HLM	human liver microsomes
HPLC	high performance liquid chromatography
HTS	high throughput screening

IC50	half maximal (50%) inhibitory concentration (IC) of a substance
K_m	Michaelis constant, substrate concentration yielding 50% of V_{max}
K_{si}	dissociation constant for substrate inhibition interaction
LC	liquid chromatography
LC-MS	liquid chromatography-mass spectrometry
LC-MS/MS	liquid chromatography-tandem mass spectrometry
LLC-PK1	renal epithelial cell line derived from porchine kidneys
LS180	human colon adenocarcinoma cell line
LSC	liquid scintillation counter/ing
MCC	Matthews correlation coefficient
MCT1	monocarboxylic acid transporter 1
MDCK	Madin-Darby canine kidney cells
MDR1	multidrug resistance protein 1, P-gp
MgATP	magnesium salt of adenosine triphosphate
MOPS	3-morpholinopropane-1-sulfonic acid
mRNA	messenger ribonucleic acid
MRPs	multidrug resistance-associated proteins
NADH	β-nicotinamide adenine dinucleotide
NADPH	nicotinamide adenine dinucleotide phosphate
NCI	National Cancer Institute of U.S.A.
NMR	nuclear magnetic resonance
OATPs	organic anion transporting polypeptide
OCT1	organic cation transporter 1
OSTα/β	heteromeric organic solute transporter
$P_{app\ (A-B)}$	apparent permeability, from apical to basolateral direction
$P_{app\ (B-A)}$	apparent permeability, from basolateral to apical direction
PAPS	3'-phosphoadenosine-5'-phosphosulfate
PEPT1	peptide transporter 1
pGlu	negative logarithm of probe glucuronidation rate
PhA	pheophorbide A
q^2	correlation coefficient with leave-one-out crossvalidation
RPMI	Roswell Park Memorial Institute medium
S/B	signal to base ratio
S/N	signal to noise ratio
SEE	standard error of estimate
Sf9	an insect cell line from the ovarian tissue of the fall army worm *Spodoptera frugiperda*
SLC	solute carrier transporter
SOP	standard operating procedure
SPA	scintillation proximity assay
SRB	sulforhodamine B
SULT	sulfotransferase
SVM	support vestor machine
TC	tip/tubing cleaning
TCA	trichloroacetic acid

TEER	trans epithelial electrical resistance
TH	tip height
TR-FRET	time-resolved fluorescence energy transfer
Tricine	N-(2-hydroxy-1,1-bis(hydroxymethyl)-ethel)glycine
UDP	uridine diphosphate
UDPGA	uridine-5-diphosphoglucuronic acid
UGTs	UDP-glucuronosyltransferases
UPLC	ultra performance liquid chromatography
UV	ultraviolet
V79	Chinese hamster lung fibroplast cell line
VBL	vinblastine
V_{max}	maximum velocity for an enzymatic reaction

1 Introduction

Robotic workstations were first established in clinical diagnostics to prepare samples for analysis in the early 1980s. Soon after, pharmaceutical industry started to apply them in drug activity and potency testing. In mid 1980s, the successful miniaturization of *in vitro* activity assays led to the establishment of high throughput screening concept, which, furthermore, increased the need for automation in the drug discovery laboratories. Indeed, automation is considered one of the main contributors to the fast increase in assay throughputs during the mid 1990s. More user-friendly workstations together with advancements in liquid handling and analytical techniques pushed the development towards even higher density assay formats.

During the mid 1990s, the HTS concept emerged also to the ADMET (absorption, distribution, metabolism, excretion, toxicity) studies. At that time, it was noticed that a high number of compounds failed in clinical studies due to the poor pharmacokinetic properties and toxicity. That evoked need for more efficient testing of the pharmacokinetic properties before performing the laborious, expensive and non-ethical *in vivo* assays. The first HTS assays in the ADMET area were microsomal CYP, protein binding, Caco-2 permeability and cytotoxicity assays. Since the mid 1990s, the number of the assays has expanded. Especially, the growing understanding on the importance of the multiple drug transporters and metabolizing enzymes on pharmacokinetics of drugs in many organs, has paved the way towards new and more detailed mechanistic assays.

One of the important organs, in which the drug transporters and metabolic enzymes affect the pharmacokinetics of drugs, is human intestine. Although the liver is considered the main metabolizing organ in the human body, contribution of intestinal metabolism in total metabolic clearance of many drugs is well recognized. Metabolic enzymes in the intestine have also been reported to take part in clinically relevant drug-drug interactions. The risk for both transporter and metabolic drug-drug interactions is considered to be pronounced due to the higher drug concentrations that the transporters and metabolic enzymes face in the intestinal wall. Despite the extensive research on the area, the prediction of intestinal absorption taking into account also the many transporter and metabolism-related processes, has not been fully accomplished yet. That is mainly due to the lack of high quality data, generation of which requires appropriate use of the existing methods and development of new tools to complement the existing ones.

This work focuses on the automatable microplate-based *in vitro* assays that are amenable to predicting the drug transport and metabolism in the intestine level. However, it should be noted that since most of the transporters and metabolizing enzymes discussed here are not expressed exclusively in human intestinal tissue, many of the assays are applicable in predicting the drug behaviour also in other tissues.

During the course of this thesis work, a new high throughput screening tool for detecting compound interactions with one of the intestinal UGT isoforms (UGT1A6) was developed (**I**). The fluorescence-based assay is the first of a kind enabling the

direct determination of the probe reaction at the product site without separation or secondary reactions. The assay was also shown to be useful in providing data for computational model development (**II**). The resulting classification and 3D-QSAR models indicated physicochemical parameters and functional groups important to the compound interactions with the UGT1A6. Interactions of two drug compounds (indomethacin and diclofenac) with UGT1A6 were more thoroughly studied. The effect of pH on the interaction was examined in human liver and intestinal microsomes, as well as with an extensive set of individual recombinant UGT enzymes (**III**). The results indicated that the effects of pH were variable and enzyme specific. Finally, automation of fairly complex, but highly predictive intestinal *in vitro* transport models were studied in detail to further improve the utilization potential of automated screening assays (**IV**).

2 Review of the literature

2.1 Intestinal drug absorption

Human small intestine is approximately 5-6 m long tube having a highly folded surface structure (reviewed in Washington et al., 2001). Due to its special features, such as Kerckring valves, villus and microvillus (Fig. 1), the absorptive surface area is markedly higher than would be expected solely based on its length and diameter.

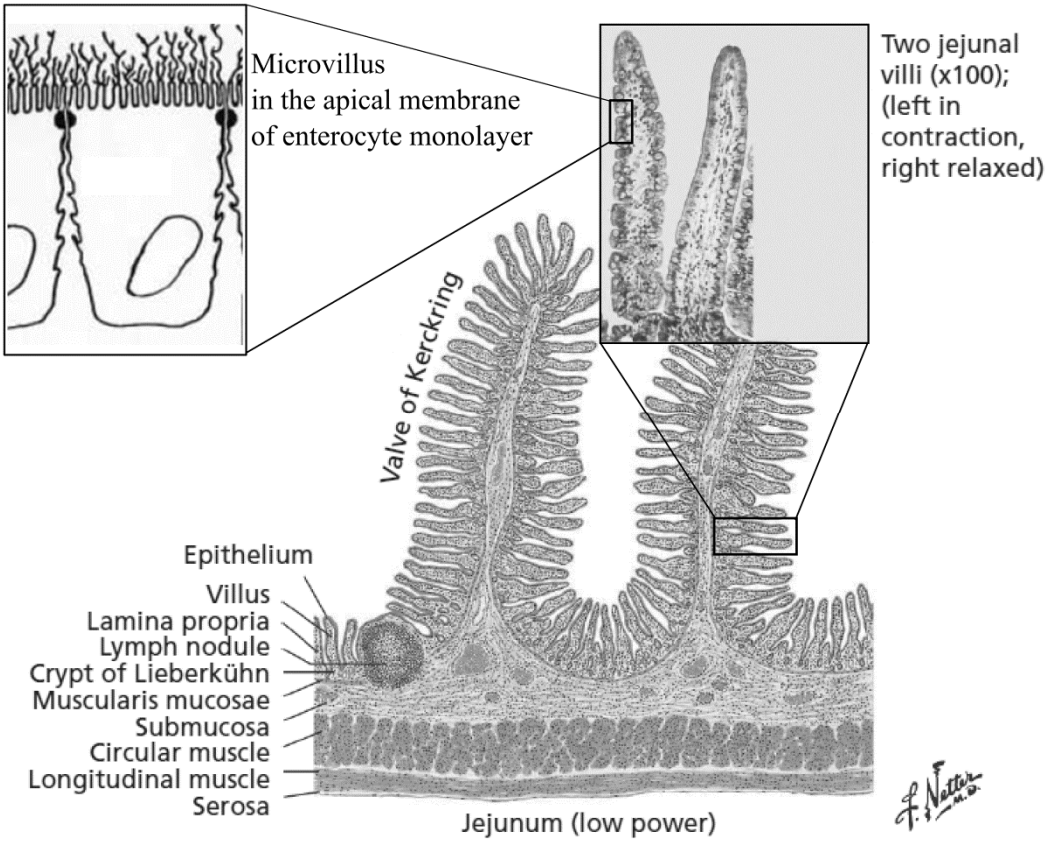

Figure 1. *Structure of human small intestine (Modified from Avdeef, 2001 and Thelen and Dressman, 2009, where in Hansen and Koepen, 2002).*

The enterocyte monolayer lining the intestinal wall is considered an important barrier for the oral drug absorption (Fig. 2) (reviewed in Chan et al., 2004). The processes affecting the drug absorption across the enterocyte monolayer are passive permeation (Fig. 2A), facilitated and efflux transport (Fig. 2B-2C) and intestinal metabolism (Fig. 2D), which may also co-operate with the efflux transport (Fig. 2E).

2.1.1 Passive permeation

Passive diffusion across the enterocyte monolayer may occur either via transcellular or paracellular pathway (Fig. 2). Overall, the most important route for intestinal drugs absorption is the transcellular diffusion through the cells (reviewed in Lennernäs, 2007). In that process, the physicochemical properties of a drug mainly dictate how well it is partioned into and diffused through the apical membrane of the enterocytes (reviewed in Krämer et al., 1999 and Avdeef et al., 2001). According to the well-established "Lipinski´s Rule of 5", compounds having molecular weight of higher than 500, logP of higher than 5, and more than 5 hydrogen bond donors or more than 10 hydrogen bond acceptors, are prone to be poorly absorbed (reviewed in Lipinski et al., 2001).

The paracellular drug transport is efficiently hindered by tight junctions located between the cells. Therefore, the paracellular pathway may contribute to the transport of only small hydrophilic compounds, which are small enough to fit through the paracellular space, with pore radii of 7-13 Å (Fine et al., 1995, Linnankoski et al., 2010). Compounds utilizing this route are not subject to intracellular metabolism, which may be an advantage (reviewed in Thelen and Dressman, 2009).

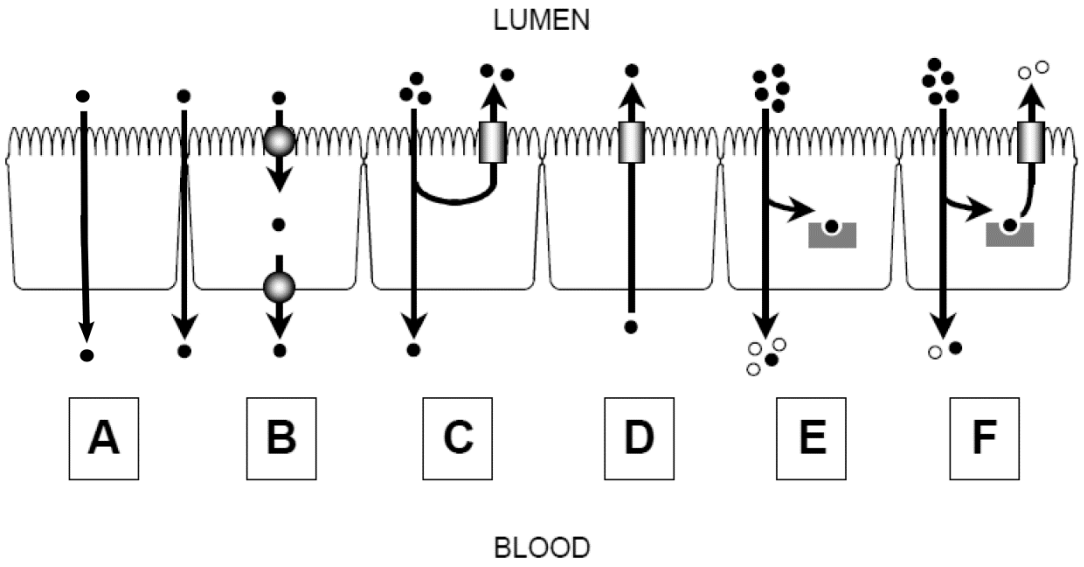

Figure 2. *Drug absorption through the enterocyte monolayer may occur (A) passively either via trancellular or paracellular pathway. (B) Carriers, such as uptake transporters, may facilitate the transport of drugs that have low passive permeation. (C) Efflux transporters located on the luminal site of the monolayer are able to pump drugs back to the intestinal lumen, and thus restrict the absorption. (D) Efflux transporters may also participate in excretion of drug from blood circulation. (E) The panel of metabolic enzymes inside the enterocytes is capable of transforming the drug into metabolites that differ in their activity and toxicity from the parent compound. (F) Metabolism and efflux transporter may also co-operate (Modified from Chan et al., 2004).*

2.1.2 Intestinal drug transport

Several uptake and efflux transporters take part in the intestinal nutrient absorption as well as in preventing hazardous xenobiotics to enter the body or accumulate into the cells (Fig. 2) (reviewed in Chan et al., 2004; Szakács et al., 2008 and Oostendorp et al., 2009). Many of these uptake and efflux proteins have been reported to affect also the drug absorption, either by enhancing or inhibiting it.

ABC transporters MDR1, MRP2 and BCRP are considered the main efflux transporters on the apical membrane (reviewed in Higgins, 1992, Chan et al., 2004 and Giacomini et al., 2010). They pump drugs back to the intestinal lumen against the concentration gradient by utilizing the energy released in ATP hydrolysis. Substrate and inhibitor specificities of these efflux transporters are broad and overlapping, but not equal. Many widely used cardioactive and anticancer drugs, as well as antivirals, antibiotics, antihypertensives and corticosteroids and their metabolites, among others, are either substrates or inhibitors of these efflux transporters.

In contrast to the ABC transporters, apical SLCs, such as OATPs, PEPT1, ASBT and MCT1, may facilitate the absorption of drugs that structurally resemble their natural substrates (reviewed in Zhang et al., 2002, Klaassen and Aleksunes, 2010 and Varma et al., 2010). The facilitated diffusion via a transporter follows the concentration gradient of the compound and is coupled with the flow of H^+ and/or Na^+ ions across the cell membrane. The function of at least OATP2B1, PEPT1 and MCT1 is pH dependent (reviewed in Anderson and Thwaites, 2010). The affinities of substrates to PEPT1 and MCT1 are generally low, from micro- to millimolar range, but transporting capacities are high, whereas the opposite applies to intestinal OATPs (reviewed in Varma et al., 2010). Drugs transported across the apical cell membrane by the intestinal OATPs, PEPT1 and MCT1 include statins (e.g atorvastatin), β-lactam antibiotics (e.g. cephalexin) and carboxylic acids (e.g. valproic acid), respectively (Tamai et al., 1999; reviewed in Brandsch et al., 2008 and Kalliokoski and Niemi, 2009). Whereas, ASBT is considered more a potential target for future prodrugs (reviewed in Balakrishnan and Polli, 2006)

The transporters located on the basolateral membrane are less thoroughly studied. The ABC transporter MRP3 is considered to take part in the enterohepatic recirculation of bile acids, as well as in protecting the enterocytes against some organic anions, such as anticancer drugs (reviewed in Borst and Elferink, 2002), whereas solute carrier OCT1 is involved in intestinal secretion of e.g. metformin and quinidine (reviewed in Jonker and Shinkel, 2004). In addition, OSTα and OSTβ are known to have an important role in the reabsorption of bile acids and steroid derivatives (Ballatori et al 2005).

2.1.3 Intestinal drug metabolism

In addition to and together with the active efflux, intestinal metabolism may substantially lower the bioavailability of orally administered drugs (Fig. 2) (reviewed

in Suzuki and Sugiyama, 2000). Even though the total metabolizing capacity of the intestinal tissue may be lower compared to that of liver, mainly due to the smaller size of the epithelial tissue, intestine is an important contributor to the first pass metabolism of drugs (reviewed in Lin et al., 1999, Kaminsky and Zhang, 2003 and Thelen and Dressman, 2009).

CYPs are the major players in phase I oxidative drug metabolism in the small intestinal epithelium; CYP3A contributing 82% and CYP2C 16% of the intestinal CYP expression (Paine et al., 2006). They are located in the endoplasmic reticulum of the enterocytes in conjunction with NADPH-cytochrome P450 reductase, which provides the electrons for the CYP, and thus enables the oxygenation of the substrate (reviewed in Nebert and Gonzales, 1987 and de Montellano, 1999).

Several enzymes responsible for phase II conjugation reactions, such UGTs (Peters et al., 1991; Ohno and Nakajin, 2009; reviewed in King et al., 2000 and Gregory et al., 2004) and SULTs (Chen et al 2003; Riches et al 2009), are expressed and functional in the intestinal wall. Of UGTs, isoform 1A1 is the most active in the intestinal level (Fisher et al., 2000); activities even higher than in the liver have been reported. In addition, the highest SULT expression levels have been detected from intestine, where SULT1B1 and SULT1A3 both accounted for about one third of the total SULT expression (Riches et al., 2009).

The conjugation reactions aim primarily at inactivation and/or detoxification of the compound or its metabolite by adding a hydrophilic residue to the parent compound. The increased water solubility also results in an impoved excretion. However, there are examples of metabolites that are pharmacologically more active than the parent compound, e.g. morphine-6-glucuronide (Osborne et al., 1990), or more toxic like the reactive acyl glucuronides (Williams et al., 1992) or the sulfate conjugate of troglitazone (Saha et al., 2010).

The major contributors in the phase II metabolism, the UGTs, catalyze the addition of a sugar residue into a substrate having a nucleophilic functional group, most often a hydroxyl, a carboxylic acid or an amine (reviewed in King et al., 2000). The most abundant UGT subfamilies in humans are 1A and 2B, which utilize the glycosyl group from a co-substrate UDPGA to form a glucuronidated substrate (β-D-glycopyranosiduronic acid conjugate). As a co-product, also UDP is formed. According to the common understanding, the UGTs are localized in the inner membrane of the ER, and therefore the substrates need to first pass through the ER membrane before getting in contact with the enzyme (King et al., 2000 where in Tephly and Burchell, 1990).

In addition to the above mentioned phase I and II enzymes, also expression of glutathione S-transferases (GSTs) (Peters et al., 1991; Coles et al 2002), alcohol, aldehyde and NAD(P)H dehydrogenases, epoxide hydroxylases, esterases, monoamine oxidases, acetyl transferases, catechol-O-methyltransferases and acetylserotonin-O-methyltransferases, among several other enzymes, have been detected in small intestinal tissue (Nishimura and Naito, 2006).

2.2 In vitro model systems for intestinal transport and metabolism

Involvement of uptake and efflux transporters in drug absorption through the intestinal wall can be studied with *in vitro* model systems of varying complexity and equivalency to human intestinal wall. Each model system has its advantages and limitations, which should be carefully considered, when choosing the biological model system for a particular assay (Table 1). The same applies to the model systems for metabolism studies. In general, the cellular systems often represent the most complex and biologically equivalent structures, whereas the transporters reconstituted on artificial lipid membranes or recombinant enzymes separated from cellular environment do not possess many structural similarities to the human intestinal wall. However, these models are useful in providing mechanistic information on the possible transport and metabolism processes.

Table 1. *Summary of advantages and limitations of in vitro model systems suitable for intestinal drug transport and metabolism screens.*

	Advantages	**Limitations**	**References**
Cellular models	Full cellular machinery Intact cell membrane Transporters and metabolizing enzymes present (more or less) Monolayer formation HTS and automation compatible Commercially available	Laborious Lab-to-lab variation Barrier properties are not equal to human intestinal wall Difficult to miniaturize SOPs needed Transporter conformation and activity may differ depending on the host cell	Ganapathy et al 1995; Artursson et al 1996b; van de Kerkhof et al, 2007; An and Tolliday, 2010
Intestinal microsomes and S9 fraction	Can be derived from human or animal tissue Several metabolizing enzymes present Easy to use Can be stored frozen HTS compatible Commercially available	Lack of drug transporters Micromes are lacking the cytosolic enzymes Co-factors need to be added High variation in enzyme activity Enzyme expression dependent on the segment of intestine where extracted Enzyme activities lower than *in vivo* Freezing and thawing cycles reduce the enzyme activity	van de Kerkhof et al, 2007; Laine, 2008; Gertz et al., 2011

Table 1. *Continued…*

	Advantages	Limitations	References
Recombinant enzymes	Can be used for reaction phenotyping without spesific substrates/inhibitors (only one enzyme) Can be used for screening metabolic stability or evaluation of inhibition potential Experimental conditions can be controlled tightly Effect of rare enzyme polyforms can be assayed HTS compatible Commercially available Easy and fast to use	Relative contribution of enzymes in metabolism of a compound may be difficult to determine (only one enzyme) IC50 values may not be compatible with the values obtained with microsomes (often lower) Enzyme conformation / activity may be dependent on the batch and recombinant system Co-enzymes and co-factors may need to be added	Gonzalez and Korzekwa, 1995; Radominska-Pandya et al, 2005; Tang et al, 2005; Kumar et al., 2006; Fujiwara et al, 2008; Miners et al, 2010; Parkinson et al, 2010
Membrane vesicles and reconstituted transporter systems	Involvement of a single transporter can be assayed Enables studies with different transporter polymorphs HTS compatible Commercially available Easy and fast to use	Artificial system composed only of the membrane and transporter(s) Laborious preparation procedures Membrane composition may affect the transporter function (reconstituted)	Xia et al 2007; Jin and Di 2008; Hegedűs et al 2009

2.2.1 Cellular models

Both primary enterocytes of animal and human origin (e.g. Hansen et al., 2000; Glaeser et al., 2002) and several cell lines (Table 2) can be used in studying the involvement of intestinal transporters and/or metabolism in drug absorption. However, poor availability, varying quality, as well as laborious and error-prone separation techniques of primary enterocytes limit their use (Weiser, 1973; Zhang et al., 1999b; Glaeser et al., 2002). Therefore, continuous cell lines presented in Table 2 are often preferred.

Caco-2 is the best characterized and the most widely used cell line for studying mechanisms of intestinal drug absorption (e.g. Pinto et al., 1983; Hidalgo et al., 1989; reviewed in Artursson et al., 1996b). Even though derived from colon cancer, it polarizes and differentiates into a cell monolayer resembling that of the intestinal epithelia when cultured *in vitro* on a permeable membrane for three weeks. It has tight junctions and microvillus structure closely resembling that of the mature enterocytes. In addition, several transporters, such as MDR1, MRP2-3, BCRP and PEPT1 (Hunter et al., 1993; Augustijns et al., 1993; Taipalensuu et al., 2001; Seithel et al., 2006), and intestinal metabolizing enzymes, including UGTs (Abid et al., 1995; Siissalo et al., 2008; Zhang et al., 2011), GSTs (Peters and Roelofs, 1989),

SULTs (Meinl et al., 2008) and esterases (Imai et al., 2005), are expressed and functional also in the differentiated Caco-2 model. However, the expression levels of these transporters and enzymes often differ from that in human duodenum (Taipalensuu et al., 2001; Sun et al., 2002; Seithel et al 2006; Zhang et al., 2011). In particular, it is important to note that the expression levels of CYP enzymes in these cells are low, making this cellular model not suitable for studying intestinal CYP-mediated metabolism. Furthermore, the properties of the cell line vary remarkably lab-to-lab, which highlights the need for using known marker compounds for standardizing the Caco-2 system in use (Hayeshi et al., 2008; reviewed in Artursson et al., 1996b).

Table 2. *Cell lines used for evaluating the role of intestinal drug transporters and metabolic enzymes in drug absorption.*

Cell model	Origin	Properties and use	Reference
Caco-2	human colon carcinoma	Resambles the most the intestinal epithelia, FDA recommended* →*bidirectional transport, uptake and efflux assays	Artursson et al., 1996b; FDA, 2006
MDCK	canine kidney	Suitable for transfection, fast differentiation, FDA recommended* →*bidirectional transport, uptake and efflux assays	Horio et al., 1989; FDA, 2006
LLC-PK1	porcine kidney	Suitable for transfection, fast differentiation, FDA approved* →*bidirectional transport, uptake and efflux assays	Adachi et al., 2003; FDA, 2006
CHO	chinese hamster ovary	Suitable for transfection →uptake and efflux assays	Covitz et al., 1996
LS180	human colon carcinoma	PXR expression →efflux transporter and CYP3A4 induction assays	Pfrunder et al., 2003; Hartley et al., 2006;
Caco-2/TC7	Caco-2 subclone	Higher CYP and UGT activities than in parent Caco-2 →Alternative for parent Caco-2 cells. Potential for studying simultaneously both transport and metabolism?	Caro et al., 1995; Bock-Hennig et al., 2002

Human recombinant DNA technologies have been utilized in tailoring the cellular models to better resemble the intestinal wall. For example, increased expression of CYP3A4, MDR1 or PEPT1 in transfected Caco-2 cells has been reported (Crespi et al., 1996; Han et al., 1998; Brimer et al., 2000). However, most commonly these techniques are utilized in developing cell lines that overexpress one or few transporters and/or metabolic enzymes. That kind of cell lines are useful in defining whether or not a certain transporter or metabolizing enzyme is involved in the transport and/or metabolism of a compound. One of the cell lines for this purpose

is MDCK (Cho et al., 1989). MDCK II clones transfected with one single transporter, e.g. MDCKII-MDR1, are most commonly utilized (Lowes and Simmons, 2002), but also double- (MDCKII-OCT1/MDR1) and triple-transfected (MDCKII-OATP1B1/ UGT1A1/MRP2) MDCKIIs have been reported (Nies et al., 2008; Fahrmayr et al., 2011). Also LLC-PK1 and CHO cell lines have been shown to be suitable for transfection purposes (Covitz et al., 1996; Brimer et al., 2000; Adachi et al., 2003).

2.2.2 Intestinal microsomes and S9 fraction

Human intestinal microsomes (HIM) are prepared by differential centrifugation from homogenized human enterocytes (Paine et al., 1997; Zhang et al., 1999b). High quality intestinal microsomes have turned out to be more difficult to prepare than liver microsomes. Variation in the enzymatic activity is considered to be mainly due to the differences in experimental procedures used, e.g. the metabolizing enzymes in the cells may be damaged during the detachment procedure and exposed to proteolytic enzymes (Galetin and Houston, 2006). That can be minimized by adding protease inbitors to the elution media (Zhang et al., 1999b). Similar to liver microsomes, intestinal microsomes contain all the enzymes bound to ER membrane, such as CYPs and UGTs, but not the cytosolic ones, such as SULTs. Whereas S9 fraction, the supernatant separated by centrifugation of the lyzed tissue or cells at 9750g, contains both the microsomal and sytosolic enzymes (Sohlenius-Sternbeck and Orzechowski, 2004). As the expression levels of transporters and metabolizing enzymes differ along the intestinal track (Sun et al., 2002), the segment of the intestine where the cells used to prepare the microsomes and S9 fraction have been extracted from, is of great importance.

Despite the challenges related to preparation, HIMs have been successfully used for assessing the intestinal CYP- and UGT-mediated first-pass metabolism (e.g. Sabolovic et al., 2004; Cubitt et al., 2009; Gertz et al., 2010). To lesser extent, also the intestinal S9 fraction has been utilized in studying the involvement of cytosolic enzymes, such as carboxyl esterases, in the intestinal metabolism of drugs (Ahmed et al., 1999; Yan et al., 2010).

2.2.3 Recombinant enzymes

Recombinant DNA technologies can be utilized to produce individual enzymes in suitable host cells, which have low or no inherent expression of the particular enzyme. Production of CYPs and UGTs by transient or stable transfection has been reported in several mammalian, bacteria and yeast cells, e.g. monkey kidney (COS) Chinese hamster lung fibroplast (V79) *E. coli* and *Sacharomyces cerevisae* or *Pichia Pastoris* (reviewed in Crespi and Miller, 1999 and Radominska-Pandya et al., 2005). In addition, high levels of CYPs and UGT enzymes can be expressed in baculovirus infected *Spodoptera frugiperda* (Sf9) insect cells (Buters et al., 1994;

Nguyen and Tukey, 1997; Kurkela et al., 2003). The recombinant enzymes are used either as purified proteins or, mainly in the case of membrane proteins, as a suitable membrane preparation, such as microsomes.

In the case of CYPs, also the amounts of their electron donor partners, such as NADPH-P450 oxidoreductase and cytochrome b_5, affect the activity of the recombinant CYP enzymes (Shaw et al., 1997). These electron transfer partners may be expressed separately or as a fusion protein (Fisher et al., 1992; Rodriques et al., 1995). The functionality of purified CYPs has been reported after purification from yeast and insect cells (Buters et al., 1994; Imaoka et al., 1996), whereas the activity of UGTs is easily lost upon extraction with detergents from the membrane (Kurkela et al., 2003), and therefore, the recombinant UGTs are used as membrane-bound protein preparations.

2.2.4 Membrane vesicles and reconstituted transporter systems

Membrane vesicles can be formed by disrupting cells in a buffer of low ionic strength in the absence of bivalent cations (Steck et al., 1970) or by nitrogen cavitation (Loe et al., 1996). As a result, a mixture containing membrane lamellae and vesicles of inside-out and right side-out orientation are formed. Most often, the membrane preparations are used as a mixture, but the relative amount of inside-out vesicles in the mixture can be increased by a special centrifugation procedure (Meier et al., 1984). Biological membranes containing transporters, such as intestinal brush border membranes (Murer et al., 1974) or cells genetically engineered to over-express a particular transporter (Sarkadi et al., 1992; Lechner et al., 2010), can be used as a source material. However, membrane vesicles prepared from original human or animal tissue have often several different transporters embedded in the membrane, which complicates the interpretation of the transport mechanism in these vesicles. In addition, the presence of three types of membrane systems in the preparation further complicates the studies with more than one compound at a time.

Vesicles are mainly used for studying compound interactions with the ATP-dependent efflux transporters, and therefore, preferred orientation is inside-out. That enables monitoring the ATPase activity on the surface of the vesicles (Sarkadi et al., 1992; Bakos et al., 1998), as well as uptake and accumulation studies with the efflux transporters (Horio et al., 1988).

Transporters can be also reconstituted into lipid bilayers of artificially prepared membrane vesicles. The purified transporter can be inserted into a liposome membrane by first mixing the detergent-solubilized transporters with detergent-destabilized liposomes, and then removing the detergents e.g. by adsorption to polystyrene beads (Geertsma et al., 2008). Liposomes composed of several different mixtures of synthetic phospholipids, such as dimyristoyl-phosphatidylcholine and 1-palmitoyl-2-phosphatidylcholine (Lu et al., 2001), egg yolk L-α-phosphatidylcholine and L-α- phosphatide with cholesterol (Jacobs et al., 2011), soybean phospholipids together with phosphatidylserine and cholesterol (Borgnia et al., 1996) and lipid extracts of bovine brain (Bucher et al., 2007) or E. coli –bacteria (Newman and

Wilson, 1980; Geertsma et al., 2008) have been successfully utilized as membrane support for the intestinal ABC-transporters. Studies with liposomes prepared of egg-phosphatidylcholine in the absence and presence of cholesterol revealed the importance of cholesterol, or structurally similar compounds, to the function of MDR1 through their effect on ATPase activity (Bucher et al., 2007).

2.3 Intestinal transporter assays

In vitro assays that are widely used for screening the involvement of transporter(s) in intestinal drug absorption can be divided into three categories: 1) assays detecting the function of an ABC-transporter indirectly by measuring ATPase activity (ATPase assay), 2) assays following the uptake or accumulation of a compound into cells or vesicles, (uptake, accumulation and efflux assays), and 3) assays measuring the passage of a compound across a cell monolayer that resembles the intestinal epithelia (bidirectional transport assay).

2.3.1 ATPase assay

Energy required for the function of ABC-transporters is released in an ATPase catalysed cleavage of ATP. Detection of that reaction, either by detecting the liberation of organic phosphate, formation of ADP or consumption of ATP, forms the basis for ATPase assays (Fig. 3) (Sarkadi et al., 1992; Garrigues et al., 2002; Ma and Cali, 2007). Several assay kits based on the above mentioned principles are also commercially available.

Experimentally, the ATPase assay is the most straightforward of the *in vitro* transport assays. Compound(s) are simply incubated with the membrane preparation, either inside-out vesicles, open membrane lamellae or reconstituted transporters system, in the presence of MgATP, and the resulting absorbance or luminescence is recorded at the end (Sarkadi et al., 1992; Borgnia et al., 1996; Garrigues et al., 2002; Ma and Cali, 2007). The assay can be performed either in stimulation mode by detecting the increase in ATPase activity due to the compound transport or in inhibition mode by following the decrease in e.g. verapamil stimulated ATPase activity. Often inhibitors for non-ABC transporters, such as ouabain, sodium azide and EGTA, are added to the incubation buffer to minimize the contribution of other ATPase linked reactions. Results are usually reported as vanadate-sensitive ATPase activity representing the compound-related ATPase activation that can be inhibited by sodium orthovanadate.

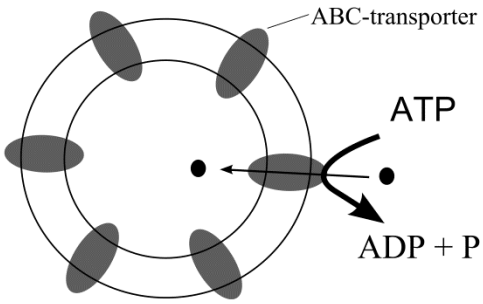

Figure 3. *Assay principle of ATPase assay in inside-out membrane vesicles.*

ATPase assay has been successfully used in defining compound interactions with MDR1, MRPs and BCRP (e.g. Litman et al., 1997a; Garrigues et al., 2002; Lespine et al., 2006; Glavinas et al., 2007; Holland et al., 2008). Compounds stimulating the ATPase activity are generally considered to be substrates of the particular transporter and those inhiting the stimulated activity either substrates or inhibitors. However, it should be kept in mind that ATPase is an indirect assay and does not measure the compound transport itself. Therefore, the results should be considered suggestive, rather than decisive (Polli et al., 2001; Scwab et al., 2003).

Several compound properties may impair the results. Especially, results obtained with compounds having extremely low or high passive membrane permeability, should be treated with caution (Polli et al., 2001; Scwab et al., 2003). The low permeability compounds may not be able to partition into the membrane at high enough concentrations to produce detectable ATPase conversion, even though they were substrates of a transporter, and the transporter would markedly impair their already poor absorption. With high permeability compounds the situation is opposite. In addition, high lipophilicity of a compound may lead to nonspecific binding, and decrease the effective compound concentration in the assay. Furthermore, test compounds may also interfere with the detection of inorganic phosphate liberation (Shirasaka et al., 2006).

2.3.2 Uptake, accumulation and efflux assays

Compound uptake and accumulation into membrane vesicles and cells or efflux from the cells allows the identification of substrates and inhibitors of a particular transporter (e.g. Horio et al., 1988; Holló et al., 1994; Vaidyanathan and Walle, 2003; Lohman et al., 2007; Zhang et al., 2007; Siissalo et al., 2009). They also provide useful information of drug-drug interaction potential. Such assays can be performed either by following the uptake and accumulation of a compound into the vesicles or cells (direct mode), or by following the effect of a test compound on the uptake and accumulation or efflux of a suitable reporter substrate (indirect mode).

In the direct assay mode, the compounds are incubated with the transporter system, either vesicles or cells, and after a specified time, the transporter function is terminated by the addition of ice-cold buffer (Horio et al., 1988; Bakos et al., 1998; Vaidyanathan and Walle, 2003; Zhang et al., 2007). Vesicles are then collected on filter (rapid filtration technique) and washed to remove the compounds that are bound nonspecifically to the external surface of the vesicles. In the cases of radiolabelled or fluorescent compounds, the amount of compound accumulated into the vesicles can be determined by quantifying the radioactivity in the filter (Horio et al., 1988). Also scintillation proximity assay technologies have been utilized in the detection of compound uptake into the tranporter-overexpressing cells (Lohmann et al., 2007). In cellular uptake assays, the cells are usually lysed after the stoppage of transporter function and prior to the compound analysis (Vaidyanathan and Walle, 2003). If radiolabelled compounds are not available, compound concentration inside

the cells or vesicles can be quantified with UV-detector after HPLC separation (Vaidyanathan and Walle, 2003) or with LC-MS/MS system (Putnam et al., 2002).

Indirect uptake, accumulation and efflux assays utilize known substrates as reporter compounds. Calcein-AM assay is a widely utilized indirect assay that can be used for identifying compounds interacting with MDR1 (Holló et al., 1994; Eneroth et al., 2001; Crivori et al., 2006). The assay relies on the high passive permeation of calcein-AM through the cell membrane and its subsequent hydrolysis by intracellular esterases (Fig. 4). That reaction yields hydrophilic and highly fluorescent calcein, which cannot permeate the cell membrane passively, or be transported by the MDR1. Inhibition of the calcein-AM efflux is detected as the accumulation of calcein into the cells, and thus, as fluorescence increase. In another commonly used approach, cells are loaded with a compound that is not a substrate for the particular transporter, but can passively permeate the cell membrane. Inside the cell the compound is transformed into a hydrophilic substrate that can escape the cell only via the transporter. One such substrate is a fluorescein derivative CDCFDA, a substrate for MRP2, which is hydrolysed to fluorescent CDCF inside the cells (Siissalo et al., 2009). The interaction of compounds with MRP2 can be detected as a lowered level of CDCF, and thus fluorescence, in the buffer.

In principle, also many other good transporter substrates can be used as probes, if their passive permeation through the membrane is low enough to avoid leakage through the membrane during the assay. For example, rhodamine 123 is a commonly used reporter substrate in MDR1 cellular uptake assays (Perloff et al., 2003), and PhA has been successfully used with BCRP (Henrich et al., 2006). However, the probe should be carefully considered, since the choice of the probe substrate has been demonstrated to affect the results, as is discussed in more detail under the chapter 2.3.3 Bidirectional monolayer transport assay.

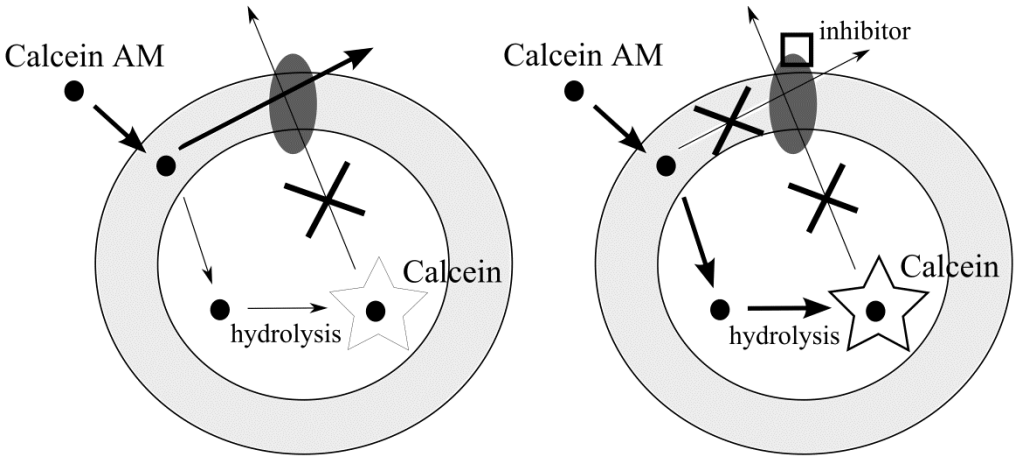

Figure 4. *Assay principle of Calcein AM assay (Modified from Kerns and Di, 2008).*

The assay conditions should be optimized for each combination of the transporter and biological model system, taking into account the properties and requirements of both. For example, in vesicular transport assays with ATP-dependent transporters, care must be taken to ensure sufficient amounts of ATP during the assay. If needed, ATP-regenerating system, creatine phosphokinase together with creatine phosphate, may be added to the system (Hirouchi et al., 2004). On the other hand, in the case of PEPT1, pH dependency should be considered, namely by providing a H^+ gradient in the experimental setting, e.g. by performing the assays in a slightly acidic buffer (Ganapathy and Leibach, 1983; Vig et al., 2006).

The observed uptake, accumulation or efflux of a compound is a combined result of both passive diffusion through the membrane and transporter-mediated passage. Therefore, care should be always taken to define also the non-transporter related transport, and subtract that from the observed total transport (e.g. Bakos et al., 1998). In the case of ATP-dependent transporters, vesicular uptake assay performed with AMP instead of ATP, or just without ATP, can be used to define the non-transporter related uptake (Bakos et al., 1998), whereas the experiments at pH 7.4 are appropriate for defining the PEPT1 unrelated transport (Ganapathy and Leibach, 1983). Also inhibitors of particular transporters may be utilized in defining the extent of passive permeation (Scow et al., 2011). That is useful especially in the cases of cells expressing several transporters.

In uptake, accumulation and efflux assays, many compound properties may affect the reliability of the results. Highly lipophilic compounds may show false negative results (Polli 2001). Compounds may leak through the membrane or non-specifically bind to the membrane, and thus, the accumulation of compounds inside the vesicles or cells may be underestimated. Also compounds having a very low membrane permeability may not be able to partition into the membrane at high enough concentration and compete with the MDR1 probe substrates. In addition, in the cellular uptake assays, toxicity issues should be considered to reduce the risk of false negatives and positives due to the cellular damage.

2.3.3 Bidirectional monolayer transport assay

Comparison of apparent permeability, P_{app} –values, or flux, of a compound across a cell monolayer in absorptive (A-B, apical to basolateral) and secretive (B-A, basolateral to apical) directions provides useful information on the involvement of efflux or uptake transporter(s) in drug absorption (e.g. Inui et al., 1992; Augustijns et al., 1993; reviewed in Artursson et al., 1996a; Hubatsch et al., 2007). Most commonly, and also recommended by the FDA for identifying substrates and inhibitors for MDR1, bidirectional monolayer transport assays are performed across Caco-2 or transporter overexpressing MDCKII or LLC-PK1 monolayers (Adachi et al., 2001; Tang et al., 2002; reviewed in Zhang et al., 2006; FDA, 2006).

In practice, a monolayer transport assay is performed by adding the compound(s) of interest either to the apical or basolateral compartment, and by detecting the appearance on the opposite site of the monolayer (Fig. 5) (reviewed in Artursson et

al., 1996a; Hubatsch et al., 2007). The analysis of the samples is usually carried out either by HPLC with UV or fluorescence detector or by LC-MS/MS (e.g. Inui et al., 1992; Wang et al., 2000). In the case of fluorescent or radiolabelled compounds, also fluorescence plate reader and liquid scintillation counting can be utilized (Tang et al., 2004; Xia et al., 2005). If the ratio ($P_{app\ B\text{-}A}/P_{app\ A\text{-}B}$) with Caco-2 cells or the difference of the ratios observed with transfected and wild type cells ($ratio_{transfected}$ / $ratio_{wild\ type}$) markedly deviate from one, a compound may be a substrate for an efflux or an uptake transporter(s) (e.g. Adachi et al., 2001; Tang et al., 2002). The involvement of transporter(s) may be further confirmed by performing the assay in the presence of inhibitors through a cell monolayer in which the expression level and functionality of transporters are well demonstrated (Augustijns et al., 1993; Hunter et al., 1993; Tang et al., 2002; Bjornsson et al., 2003; Xhang et al., 2006). For detecting inhibitors, the transport of a substrate can be followed in the presence and absence of the compound of interest (e.g. Fromm et al., 1999; Bjornsson et al., 2003; Zhang et al., 2006).

To avoid erroneous results due to the leakage of the compound through possible gaps in the monolayer, TEER is usually measured before and after the assay (reviewed in Artursson et al., 1996a; Hubatsch et al., 2007). Also permeation of passive paracellular transport markers, such as [^{14}C]-mannitol, is often monitored in parallel with the transport of the compound(s) of interest.

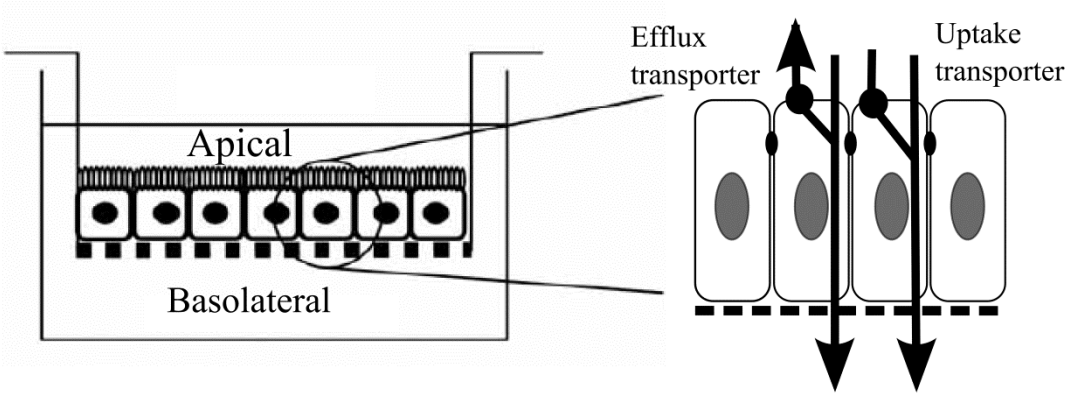

Figure 5. *Assay principle of the bi-directional transport assay (modified from Jin and Li, 2008).*

The choice of inhibitors and substrates for the assay is complicated by several factors. Firstly, the transporters may have several binding sites, as clearly demonstrated in the case of MDR1 (Ayesh et al., 1996; Litman et al 1997b; Shapiro and Ling, 1997; Martin et al., 2000). Secondly, many of the compounds are transported by or inhiting/modulating the function of more than one transporter. For example, vinblastine is transported by MDR1 and MRP2 (Horio et al., 1988; Evers et al., 2000) and GF120918 is an inhibitor for three different transporters, MDR1, BCRP and MRP2 (Matsson et al., 2009). Thirdly, the function of substrates and inhitors may be dependent on the cellular system (van der Sandt et al., 2000; Wang et al., 2008b).

Of the MDR1 substrates, digoxin is usually the primary choice due to its selectivity towards MDR1 and applicability to both *in vitro* and *in vivo* drug interactions studies (Keogh and Kunta, 2006; Rautio et al., 2006). Also the use of vinblastine, colchicine and quinidine is well established (Taub 2005; Rautio et al., 2006; Patil et al., 2011). In addition, rhodamine 123 and Hoechst 33342 can be used as probes for detecting the specific binding site within MDR1 (Tang et al., 2004). However, rhodamine 123 was shown to require carrier mediated influx for its activity as a MDR1 substrate in Caco-2 cells (Troutman and Thakker, 2003). Whereas, methotrexate and estrone-3-sulfate have been used as probe substrates for BCRP, although they are not specific substrates for BCRP (Xia et al., 2005). As for inhibitors, GF120918, verapamil, MK-571 (MDR1, BCRP, MRP2) and Ko143 (BCRP, MRP2) are among the widely used inhibitors (Ozawa et al., 2004; Matsson et al., 2009).

The main drawbacks related to the bidirectional transport assays are the long culturing time of the cells and the often laborious compound analysis. Attempts have been made to decrease the culturing time of the Caco-2 monolayer (Yamashita et al., 2002; Alsenz and Haenel, 2003; Miret et al., 2004; Galkin et al., 2008). However, the transporter profiles have not been comparable to those of mature monolayers (Miret et al., 2004). Similar to metabolism assays, compound cocktail and sample pooling have been also suggested as means of more efficient sample analysis in the bidirectional Caco-2 transport assays (Bu et al., 2000; Hakala et al., 2003; Laitinen et al., 2003; Koljonen et al., 2006).

Despite the challenges, the bidirectional monolayer transport assay is considered to be the most reliable microplate-based *in vitro* method for evaluating drug interaction potential occuring via the MDR1 (Polli et al., 2001; Schwab et al 2003; FDA, 2006). The assay may be unable to detect lipophilic substrates due to their high passive permeation through the membrane (Lenz et al., 2000; Polli et al., 2001). Nevertheless, this should not be a major issue, since in the case of lipophilic compounds, the contribution of efflux transporters to the total drug absorption is negligible.

2.4 Intestinal metabolism assays

2.4.1 Metabolic (in)stability

The metabolic stability of a drug is routinely assayed i*n vitro* using subcellular liver fractions (microsomes, sytosolic, S9) to predict the metabolic first-pass clearance of a drug (reviewed in Jia and Liu, 2007). With increasing understanding on the contribution of the intestinal metabolism to the total first-pass metabolism of many orally administered drugs, interest in taking into account also the contribution of intestinal biotransformation on the total first-pass metabolism has increased (e.g. Thummel et al., 1996; Cubit et al., 2009). So far, the models and assays used for studying drug metabolism at the intestinal level are not as well validated and reliable as the ones routinely used for studying metabolism in liver.

In intestinal level, metabolic stability, metabolite identification and reaction phenotyping can be assayed in the subcellular intestinal fractions, most often human intestinal microsomes (HIM), but also with the S9 fractions (e.g. Thummel et al., 1996; Ahmed et al., 1999; Galetin and Houston, 2006; Cubit et al., 2009) and in individual recombinant enzymes (reviewed in Crespi and Miller, 1999 and in Tang et al., 2005). Subcellular fractions of animal intestine can be used to predict species differences (e.g. Mazur et al., 2010; Yan et al., 2010). In addition, enterocyte homogenates of human and intact enterocytes of animal origin have shown utilization potential (Glaeser et al., 2002; Bonnefille et al., 2011).

The experimental set up of the metabolism assay depends on the enzyme source used. With subcellular fractions, reaction co-factors, such as NADPH for CYPs, UDPGA for UGTs, PAPS for SULTs and GSH for GSTs, need to be added, whereas in intact cells those co-factors are expected to be present inherently (reviewed in van de Kerkhof et al., 2007). With intestinal microsomes, the pore forming agent alamethicin increases the activity of UGTs, probably through increasing the access of UDPGA to the enxyme UDPGA binding site, inside the microsomes. Recombinant UGTs do not benefit markedly from alamethicin addition (Kemp et al., 2002; Zhang et al., 2011), probably since the membrane preparations for the Sf9 insect cells, where they reside, are already permeable for the UDPGA. Differences in sensitivity to organic solvents, such as DMSO, ethanol and methanol, have been noted for CYPs, whereas UGTs are commonly much less sensitive to this solvent (Busby et al., 1999; Uchaipichat et al., 2004; Zhang et al., 2011). Contrary to the prediction of metabolic clearance with liver microsomes, extent of plasma protein binding, measured rutinely *in vitro* as drug binding to bovine serum albumin, does not seem to have that important role in determining intestinal metabolic clearance during the intestinal drug absorption (Hall et al., 1999; Yang et al., 2007). Nevertheless, the addition of BSA to remove the inhibitory fatty acids that bind to some of the UGTs, probably during the microsome preparation, has recently shown to be highly beneficial (Rowland et al., 2008; Manesvki et al., 2011). In addition, acidic and basic assay conditions have been found to increase the glucuronidation of acidic and basic drugs, respectively (Chang et al., 2009). Furthermore, the extent of

nonspecific binding of drugs to microsomes has been found to be mainly dependent on the lipophilicity and the charge state of the drug (Soars et al., 2002; Gao et al., 2008; Benoit-Biancamano et al., 2009).

With each assay performed with subcellular fractions or recombinant enzymes, several control incubations are recommended, namely without the parent compound, without the co-substrate and without the enzyme source (reviewed in Jia and Liu, 2007). In addition, incubations with microsomes prepared from untransfected cells or membranes of cells transfected with the mock virus, can also serve as good controls, since they allow for taking into account the effect of inherent enzymatic processes in the host cell and drug binding to the membranes that carry the recombinant enzyme (e.g. Manevski et al., 2011).

The analysis of either the parent compound or the formed metabolites is most often performed, with appropriate LC-MS set ups, from the supernatant of the incubation mixture after protein precipitation and centrifugation (reviewed in Lahoz et al., 2008 and Tolonen et al., 2009). Acetonitrile, trichloroacetic acid and zinc as sulfate salt have shown to be efficient in precipitating proteins (Polson et al., 2003). Although LC-MS is considered the standard method in metabolite analysis due to the high sensitivity and decreasing analysis times, it may not be able to identify all the minor metabolites, the site within the parent compound, where the metabolic reaction has occurred, or to quantify the metabolites if the authentic metabolites are not available (reviewed in Liu and Jia, 2007). In addition, the outcome of the MS analysis is highly dependent on the instrument used (reviewed in Tolonen et al., 2009). Microscale LC-MS combined with microdroplet NMR was lately reported (Lin et al., 2008), and perhaps future developments in the sensitivity and speed of NMR analysis will support the use of this technology also in routine metabolite identification.

2.4.2 Metabolic inhibition and induction assays

In vitro metabolic enzyme inhibition and induction assays provide important information on drug-drug interaction potential of a compound before *in vivo* experiments, and may also be used to further confirm the mechanism of inhibition or induction observed *in vivo* (reviewed in Jia and Liu, 2007). Many inhibition assays have also been succesfully miniaturized and are rutinely run in high density plate formats (e.g. Crespi et al., 1997; Moody et al., 1999; Trubetskoy et al., 2005; Larson et al., 2011; reviewed in Lahoz et al., 2006). Due to the important role of CYP(s) in drug metabolism, most effort has been put on developing assays for detecting the inhibitors and inducers for CYPs. However, assays are emerging also for other metabolic enzymes, e.g. UGTs, as the knowledge on their importance on drug metabolism is increasing.

Inhibition of a metabolic enzyme in the intestine can be studied *in vitro* by following the effect of a compound on probe substrate metabolism in incubations with intestinal microsomes or recombinant enzymes (e.g. Gibbs et al., 1999; Zhang

et al., 2007). The experimental conditions discussed in chapter 2.4.1 Metabolic stability apply to the enzymatic inhitibition assays as well.

Contrary to the inhibition assays, induction of enzyme expression can only be determined in intact cells that contain the nucleus and all the needed enzymes. The cell model LS180 was shown to be suitable for induction studies at the intestinal level (e.g.; Hartley et al., 2006; Harmsen et al., 2008; Fan et al., 2011). Typically, the cells are exposed to the compounds for 2-3 days, after which the metabolic activity of the enzyme is determined with an appropriate probe substrate or via reporter gene activity assay, and compared to the values of unexposured cells. In addition, changes in protein levels and mRNA levels give valuable information on the induction of gene expression (Cotreau et al., 2000; reviewed in Worboys and Carlile, 2001).

The choice of a probe substrate is of great importance for inhibition and induction assays. Drug probes are considered to provide more *in vivo* relevant data than fluorescent or luminescent counterparts (Cohen et al., 2003; Bell et al., 2008). However, if not radiolabelled, the detection of most of the drug probe substrate metabolism requires LC-MS analysis, which is still, despite the recent advancements in LC-MS analysis (reviewed in Liang et al., 2011), more time-consuming than the detection of radiolabelled, fluorescent or luminescent probe reactions with simple plate readers. Properties of an ideal probe substrate for metabolic inhibition and induction assays are presented in Table 3.

Thorough reviews on recommended probe substrates, inhibitors and inducers for CYPs are available (Tucker et al., 2001; Liu et al., 2007). Of the drug probes, midazolam and testosterone are considered the golden standards for CYP3A (Thummel et al., 1994; Obach et al., 2001), and diclofenac and S-mephenytoin for CYP2C9 and CYP2C19, respectively (Obach et al., 2001). Several nonspecific fluorescent probes, such as 3-cyano-7-ethoxycoumarin, resorufin benzyl ether (Crespi et al., 1997), 3-(3,4,-difluorobenzyloxy)-5,5-dimethyl-4-(4-methyl-sulfonylphenyl)-5H-furan-2-one (Chauret et al., 1999), dibenzylfluorescein, benzyloxyresorufin (Stresser et al., 2000), 7-benzyloxyquinoline, 7-benzyloxy-4-trifluoromethylcoumarin (Stresser et al., 2002) and Vivid® substrates (Trubetskoy et al 2005) have been succesfully used in high throughput CYP screens. In addition, assays utilizing proluminescent substrates have emerged for CYPs, offering less compound interference problems with the fluorescent compounds than the fluorescencent probes (reviewed in Cali et al., 2006). Proluminescent substrates have a common luciferin structure, which is then further modified with different functional groups to guide the substrate specificity. For example, different proluciferin acetals have been suggested as appropriate substrates for the CYPs (Meisenheimer et al., 2011). Fluorescence and luminescence-based assay kits for several CYPs are currently commercially available.

For other intestinal metabolic enzymes, clear consensus on appropriate probe substrates have not been reached yet. Fluorescence- and luminescence-based assays exist also for the UGTs (Collier et al., 2000; Larson et al., 2011), and a luminescent assay is also commercially available.

Table 3. *Properties of an ideal probe substrate in in vitro metabolic inhibition and induction assays.*

Property	Reference
K_m of the substrate is in the same range as clinically relevant IC50 values	Cohen et al., 2003
Aqueous solubility of the substrate >> Km	Cohen et al., 2003
Unique single product is formed.	Cohen et al., 2003
Formation of product is detectable at 1% conversion	Cohen et al., 2003
Product is stable. It is not further metabolized or degraded under the assay conditions.	Cohen et al., 2003
No mechanism-based inactivation of the enzyme by the substrate.	Cohen et al., 2003
Saturable and monophasic kinetics.	Cohen et al., 2003
Absorbance, fluorescence or luminescence of the substrate and the product differ (if analysis by plate-reader is aimed) and the signal intensity is high enough to enable sensitive detection in aqeous solutions.	Cohen et al., 2003; Meisenheimer et al., 2011
Detection based on the appearance of the product rather than the disappearance of the probe substrate	Tucker et al., 2001
The higher the detection wavelength the less compound interference in likely to occur (absorbance, fluorescence). λ_{ex} > 420 nm in CYP assays with fluorescent probe recommended to avoid photo damage.	Cohen et al 2003; Simeonov et al., 2008
[S] ≤ Km of the substrate can be used in the assay.	Copeland et al., 2003
The probe is selective towards the enzyme in question (subcelluar fractions).	Yuan et al., 2002
Feasible for both *in vitro* assays and *in vivo* studies.	Palmer et al., 2001
Substrate and metabolite(s) should be commercially available.	

Inhibition profiles of many metabolic enzymes have been reported to be substrate dependent (Kenworthy et al., 1999; Stresser et al., 2000; Wang et al., 2000). In the case of CYP3A4, the most thoroughly studied of the enzymes, this is considered to be due to the possibility of multiple substrates to bind to the enzyme simultaneously (e.g. Shou et al., 1994) or the non-Michaelis Menten kinetics that has been observed with many of the substrates (Kronbach et al., 1989, Ueng et al., 1997), including different inhibition modalities (reviewed in Zhang and Wong, 2005). Lately, multiple substrate binding with UGT2B7 (Uchaipichat et al., 2008) and substrate dependent inhibition profiles with CYP2D6 (VandenBrink et al., 2012) have also been observed. Therefore, when evaluating the drug interaction potential of a compound with the enzymes, especially with CYP3A, inhibition profiles towards several drug probes should be determined (Kenworthy et al., 1999; Wang et al., 2000; Bjornsson et al., 2003).

2.5 Automation of transport and metabolism assays

In general, automation of *in vitro* assays increases throughput, decreases human errors and need for labour, releases working hours for more challenging tasks and improves safety issues (Banks et al., 1997).

Both fully automated and semi-automated systems have been established for the transport and metabolism assays (e.g. Jenkins et al., 2004; Hugger et al., 2003). Fully automated systems are capable of performing full assay procedures, from the test compound management through the sample preparation and sample analysis, until the data processing, unattended (Banks et al., 1997; reviewed by Saunders, 2004). Usually, they utilize a centralized robotic arm, which integrates several liquid handling stations, analytical devices, incubators and plate stackers to the system. These systems are best suited for high compound numbers assayed with fairly simple protocols. Whereas, semi-automated systems, comprising a single liquid handling workstation, are more flexible for manual interruptions and reprogramming, and therefore, usually used in executing sections of more challenging assay protocols (Sills et al., 1997; reviewed by Saunders, 2004).

An ideal assay for automation would have simple, preferably add-mix-measure -type of a homogenous assay protocol (reviewed in Bronson et al., 2001). Of the *in vitro* transport and metabolism assays used to predict these processes at intestinal level, CYP inhibition and ATPase assays fullfill these criteria the most closely (Table 4). Today, automated CYP inhibition assays, which are based on probe reactions yielding fluorescent or luminescent signal in incubations with recombinant CYPs, are rutinely run both in 384-well (Kariv et al., 2001; Larson et al., 2011) and in 1536-well formats (Trubetskoy et al., 2005; Litten et al., 2010). Vesicular transport assays should also be adaptable to at least 384-well format, but information on the plate format routinely used is not publicly available. Also ATPase assay and the efflux assays based on PhA accumulation can be run at least in 384-well format (Garrigues et al., 2002; Henrich et al., 2006). All the other assays have not been reported at higher than 96-well format. Screening of metabolic instability in liver microsomes with LC-MS analysis of metabolites (e.g. Di et al., 2003; Jenkins et al., 2004; McNaney et al., 2008), as well as calcein AM assay and bidirectional transport assays through both MDCK and Caco-2 cell monolayers (Eneroth et al., 2001; Xiao et al., 2006; Galkin et al., 2008) have been reported at 96-well format. Although no automated platforms have been reported so far for studying metabolic instability in intestinal microsomes, the assays validated for liver microsomes should be applicable with minor changes.

In the future, ligand binding assays for nuclear receptors utilizing fast detection technologies (TR-FRET, SPA) (Hereley et al 2007; Wang et al 2008a; Shukla et al 2009) and PEPT1 assays based on the measurement of the changes in electric current (Faria et al., 2004; Kelety et al., 2006) could serve as easily automatable higher throughput assay formats for screening the intestinal drug transport and metabolism. Similar to studying metabolism in liver, substrate cocktails taking into account the most important metabolic enzymes in the intestinal level would also be useful.

Table 4. *Summary of assays used for screening intestinal drug transport and metabolism at 96- or higher well formats.*

Assay type	Assay principle and detection technology	Reference
ABC transporters		
ATPase assay	P_i-molybdate complex → Absorbance	Sarkadi et al., 1992
ATPase assay	NADH consumption → Absorbance	Garrigues et al., 2002
ATPase assay	ATP consumption → Luminescence	Ma and Cali, 2007
Uptake assay	Compound accumulation → LSC	Tabas and Dantzig, 2002
Efflux assay	Calcein-AM accumulation → Fluorescence	Holló et al., 1994
Efflux assay	CDCF efflux → Fluorescence	Siissalo et al., 2009
Efflux assay	PhA accumulation → Fluorescence	Henrich et al., 2006
Bidirectional transport assay	Compound transport across cell monolayer → LC or LC-MS/MS	Xiao et al., 2006; Galkin et al., 2008
Bidirectional transport assay	Compound transport across cell monolayer → Absorbance	Alsenz and Haenel, 2003
SLC transporters		
Uptake assay	Radiolabelled substrate → LSC	Vig et al., 2006
Uptake assay	Radiolabelled compound →SPA	Lohmann et al., 2007
Phase I metabolism		
Metabolite screening	Metabolite identification → LC-MS	Shou et al., 2005
Inhibition assay	Drug probes → RapidFire LC-MS/MS	Miller, 2011
Inhibition assay	Profluorescent substrate → Fluorescence	Crespi et al., 1997
Inhibition assay	Vivid® substrate → Fluorescence	Trubetskoy et al., 2005
Inhibition assay	Proluciferin substrate→ Luminescence	Cali et al., 2006
Inhibition assay	Radiolabelled substrate → LSC	Moody et al., 1999
Inhibition assay	Radiolabelled substrate → SPA	Delaporte et al., 2001
Phase II metabolism		
Glucuronidation assay	Radiolabelled UDPGA → LSC	Di Marco et al., 2005
Glucuronidation assay	Antibody-bound tracer/UDP → FP	Kleman-Leyer et al., 2009
Inhibition assay	Proluciferin substrate → Luminescence	Larson et al., 2011
Inhibition assay	Fluorescent substrate	Collier et al., 2000; Trubetskoy et al., 2007
Inhibition assay	β-glucuronidase → Fluorescence	Trubetskoyand Shaw, 1999
Inhibition assay	Proluciferin substrate → Luminescence	Yasgar et al., 2010
Inhibition assay	Halogenated substrate → Absorbance	Skopelitou and Labrou, 2010

Several issues need to be considered when assays are set up on liquid handling workstations (Table 5). The precise and accurate liquid handling is the key issue in assay quality, but on the other hand, the assay throughput should not be too much affected. Contaminations should be carefully detected and minimized by choosing the most appropriate tips and liquid handling settings for each chemical. Whereas, the mixing efficiency is dependent on the correct combination of liquid volume and

method used. When working with transporters and metabolic enzymes, it must be remembered that too vigorous stirring may cause degradation and impair the functionality of the proteins. Evaporation of liquids may become a problem during prolonged incubations, if the plates cannot be sealed. The transport and metabolism studies are normally run at +37ºC, which promotes the evaporation. In addition, the assay volume determines the plate format and the choice of liquid handling device. Today, automated liquid handling devices capable of dispensing liquids at micro-, nano- and picoliter scale are available (reviewed in Hong et al., 2009; Arrabito and Pignataro, 2010). So far, most of the microplate-based transport and metabolism assays are mainly run in microliter scale as they are performed in no higher than 384-format (Table 4). However, nanoliter scale liquid dispensing may be useful in the assays run at 1536-well format.

Table 5. *Issues to be considered when setting up in vitro assays on an automated liquid handling workstation.*

Issue	Factors affecting	Reference(s)
Pipetting accuracy and precision	Liquid handling settings (speed, height, extra volumes) Single dispense vs multidispense Fixed vs disposable tips Liquid properties (e.g. foaming, dripping) Detection method (gravimetric or colorimetric)	Berg et al., 2001; Taylor et al 2002; Frégeau et al 2007; Gu and Deng, 2007; TECAN, 2007
Pipetting throughput	Single vs multidispense Single vs multitip system up to 384 tips	Lorenz, 2004; TECAN, 2007
Contamination	Fixed tips cleaning (carry-over) Disposable tip quality (leachables) Liquid properties (e.g. volatile, dripping)	Astle and Acowitz, 1996; Maddox et al., 2008
Mixing	Liquid volume Method (orbital shaker, magnetic stirrer, ultrasound, organic solvent drop)	Berg et al., 2001; V&P Scientific Inc; Oldenburg et al., 2005 Mitre et al., 2007
Evaporation	Liquid volume Sealed or open plate Incubation time Temperature	Berg et al., 2001

3 Aims of the study

The importance of several drug transporters and metabolizing enzymes on the overall intestinal drug absorption of many drugs is well known. In order to be able to predict the involvement of the transporters and metabolizing enzymes in drug absorption at the different stages of drug discovery, *in vitro* tools of varying complexity and predictivity are needed.

The more specific aims of the thesis work were:

1. To develop a fluorescence-based high throughput screening assay for detecting drug interactions with UGT1A6 (**I**).

2. To utilize the UGT1A6 screen to provide data for developing computational models for predicting the compound interactions with the UGT1A6 (**I, II**).

3. To further evaluate the effects of pH on the interactions of model drugs, diclofenac and indomethacin, with the human UDP-glucuronosyltransferases (**III**).

4. To test the feasibility of three different types of cell-based assays on a robotic workstation, to address the critical liquid handling parameters in each assay, and to evaluate the factors affecting the ease and benefits of the obtained automated assays (**IV**).

4 Experimental

4.1 Compounds

Antipyrine (**IV**), atenolol (**IV**), doxorubicin hydrochloride (**IV**), 5-fluorouracil (**IV**), (±)metoprolol tartrate (**IV**), hydrochlorthiazide (**IV**), nadolol (**IV**), α-propranolol (**IV**), ranitidine hydrochloride (**IV**), fluorescein sodium (**IV**), 1-naphthol (**I, II, III**), 1-naphthylglucuronide (1-NG) (**I, III**), 4-methylumbelliferone (**III**), 4-methylumbelliferone glucuronide (**III**), 5-methylsalicylic acid (**I, II**), 5-bromosalicylic acid (**I, II**), 5-chlorosalicylic acid (**I, II**), 5-fluorosalicylic acid (**I, II**), sodium salicylate (**I, II**), diclofenac sodium (**I, II, III**), indomethacin (**II, III**), naproxen (**II, III**) and scopoletin (**I, II**) were purchased from Sigma-Aldrich Chemie (Steinheim, Germany). Vinblastine sulphate (**IV**) and rhodamine 123 (**IV**) were from Fluka Chemie (Buchs, CH), ketoprofen (**II, IV**) from MP Biochemicals LLC (Aurora, OH) and carbamazepine (**IV**) from Hawkins, Inc. (Minneapolis, MN). Dexibuprofen (**I, II**) was from Sekhsaria Chemicals Limited (Thane, India), ibuprofen (**I, II**) from Francis s.p.a. (Italy) and 4-hydroxyindole (**I, II**) from TCI Europe (Zwijndrecht, Belgium). D-[1-^{14}C]-mannitol (specific activity 59 mCi/mmol) (**IV**) was purchased from Amersham Pharmacia Biotech UK Ltd. (Amersham, England) and [3H(G)]-digoxin (specific activity 21.8 Ci/mmol) (**IV**) from PerkinElmer (Boston, MA).

The Caspase-Glo® 3/7 assay kit (**IV**) was provided by Promega Corporation (Madison, WI). The tetra-His antibodies, from QIAGEN (Hilden, Germany), were used to determine the relative expression levels of the individual recombinant UGTs (Kurkela et al., 2007). All the solvents were HPLC grade.

4.2 Model systems

Recombinant human UGTs (**I, III, IV**), all except UGT2B15, were expressed in baculovirus-infected insect cells, as previously reported (Kurkela et al., 2003; Sneitz et al., 2009). Recombinant UGT2B15 “supersomes”, human liver microsomes and human intestinal microsomes were from BD Biosciences (Franklin Lakes, NJ, USA) (**III**).

The colon carcinoma cell line Caco-2 was originally from the ATCC (Rockville, MD) and the prostate cancer cell line DU-145 was a generous gift from the Medical Biotechnology Department of Technical Research Center of Finland (VTT Turku). They were both cultured for the experiments as reported in original publication **IV**.

4.3 TECAN workstation

The assays (**I, II, IV**) were automated on a TECAN Genesis RSP 150/8 workstation (TECAN Schweiz AG, Männedorf, Switzerland) equipped with a Liquid Handling

Arm and a Robotic Manipulator Arm. Gemini 3.4 (TECAN software GmbH, Hannover, Germany) and FACTS (Flexible Assay Composer and Task Scheduler) 4.81 (TECAN Schweiz AG) softwares were used to generate and operate the pipetting scripts and assay protocols. Pipetting precision was assessed using colorimetric methods as described in original publication **IV**.

4.4 Assay protocols

4.4.1 Automated HTS assay for UGT1A6 (I, II)

The reaction mixture consisted of, if not otherwise specified, 50 mM phosphate buffer (pH 7.4), 10 mM $MgCl_2$, 1-100 µg/ml of protein (insect cell membranes that contained the recombinant UGT1A6) and 2 mM UDPGA, in milli-Q water (resistance 18.2 $M\Omega cm^{-1}$). The aglycone substrate 1-naphthol was used as the probe. Also artifact samples, 2.5 µM of 1-naphthylglucuronide (1-NG) in reaction mixture with and without investigational compound, were run to detect and enable correction of possible compoud interference with 1-NG signal detection. More detailed HTS protocol is presented in Figure 6.

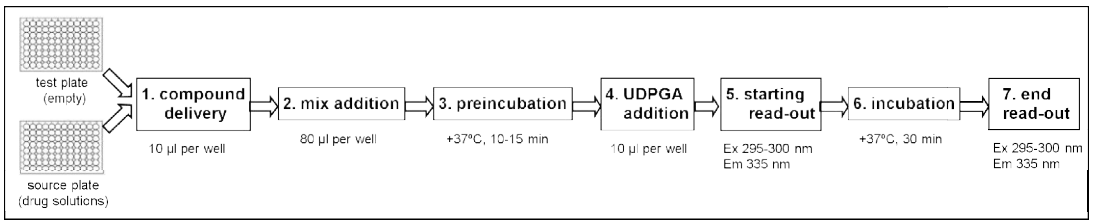

Figure 6. *The UGT1A6 screening assay was initiated by delivering the compounds (step 1) and reaction mixture (step 2) into the test plate, after which the plate was preincubated (step 3). The reactions were initiated by UDPGA addition (step 4). The fluorescence was recorded immediately after the initiation (step 5) and after 30 min incubation (steps 6-7).*

4.4.2 Inhibition of 1-naphthol glucuronidation (I, III)

Glucuronidation reactions were performed similarly to those done in the HTS assay, with the exceptions that the reactions were carried out in 1.5 ml tubes, stopped by adding 10 µl of ice-cold 4 M perchloric acid followed by 10-15 min incubation on ice, and centrifuged to sediment the proteins. The formation of 1-NG was determined from the supernatant aliquots by HPLC with fluorescence detector.

4.4.3 Glucuronidation assays (III)

The reaction mixture, total volume of 100 µl, contained 50 mM phosphate buffer (pH 5.5 - 8.0), 10 mM $MgCl_2$, 2-5 mM UDPGA, UGT-enriched insect membrane, HIM or HLM, and DMSO for the glucuronidation assay. In the case of HIM and HLM, the reaction mixtures also included 10 µg/ml of alamethicin. More detailed information on the assay conditions are presented in the original publication **III**.

The enzyme source, substrates and inhibitors, were pre-incubated at 37°C for 5 min in the reaction mixture in the absence of UDPGA, followed by reaction initiation with the addition of UDPGA. The glucuronidation reactions were carried out at 37°C and the incubation times were 30-60 min depending on the substrate. The reactions were terminated by adding 10 µl of 4 M perchloric acid followed by cooling on ice for 10 min and subsequent centrifugation at 13,000 rpm for 10 min in a bench top centrifuge. The supernatants from the latter centrifugations were analyzed by either by LC-MS, or by LC with UV or fluorescence detection.

The glucuronidation rates were corrected (normalized) according to the enzyme expression level (with the exception of UGT2B15), using UGT1A10 as a reference. The relative expression level determination was based on immunodetection using monoclonal antibodies to the 6 His residues (His-tag) in the C-terminal fusion peptide (Kurkela et al., 2007). The relative expression levels in the specific batches of recombinant UGTs are reported in the original publication **III**.

4.4.4 Automated bidirectional Caco-2 transport assay (IV)

Wells A1-A3, B1-B3, C1-C3 and D1-D3 were used for studying drug transport of four different drugs (n=3 for each) in the A-B direction, while in the wells A4-A6, B4-B6, C4-C6 and D4-D6 the transport was studied in the B-A direction. Two permeability protocols were automated: 1) primary first-stage bidirectional Caco-2 permeability assay for fast permeating compounds and 2) secondary assay for slowly permeating compounds (Fig. 7). In the primary assay the incubations were scheduled as short as possible within the technical limits of TECAN workstation (sampling at 5, 10, 15 and 20 min time points). In the secondary assay samples were taken every 30 minutes until 120 minutes. Samples were analyzed either with HPLC equipped with UV and fluorescence detectors (injected directly from the sample plates) or with fluorescence plate reader. Samples for scintillation counting were prepared manually.

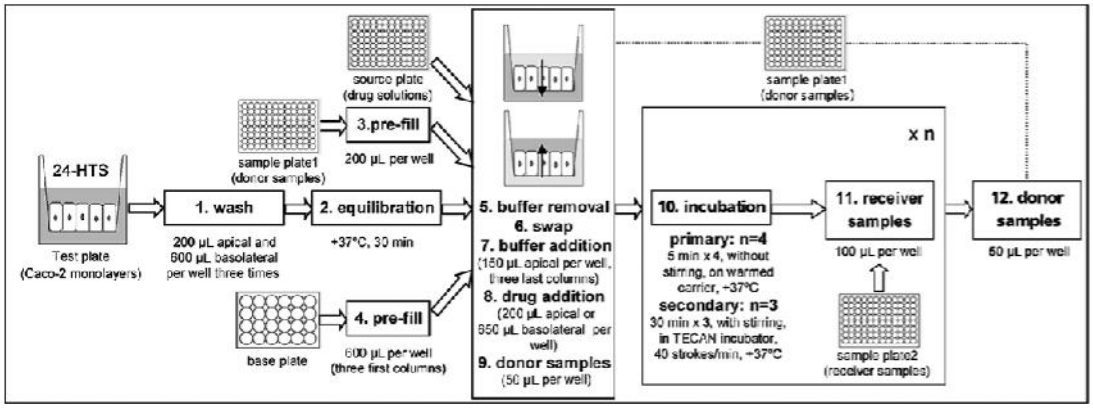

Figure 7. *Assay protocol for the automated bidirectional Caco-2 transport assay. The monolayers grown on test plate were first washed with buffer (step 1). During the equilibration (step 2) a new base plate and a sample plate for donor samples were pre-filled (steps 3-4). The equilibration buffer was then discarded (step 5), the insert part was transferred onto the new base plate (step 6) and the experiments were initiated by adding the receiver volumes and drug solutions (step 7-8). Immediately thereafter, a start sample was withdrawn (step 9). In the primary protocol the test plate was kept on the warmed carrier during the incubations and in the secondary protocol the incubation was carried out in the TECAN incubator (step 10). In the primary experiments number of sampling time points was four and in the secondary experiments it was three (step 11). After the withdrawal of the last receiver sample, end samples were withdrawn from the donor compartments (step 12).*

4.4.5 Cytotoxicity assays (IV)

Heterogeneous SRB assay, used in studying toxicity and anticancer activity, is a protein staining assay detecting the total cellular protein amount (Skehan et al., 1990). The automated SRB assay followed the protocol by NCI. Except pre-seeding of the test plate, the assay was carried out automated using separate processes (Fig. 8). The volumes are stated per well.

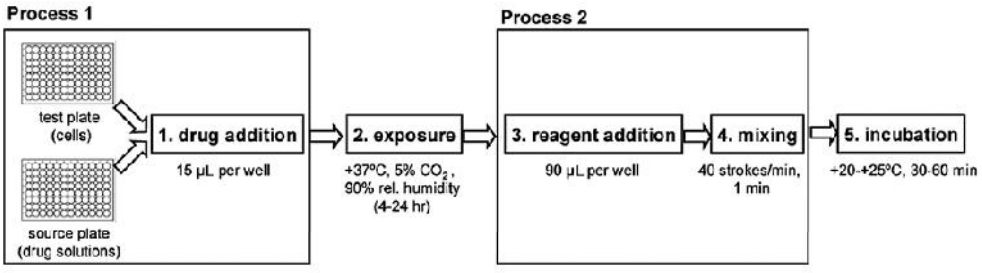

Figure 8. *The Caspase-Glo® 3/7 assay was initiated by adding the compounds into the test plate (step 1). After exposure (step 2) the reagent was added (step 3) and the test plate was mixed (step 4) and incubated (step 5). Finally, luminescence was measured.*

The homogeneous Caspase-Glo® 3/7 assay kit measures the activation of caspase enzymes 3 and 7 in cells undergoing apoptotic cell death (O´Brien et al., 2005). The assay was performed according to the instructions by Promega. Two simple processes were created and the assay was performed in automated mode after seeding the cells into the test plate (Fig. 9). The automated assay process was the following (volumes stated per well):

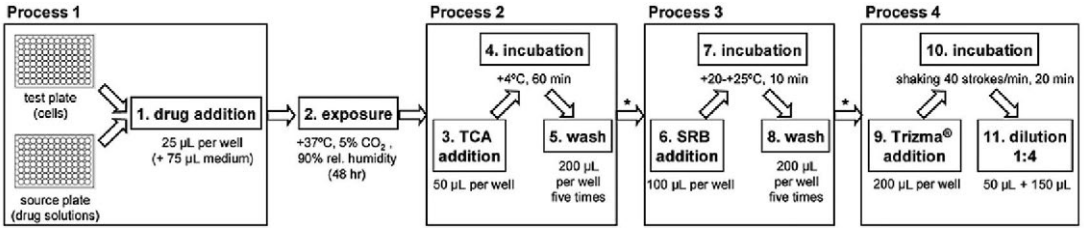

Figure 9. *The sulforhodamine B (SRB) assay was initiated by adding drug solutions into the test plate (step 1). After the exposure (step 2) the cells were fixed with TCA (steps 3-4), and the cell fixate was washed with mQ-water (step 5). Then, it was stained with SRB (steps 6-7) and the protein unbound dye was removed by washing with dilute acetic acid (step 8). Finally, the protein bound dye was dissolved into Trizma® base (steps 9-10) and diluted (step 11) prior to the absorbance measurements.*

4.5 Analytical methods

The multiple glucuronidation products were analyzed by UPLC-MS at Novamass Ltd. (Oulu, Finland). Agilent 1100 series HPLC, Shimadzu HPLC or Water Acquity UPLC with UV or fluorescence detection were used in house to detect samples from the Caco-2 permeability (**IV**) and glucuronidation experiments (**III**).

1-naphthylglucuronide (**I, II**), sulforhodamine B (**IV**), and erythrosine (**I, IV**) were detected with Varioskan plate reader, fluorescein (**IV**) and rhodamine (**IV**) with Wallac Victor® 1420 multilabel counter, and ^{14}C-mannitol (**IV**), ^{3}H-digoxin (**IV**) and Caspase-Glo® 3/7 reagent with Wallac 1450 Mikrobeta/Trilux scintillation counter.

The analytical methods are described in more detail in the original publications (**I, III, IV**).

4.6 Data analysis

4.6.1 Kinetic parameters (I, II, III, IV)

Apparent permeability coefficient, P_{app} (IV) was calculated according to the following equation (Artursson et al., 1996a),

$$P_{app} = \frac{(dQ/dt)}{(A * C_0 * 60)} \quad (1)$$

where *dQ/dt* is cumulative transport rate (nmol/min), *A* the surface area of the insert (0.33 cm^2), and C_0 the initial donor concentration (nmol/ml).

Efflux ratio (IV) was obtained as a ratio of $P_{app\ B\text{-}A}$ and $P_{app\ A\text{-}B}$.

Probe glucuronidation rate (I, II). The fluorescence intensity was measured at least at the 0 and 30 min time points. The readings were collected at two excitation wavelengths, 295 and 300 nm with fixed emission to 335 nm, and the area under the signal (AUS) of the excitation spectra between 295 and 300 nm was calculated. Subsequently, the AUS values were plotted against the fluorescence measurement time, and a linear regression line was fitted through the points. The slope value (AUS/min) was used as an indicator of the reaction rate.

K_m, K_{si} (I, III). The K_m values for substrates were estimated by fitting the experimental data either to the Michaelis-Menten equation

$$v = \frac{V_{max} \bullet [S]}{K_m + [S]}, \quad (2)$$

or the substrate inhibition equation

$$v = \frac{V_{max} \bullet [S]}{K_m + [S] + \frac{[S]^2}{K_i}}, \quad (3)$$

where *v* is the initial velocity of the reaction, *S* the substrate concentration and V_{max} the maximum velocity, K_m the substrate concentration at $0.5V_{max}$ and K_i the dissociation constant for the substrate inhibition interaction.

IC50 (I, III) values for 4-hydroxyindole (**I**), scopoletin (**I**), indomethacin (**III**) and diclofenac (**III**) were estimated by fitting the experimental data to the following equation with GraphPad Prism version 4.03 for Windows;

$$\%\ inhibition = \frac{100}{1 + \left(\frac{IC50}{[I]}\right)^h}, \quad (4)$$

where *[I]* is the concentration of the inhibitor and *h* the Hill coefficient.

Growth inhibition % (GI%) (I) was calculated from the measured absorbance values according to the following equation (Vichai and Kirtikara, 2006)

$$\text{GI\%} = \left(1-\left(\frac{T_i - T_z}{C - T_z}\right)\right)*100 \quad (5)$$

where T_i is the absorbance after drug treatment (t = 48 h), T_z the absorbance indicating the protein amount before drug addition (t = 0 h), and C the absorbance of the control well indicating free cell proliferation without drug treatment (t = 48 h).

4.6.2 Correction for compound interference (I, II)

The assay signal in the UGT1A6 screen was corrected in the cases when interference was observed by the test compound with the fluorescent signal of the 1-NG. Procedure was modified from Shapiro et al 2009, and in case of decrease in signal, calculated as follows:

$$\textit{Corrected AUS} = \left(A2 - T1\right)\times\frac{\left(A1 - A0\right)}{\left(T2 - T1\right)} \quad , \quad (6)$$

where, $A0$ is the AUS of the reaction mixture, $A1$ is the AUS of the reference artifact sample (2.5 µM of 1-NG in reaction mixture), $A2$ is the AUS of the artifact sample (2.5 µM of 1-NG in reaction mixture with test compound), $T1$ is the AUS of test sample without probe (test compound in reaction mixture), and $T2$ is the AUS of the test sample (probe and investigational compound in reaction mixture).

If the reading of the artifact sample was higher or similar compared to the reference artifact sample reading, the reading of test sample without probe was subtracted from the reading of the test sample ($T2 - T1$).

4.6.3 Assay quality (I, II, IV)

Signal to base ratio (S/B) (I, IV) was calculated as the ratio of the signals from the means of maximum and minimum signals (n=3) (Zhang et al., 1999a).

Z´ factor (I, I) was calculated according to the equation (7) (Zhang et al., 1999a). The values of 0.5 – 1 (or 0.4 – 1 for cell based assays) indicate excellent assay.

$$\text{Z}' = 1-\frac{(3\sigma_{\max} + 3\sigma_{\min})}{\left|\mu_{\max} - \mu_{\min}\right|} \quad (7)$$

signal to noise ratio (S/N) (II) according to the formula (8) (Zhang et al., 1999a),

$$\text{S/N} = \frac{\mu_{\max} - \mu_{\min}}{\sigma_{\min}} \quad , \quad (8)$$

and ***Coefficient of variation for the assay (CV_A)*** with the equation (9) (Iversen et al., 2006),

$$CV_A = \frac{\sigma_{max}}{\mu_{max} - \mu_{min}} \quad , \tag{9}$$

where in all σ_{max} and σ_{min} are the standard deviations of maximum and minimum signals and μ_{max} and μ_{min} the means of maximum and minimum signals, respectively.

4.6.4 QSAR analysis (II)

The conformations for each of the 46 compounds were defined with Sybyl-X software (Tribos, USA). A single conformation for compounds having rotable bonds was randomly picked, and all the structures with assigned Gasteiger-Huckel charges were first energy minimized using the standard Tripos force field (Powell method and 0.05 kcal/(mol.Å) energy gradient convergence criteria).

Support vector machine (SVM) models

The 46 compounds were classified as strongly interacting (0-40% of the probe glucuronidation rate in the presence of the compounds compared to that in the absence of compounds), moderately interacting (40-70%), and non-interacting molecules (70-100%). For each of the compounds, 856 molecular descriptors were calculated, of which 712 were further used in the model development.

The SVM model was developed with a training set of 31 compounds using LIBSVM software (Chang and Lin, 2011). The rest 15 compounds were used as an external test set. Relative importance of each of the descriptors in classification was evaluated by F-score. In practise, the model was developed by adding features of the highest F-scores one after another until the validation accuracy decreased. The model giving the best accuracy (Eq. 10), sensitivity (Eq. 11), specificity (Eq. 12) and Matthews correlation coefficient (MCC) (Eq. 13) was chosen after 10-fold cross-validation.

Accuracy, sensitivity, specificity and MCC were determined according to the following equations:

$$accuracy(\%) = \frac{TP + TN}{TP + FP + TN + FN} \quad , \tag{10}$$

$$sensitivity(\%) = \frac{TP}{TP + FN} \quad , \tag{11}$$

$$specificity(\%) = \frac{TN}{TN + FP} \quad , \tag{12}$$

$$MCC = \frac{TP \times TN - FP \times FN}{\sqrt{(TP + FP) \times (TP + FN) \times (TN + FP) \times (TN + FN)}} , \tag{13}$$

in which, TP is the number of true positives, TN is the number of true negatives, FP is the number of false positives and FN is the number of false negatives.

3D-QSAR (CoMFA/CoMSIA) models

Compounds were first clustered based on their chemical structures with a hierarchial clustering program in Sybyl-X software. The largest of the three clusters, which contained in total 35 compounds and covered the whole data range, was chosen for 3D-QSAR modelling. Compounds were further divided into a training set (26 compounds) and a test set (9 compounds).

First, alignment of the training compounds were tried with several ligand-based approaches. CoMFA and COMSIA molecular fields were then calculated for the aligned compound set using the QSAR module of Sybyl-X software.

CoMFA and CoMSIA models were developed using a conventional stepwise procedure. The leave-one-out cross validation (LOOCV) was performed to determine optimum number of components leading to the highest cross-validation coefficient q^2 (Eq. 14) and the lowest standard error of prediction (SEP).

$$q^2 = 1 - \frac{\sum_y (Y_{predict} - Y_{experimental})^2}{\sum_y (Y_{experimental} - Y_{mean})^2}, \quad (14)$$

where, $Y_{predict}$ is a predicted pGlu, $Y_{experimental}$ is an experimental pGlu, Y_{mean} is the best estimate of the mean of all values that can be predicted.

After that, non-cross-validation analysis was performed to derive the final PLS regression models with the explained variance r^2, standard error of estimate (SEE) and F-ratio. The CoMFA and CoMSIA fields were graphically represented in contour maps, where the coefficients were generated using the field type ‘‘Stdev*Coeff’’. Locations of favored and disfavored fields were presented at 80% and 20% levels, respectively.

In order to test the real predictive ability of the trained CoMFA and CoMSIA models, the pGlu values of the external validation set (9 compounds) were predicted using the same CoMFA and CoMSIA calculation parameters as those used to generate the models. The non-cross validated analyses were used to make predictions of the probe glucuronidation rate (pGlu) of compounds from the test set and to display the coefficient contour maps. The actual versus predicted probe glucuronidation rate (pGlu) of the test compounds were fitted by linear regression, and the r^2_{pred} (Eq. 15), SEE, and F ratio were determined.

$$r^2_{pred} = 1 - \frac{\sum_y (Y_{predict(test)} - Y_{(test)})^2}{\sum_y (Y_{(test)} - Y_{mean})^2} \quad (15)$$

In Equation (15), $Y_{predict(test)}$ and $Y_{(test)}$ indicate predicted and experimental probe glucuronidation rates (pGlu) of the test set compounds, respectively, and Y_{mean} indicates the mean probe glucuronidation rate (pGlu) of the training set.

.

5 Results and discussion

5.1 HTS assay for UGT1A6 (I, II)

5.1.1 Detection of probe reaction (I)

The core of the assay is a probe reaction, in which 1-naphthol is glucuronidated by recombinant UGT1A6 into a highly fluorescent metabolite, 1-NG (Fig. 10). The formation of 1-NG is followed with a plate reader by detecting the excitation spectra (295-300 nm) at fixed emission wavelength (335 nm). This analytical approach allowed the separation of the 1-NG signal from the signal produced by the components of the reaction mixture. In the assay system, reaction mixture contained insoluble material, such as biological membranes and traces of other cell components, which are prone to interfere with the signal detection. The stability of the detected signal was further increased by using of the area under the excitation signal (AUS), instead of a single wavelength measurement.

This probe-based assay is the first of a kind for detecting compound interactions with any of the UGT isoforms. The possibility to follow the probe reaction at the product site, intead of detecting only the disappearance of the probe substrate (Collier et al., 2000; Broudy et al., 2001; Trubetskoy et al., 2007), helps to avoid several possible artefacts. In addition, the possibility to detect the 1-NG formation without secondary reactions or purification steps, unlikely in few of the previously reported assays (Trubetskoy and Shaw, 1999; Di Marco et al., 2005; Kleman-Leyer et al., 2009; Larson et al., 2010), reflects also to the costs of the assay.

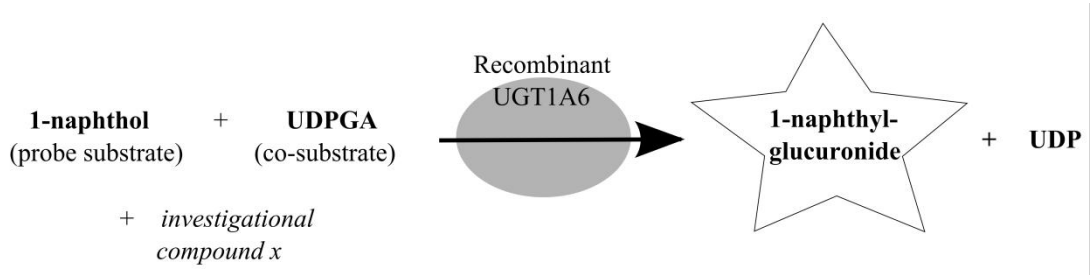

Figure 10. *Basic principle of the UGT1A6 screening assay. The assay is based on detecting the increase in fluorescence when the probe 1-napthol is glucuronidated into highly more fluorescent 1-naphthylglucuronide (1-NG). The interaction of the test compound with the enzyme is detected as decreased rate of 1-NG formation. Copyright © (2011) Mary Ann Liebert, Inc. Reprinted with the permission.*

5.1.2 Optimal conditions for the probe reaction (I)

The reaction conditions for the conversion of 1-naphthol into 1-NG, were optimized to yield high enough signal separation. A probe concentration of 5µM (K_m 7.7 ± 0.7 µM for 1-naphthol) and reaction time of 30 min with 2.5 µg of total protein per well, without stirring, gave the best linearity and signal separation with r^2 of 0.998 and S/B of 3.9, respectively. The optimal pH for the conversion was found to be around pH 7.5 (Fig. 11a) and, the highest glucuronidation rate was reached in phosphate buffer (Fig. 11b). As expected, increase in the DMSO concentration from 1% to 10% decreased the probe glucuronidation rate (Fig. 11c). Nevertheless, the signal separation was still acceptable with S/B 3.0 at 5% DMSO.

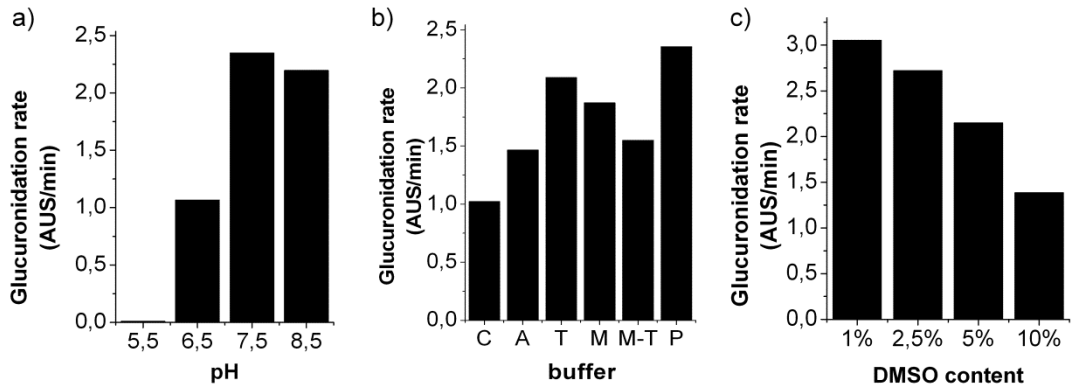

Figure 11. *Effects of a) pH, b) buffer, and c) DMSO concentration on the probe reaction rate (n=2, CV% ≤ 5). The buffers tested were C; citrate (pH 6.0), A; acetate (pH 6.0), T; Tricine (pH 7.5), M; MOPS (pH 7.5), M-T; MOPS-Tricine (pH 7.0) and P; phosphate (pH 7.4). The phosphate buffer at pH 7.4 with 5% of DMSO was selected for the screen. Copyright © (2011) Mary Ann Liebert, Inc. Reprinted with the permission.*

5.1.3 Inhibition assay (I)

The HTS assay is based on the assumption that the interaction of the test compound with the recombinant human UGT1A6 affects the rate at which the fluorescent 1-NG is formed. In the case of inhibitors, that is detected as a lower rate of fluorescence increase in comparison to the reaction with only the enzyme and the probe.

First, the effect of scopoletin and 4-hydroxyindole, two good substrates of UGT1A6 (Luukkanen et al., 2005; Manevski et al., 2010), on the fluorescent signal were determined to obtain preliminary information on the signal range of the assay at different compound concentrations. The inhibition patterns obtained with the HTS assay and a reference HPLC method with fluorescence detector were similar showing IC50 values of 108±7 and 148±6 µM for 4-hydroxyindole, and 969±58 and 869±63 µM for scopoletin, respectively. The good correlation of the results obtained

with both the methods also in detecting interactions with sets of NSAIDs and salicylic acid derivatives further convinced the functionality of the assay (Fig. 12).

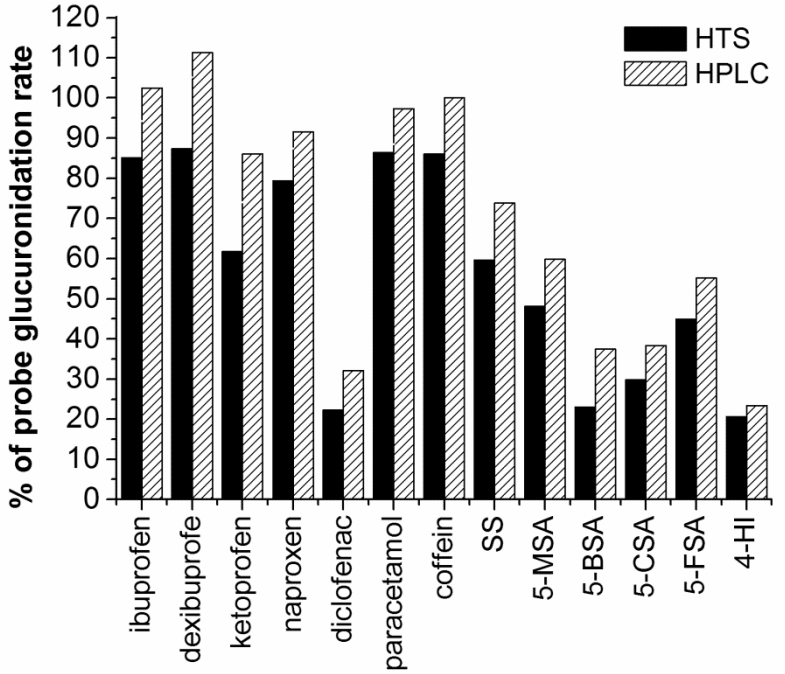

Figure 12. *Results obtained with the HTS assay and the reference HPLC method for the non-steroidal anti-inflammatory drugs and salicylate derivatives (SS, sodium salicylate; 5-BSA, 5-bromosalicylic acid; 5-CSA, 5-chlorosalicylic acid; 5-FSA, 5-fluorosalicylic acid) at 500 µM. Copyright © (2011) Mary Ann Liebert, Inc. Reprinted with the permission.*

The plate uniformity and signal variation tests with 4-hydroxyindole demonstrated robust probe glucuronidation behaviour throughout the plate and acceptable separation of the minimum and maximum signals. For all the three plates also the quality parameters, including Z´ factor values of 0.5 or higher, indicated an excellent HTS assay (Table 6).

Table 6. *Assay quality parameters for the UGT1A6 assay. The parameters were calculated from the raw data AUS values after 30 min incubation and the obtained slope values (AUS/min). Copyright © (2011) Mary Ann Liebert, Inc. Reprinted with the permission.*

	Plate 1		*Plate 2*		*Plate 3*	
	Raw data	***Slope***	***Raw data***	***Slope***	***Raw data***	***Slope***
Z´ factor	0.7	0.7	0.5	0.6	0.8	0.8
S/B	2.0	17	1.9	47	1.9	22
S/N	60	51	19	31	48	47
CV_A	7.9	7.3	11	8.5	6.2	5.3
CV_{mid}	n.c.	7.7	n.c.	6.5	n.c.	5.1

Based on the data and earlier findings on generally low affinities of substrates and inhibitors towards the UGTs (reviewed in Kiang et al., 2005), it was obvious that fairly high compound concentrations, in the range of 100-500 µM, would be needed to be used in the screening. Adding to this, also the fact that the excitation wavelengths of 1-NG are low (295-300 nm), interference with a large portion of the test compounds was inevitable. However, this drawback of the assay was successfully overcome by applying an arithmetic correction procedure (Shapiro et al., 2009).

5.1.4 Screening a set of compounds (I, II)

The developed HTS assay was succesfully used for the screening of 46 compounds, including 14 benzoic acid, 4 naphthalene, 11 phenol, 5 carboxylic acid, 3 indole, 2 flavonoid and 6 coumarin derivatives and coffein, towards the 1-naphthol glucuronidation at the compound concentration of 500 µM. The observed interactions with the probe glucuronidation covered the full range of the assay signal, from almost fully inhibited reaction to no interaction (Fig. 13). As the assay detects only the effect of a compound on probe glucuronidation, compounds decreasing the glucuronidation rate may be substrates for the UGT1A6, and thus, compete with the probe glucuronidation. Alternatively, they may only interfere with the enzyme catalysis of the probe substrate, without being glucuronidated by the UGT1A6.

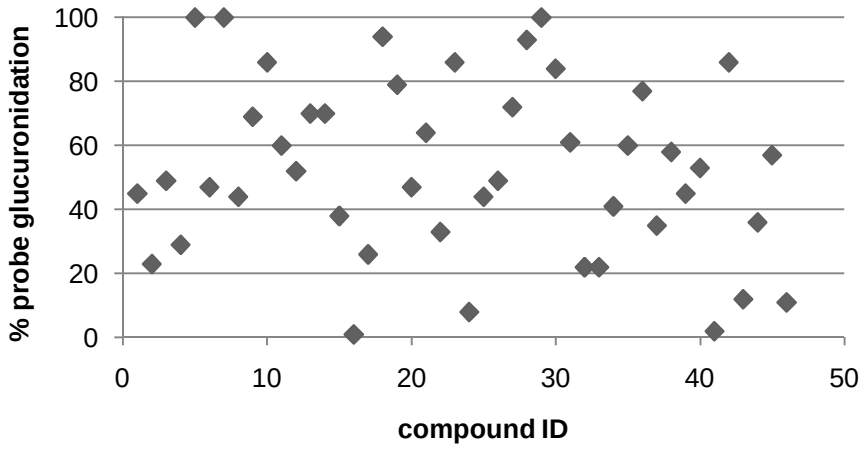

Figure 13. *Range of the data obtained in screening 46 compounds. The compound names related to the ID numbers can be found from the original manuscript (**II**).*

The newly developed and optimized UGT screening assay was demonstrated to be effective in finding potential inhibitors and/or substrates of the UGT1A6. Although the current assay was developed and optimized using only UGT1A6 as the enzyme, this assay could probably be adapted to several other UGTs, since many of them glucuronidate 1-naphthol (Kurkela et al., 2003; Uchaipichat et al., 2004).

5.2 Classification and 3D-QSAR models for UGT1A6 (II)

5.2.1 SVM model

SVM model for the classification of compounds into three classes based on their effect on 1-naphthol glucuronidation by human UGT1A6 was developed. The derived model was based on ten molecular descriptors characterizing atomic mass, nature of carbon in the molecules, molecular distance edge, hybridization state, polarization, polarizability, electrotopologigal state, size, logP, electronegativity and dipole moment. The prediction performance of the model is presented in Table 7. The specificities higher than sensitivities for both the training and test set compounds indicated that the model is able to find more reliably the compounds that do not belong to a certain class than the compounds that would belong to a certain class. These are in line with the earlier findings, both in terms of prediction performance and important descriptors for the molecular recognition and catalysis by the UGT enzymes (Ethell et al., 2002; Smith et al., 2003; Dong and Wu, 2012).

Table 7. *Prediction performance of the SVM model.*

	Accuracy (%)	*Specificity (%)*	*Sensitivity (%)*	*MCC*
Training set	77	91	83	0.75
External test set	67	83	66	0.55

5.2.2 3D-QSAR models

Of the several methods tested for aligning the training dataset, the preliminary CoMFA model developed, based on Surflex-Sim Flexible alignment (Fig. 14), gave the best predictive performance (r^2_{cv} 0.62 and r^2_{ncv} 0.95). It was, therefore, chosen as the basis for further CoMFA and CoMSIA model development.

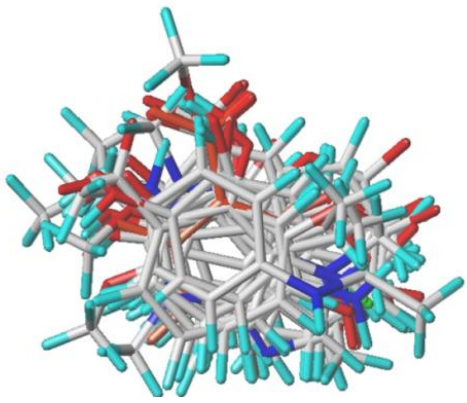

Figure 14. *Surflex-Sim Flexible alignment of the training set in the grid box (2Å).*

The CoMSIA analysis capable of taking into account steric, electric, hydrophobic and hydrogen bonding donor and acceptor fields provided more statictically reliable model than the CoMFA (Table 8). For this data set (compounds detailed in the manuscript **II**), the contributions of hydrogen bond donor fields were the most important (0.36), but also electric, hydrophobic and hydrogen bond acceptor fields had significant contributions.

Table 8. *Prediction performance parameters of CoMFA and CoMSIA models based on Surflex-Sim Flexible alignment.*

	Parameter						***Contributors***				
	q^2	r^2	*NC*	*SEP*	*F-value*	r^2_{pred}	*S*	*E*	*H*	*D*	*A*
CoMFA	0.62	0.94	5	7.5	84	0.68	0.39	0.61	-	-	-
CoMSIA	0.76	0.89	4	0.11	107	0.74	0.03	0.20	0.22	0.36	0.17

r^2 is the q^2 without the leave-one-out cross-validation; NC, number of components from PLS analysis; S, contribution of steric fields; E, contribution of electric fields, H, contribution of hydrophobic fields; D, contribution of hydrogen bond donor fields; and A, contribution of hydrogen bond acceptor fields

Also the scatter plots presenting the correlation of predicted and experimental probe glucuronidation rates revealed the better performance of the CoMSIA model (Fig. 15). The CoMSIA model was able to predict the external test of 9 compounds with the r^2_{pred} of 0.74 and CoMFA with the r^2_{pred} of 0.68.

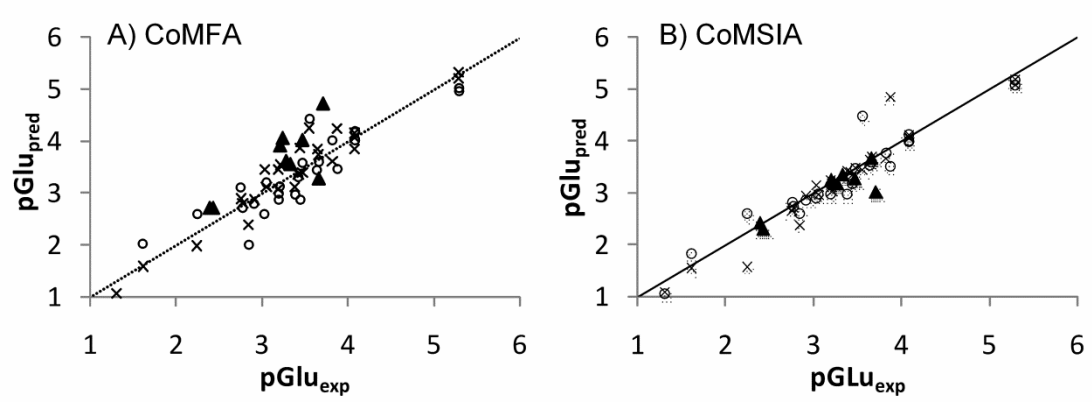

Figure 15. *Scatter plots of the experimental probe glucuronidation rate values ($pGlu_{exp}$) versus predicted probe glucuronidation rate values ($pGlu_{pred}$) for the CoMFA (A) and CoMSIA (B) models. Open circles (○) represent the predictions of training set compounds after leave-one-out crossvalidation, crosses (x) represent the predictions of training set compounds without crossvalidation, and filled triangels (▲) represent the predictions of test set compounds.*

The CoMFA contour plots are able to define the regions where bulky or charged functional groups would either be favourable or unfavourable for the interaction with the UGT1A6 (Fig. 16a). In addition to CoMFA fields, hydrophobic, hydrogen bond donor and acceptor fieds are presented as contour plots (Fig. 16b-d). The steric and electrostatic fieds obtained with CoMSIA analysis were similar to those obtained in CoMFA analysis. The CoMSIA fields further highlight the importance of hydrophobic and hydrogen bonding groups for compound interactions with UGT1A6.

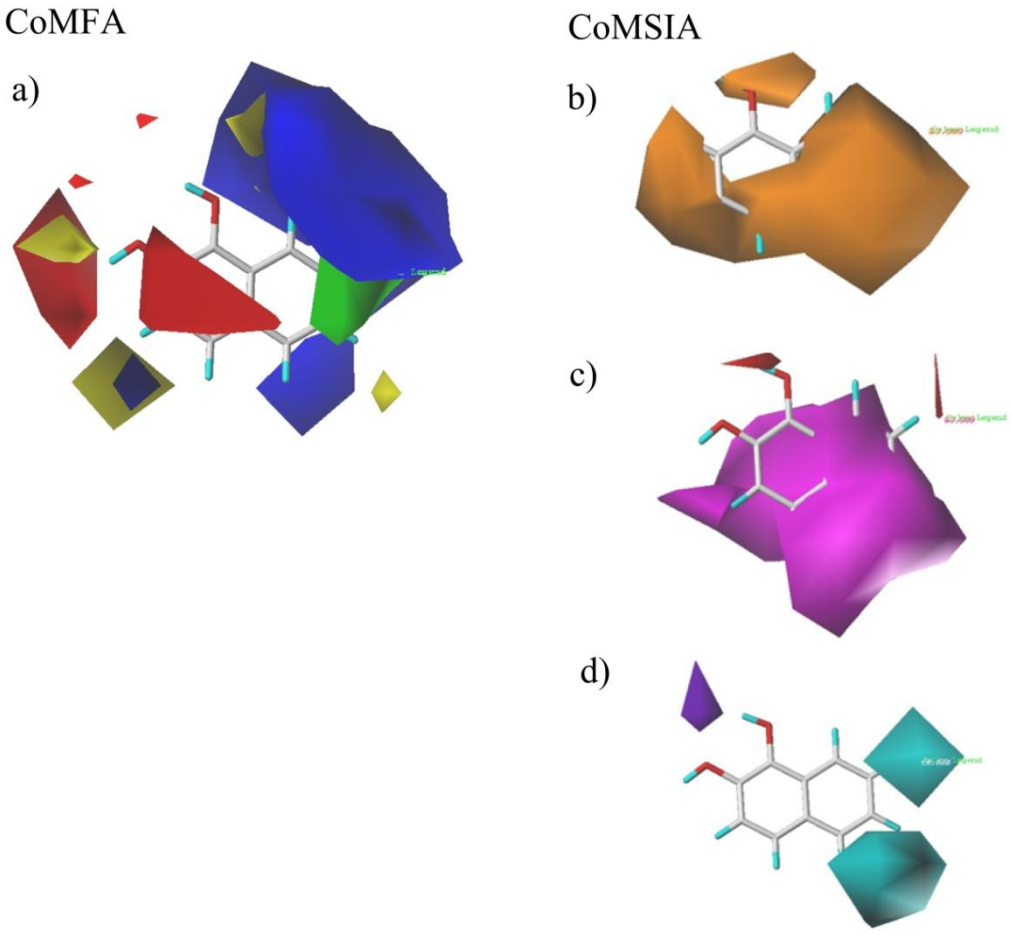

Figure 16. *Contour maps of CoMFA and CoMSIA fields using the compound 16, naphthalene-1,2-diol, as a representative structure. a) In CoMFA, green contour indicates regions where bulky groups, blue contours indicate the regions where an increase in positive charge, and red contours indicate regions where increase in negative charge are favourable for the compound interaction with the UGT1A6. Whereas, yellow contours indicates the area where large substituents are unfavorable for the interaction. In CoMSIA, b) orange contours indicate regions where hydrophobic groups are favorable for the interaction, c) magenta represents areas where HB acceptors are favorable and red areas where they are unfavourable for the interaction, and d) cyan represents areas where HB donors are favorable and purple the areas where they are unfavorable for the interaction.*

5.3 Effect of pH on compound interactions with human UGTs (III)

5.3.1 Indomethacin and diclofenac glucuronidation in HLM and HIM

More than one glucuronide products for diclofenac and indomethacin, NSAIDs bearing a carboxylic acid group in their structure, were found in LC-MS chromatograms after incubations in HLM at pH 7.4. In the case of indomethacin, the glucuronide peaks were two, whereas in case of diclofenac two main glucuronides, and traces of a third one, were detected. The decrease in pH from 7.4 to 6.0 resulted in a decrease in the relative sizes or disappearance of the minor peaks. These findings suggested that the main peaks represented the respective acyl-glucuronides, metabolites resulting from the conjugation of the carboxylic acid with glucuronide acid. The acyl-glucuronides of both drugs are known to be unstable at physiological conditions and undergo acyl-glucuronidation (Spahn-Langguth and Benet, 1992).

In the further experiments with human microsomes, the results analyzed in UPLC with UV detection revealed that lowering the reaction pH from 7.4 to 6.0 led to a 2-fold increase in the rate of indomethacin glucuronidation by both the HIM and HLM (Table 9). In the case of diclofenac glucuronidation, on the other hand, the results with HLM were similar at both pH values, while the rate of the HIM-catalyzed reaction was clearly higher at pH 6.0 than at pH 7.4.

Table 9. *Glucuronidation rates (pmol/min/mg) of diclofenac and indomethacin by HIM and HLM. Copyright © (2012) Elsevier. Reprinted with the permission.*

	Diclofenac		*Indomethacin*	
	pH 6.0	*pH 7.4*	*pH 6.0*	*pH 7.4*
HIM	196 ± 2	168 ± 3	65.5 ± 1.6	32.9 ± 1.8
HLM	1041 ± 6	1051 ± 2	220 ± 9	116 ± 6

5.3.2 Effect of pH on glucuronidation of model compounds

Glucuronidation of indomethacin and diclofenac by 19 human UGTs were screened at substrate concentration of 100 µM at pH 6.0 and 7.4. The results, corrected for the relative expression level of each UGT (except for UGT2B15), are presented in Figure 17. Diclofenac was mainly glucuronidated by UGT isoforms 1A10, 2B7 and 2B17. pH affected most the glucuronidation of diclofenac by UGT1A10 and UGT2B17. Whereas, the main isoenzymes catalyzing indomethacin glucuronidation were 1A10, 2B7 and 2A1, which were all affected by the pH change. Overall, the results revealed that the effect of reaction pH on the rate of indomethacin and/or diclofenac glucuronidation varied among the individual UGTs. For example, the glucuronidation of both indomethacin and diclofenac by UGT1A10 was highly

stimulated by lowering the reaction pH from 7.4 to 6.0, whereas in the case of UGT2A1, only the indomethacin glucuronidation rate was strongly stimulated by lowering the reaction pH from 7.4 to 6.0.

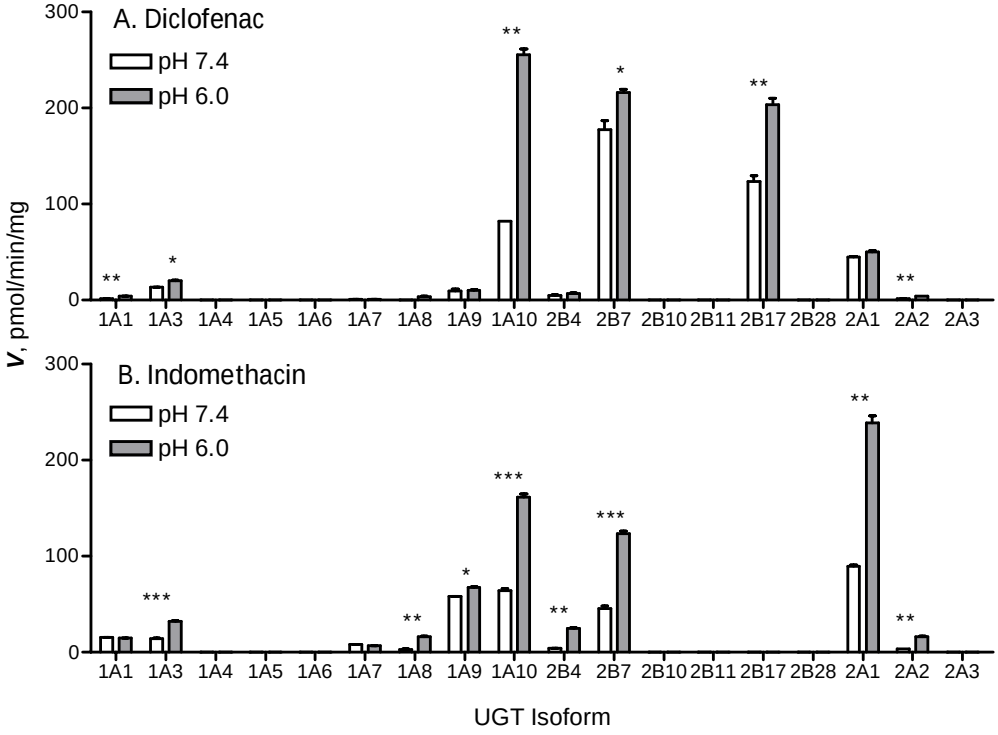

Figure 17. *Diclofenac and indomethacin glucuronidation rates (normalized) of individual human UGTs at pH 7.4 (white) and 6.0 (gray). The significance of the change between the two pH values for each of the UGT is marked as: *p=0.05, **p=0.005, ***p=0.001. Copyright © (2012) Elsevier. Reprinted with the permission.*

The effect of pH on the glucuronidation rates of diclofenac and 4-MU by UGT1A10 and UGT2B15, and that of indomethacin by UGT1A10 only, were further examined in the pH range of 5.5-8.0 (Fig. 18). Neither enzyme exhibited detectable diclofenac glucuronidation at pH 5.5, but the differences between the two enzymes at pH 6.0 were large. The optimal pH value for UGT1A10 in both diclofenac and indomethacin glucuronidation is 6.0, while UGT2B15 is practically inactive at this pH value. The lowest pH at which the UGT2B15 catalyzed diclofenac glucuronidation was 6.5, and the optimal reaction pH for this enzyme was 7.0. In addition, the effect of pH on the glucuronidation of 4-MU, a non-ionized compound, by the UGT1A10 and UGT2B15 was examined. The results indicated that while the

pH “profile” of UGT2B15 in diclofenac and 4-MU glucuronidation reactions were very similar, UGT1A10 glucuronidates 4-MU more efficiently at higher pH values contrary to the highest glucuronidation rates of diclofenac and indomethacin at pH 6.0.

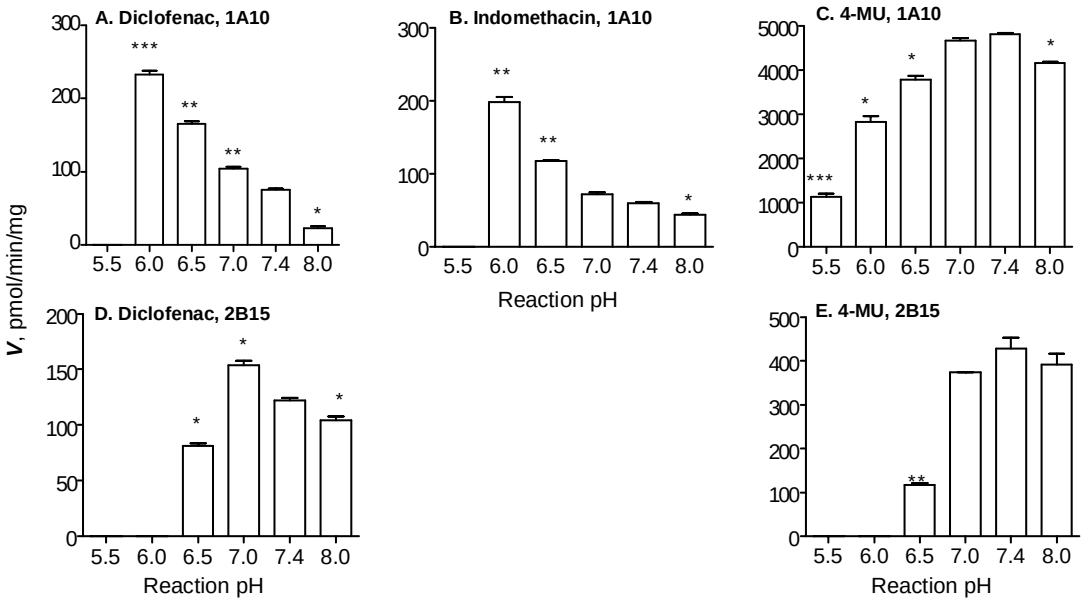

Figure 18. *Effect of pH on UGT1A10-mediated glucuronidation of diclofenac, indomethacin and 4-methylumbelliferone (4-MU), and on UGT2B15-mediated glucuronidation of diclofenac and 4-MU. Copyright © (2012) Elsevier. Reprinted with the permission.*

Kinetic analyses of the diclofenac glucuronidation by the UGT1A10 and UGT2B7 were undertaken in order to get more detailed information on how the lower reaction pH stimulated the glucuronidation activity. It was found out that lowering the reaction pH resulted in a lower K_m value for the substrate, and a higher V_{max} value with both the isoforms (Table 10). However, the difference in V_{max} values was much more pronounced in UGT1A10. Also the increased affinity of diclofenac towards the UGT1A10 led to an observed substrate inhibition. The large differences between the pH effects on the UGT1A10 and UGT2B7 strongly suggest that changes in the enzyme, probably protonation of a yet-unidentified amino acid side chains, played a major role in the pH effect of the reaction rate.

Table 10. *Kinetic constants for diclofenac glucuronidation by UGT1A10 and UGT2B7, as well as for 1-naphthol glucuronidation by UGT1A6 at pH 6.0 and 7.4. K_{si} is the substrate inhibition constant. Copyright © (2012) Elsevier. Reprinted with the permission.*

	Diclofenac		*1-naphthol*
Kinetic constants	*UGT1A10*	*UGT2B7*	*UGT1A6*
pH 6.0			
K_m (µM)	94 ± 9	25 ± 1	6.8 ± 1
K_{si} (µM)	672 ± 96		
V_{max} (pmol/min/mg)	458 ± 25	342 ± 3	3318 ± 101
pH 7.4			
K_m (µM)	153 ± 15	55 ± 3	5.1 ± 0.3
K_{si} (µM)			1639 ± 215
V_{max} (pmol/min/mg)	196 ± 8	316 ± 4	5860 ± 102

5.3.3 Effect of pH on inhibition potential

Effect of pH on the inhibition potential of diclofenac and indomethacin towards 1-naphthol glucuronidation by UGT1A6 was studied to find out if the reaction pH affects the binding of the compounds to UGT1A6, an isoform that does not glucuronidate neither of the compounds (Fig. 17). UGT1A6 was previously reported to be sensitive to inhibition by diclofenac when the assay was carried out at pH 7.4 (Uchaipichat et al., 2004; original publication **I**).

First, the effect of pH was assayed on the 1-naphthol glucuronidation activity of UGT1A6 at pH 6.0 and 7.4. The results showed that lowering the reaction pH from 7.4 to 6.0 strongly reduced the V_{max} of UGT1A6 in 1-naphthol glucuronidation, and practically eliminated the substrate inhibition that was clear at pH 7.4 (Table 10). The pH effect on the K_m value of UGT1A6 for 1-naphthol was mild, however. Due to this, the subsequent inhibition analyses were carried out in the presence of the same substrate concentration, 5 µM. The inhibition profiles showed that both the drugs inhibited the 1-naphthol glucuronidation activity of UGT1A6 more effectively at pH 6.0 (Fig. 19). This is in line with the higher affinity of UGT1A10 for diclofenac at pH 6.0 than at pH 7.4 (Table 10). In addition, diclofenac was significantly more effective as a UGT1A6 inhibitor than indomethacin at the two pH values. The derived IC_{50} values for diclofenac were 37 and 85 µM at pH 6.0 and 7.4, whereas they were 290 and 440 µM for indomethacin, respectively.

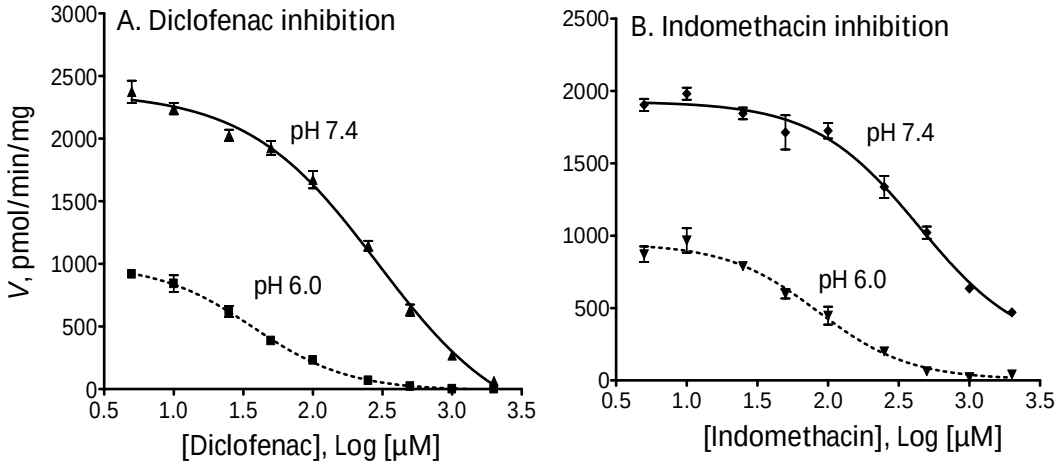

Figure 19. *Effect of pH on the inhibition of 1-naphthol by diclofenac (A) and indomethacin (B). The 1-naphthol concentration was 5 µM. Copyright © (2012) Elsevier. Reprinted with the permission.*

5.4 Automation feasibility (IV)

5.4.1 Implementation of assays on a robotic workstation

Quality of the liquid handling highly affects the quality of the results. In the three cellular assays, Caspase-Glo 3/7, sulforhodamine B and bidirectional Caco-2 transport assay, the liquid handling parameters were adjusted to acquire acceptable precision without interfering with the assay system. The critical steps and optimized parameters are listed in Table 11. In the assays studied, tolerance to the mechanical stress caused by the pipetting varied. The adherent Caco-2 and DU-145 cells and the differentiated Caco-2 monolayers required lowered dispensing speeds. In the SRB assay, the addition step of TCA had to be done extremely slowly. Too high a dispense speed could have caused the fluid shearing forces to interfere with the fixation of cell proteins (Skehan et al., 1990). Removal of the supernatant after the fixation was also critical. Differentiated Caco-2 monolayers endure normal aspiration speeds as long as the tips do not touch the cell monolayer. Thus, the tips were configured to move as close to the cell monolayer as possible to minimize dead volume in the apical chamber. Even in the optimized protocol a dilution of 16.2 ± 1.7% was observed in drug solutions added into the apical chamber.

Table 11. *Liquid handling parameters and settings for the automated assays. Copyright © (2010) SAGE Publications. Reprinted with the permission.*

	Step	*Problem*	*Critical parameter*	*Solution*
Caspase Glo® 3/7				
Process 1	1. Drug addition	cell detechment	DS	DS 200 µl/s
		contamination	TC	decontamination step
Process 2	3. Reagent addition	foaming/stickiness	DS	DS 200 µl/s
SRB				
Process 1	1. Drug addition	cell detachment	DS	200 µl/s
		contamination	TC	decontamination step
Process 2	3. TCA addition	improper fixation	DS	DS 200 µl/s
		precipitation in tubing	TC	cleaning step
	5. Wash	protein detachment,	AS	AS 10 µl/s
		background signal ↑	TH	TH z-max-0.5xmm*
Process 3	8. Wash	background signal ↑	TH	TH z-max-0.5xmm*
Caco-2 permeability				
Process 1	1. Wash	monolayer integrity ↓,	DS	DS 200 µl/s
			TH	TH z-max-0.5xmm*
	5. Buffer removal	monolayer integrity ↓,	DS	DS 200 µl/s
		dead volume		TH z-max-0.5xmm*
	7. Buffer addition	monolayer integrity ↓	DS	DS 200 µl/s
	8. Drug addition	monolayer integrity ↓	DS	DS 200 µl/s
	9./12. Donor samples	monolayer integrity ↓	TH	TH z-max-0.5xmm
	11. Receiver samples	monolayer integrity ↓	TH	TH z-max-0.5xmm

DS, dispense speed; TC, tip/tubing cleaning; AS, aspiration speed; TH, tip height

Since only fixed tips were used in the Caspase-Glo® 3/7 and SRB assays, a decontamination step, wash of tips with DMSO, was needed to prevent carry-over. In addition, a cleaning step with pure DMEM or RPMI 1640 medium was needed to remove the serum remnants from the pipette tubing, and to avoid foggy-like precipitation to appear randomly in the wells.

5.4.2 Optimization of assays

Caspase-Glo® 3/7 assay

Optimization and standardization of the automated apoptosis assay were performed on Caco-2 and DU-145 cells. With Caco-2 cells 25 000 cells per well (Fig. 20a), exposure time of 12 hours (Fig. 20b) and reagent incubation time of 30 minutes (Fig. 20c) gave the optimimal apoptosis signal. With vinblastine a Z´ factor of 0.7 with an S/B value of 1.7 indicated succesfull assay. Based on the dose-responce curves, concentrations 0.1 (min) and 50 µM (max) were suggested to be used in screening. With DU-145 cells a single exposure time could not be chosen, since the activity of vinblastine was the highest after 8 and 12 hours of exposure, and decreased markedly during prolonged incubation, while the activity of doxorubicin was only detectable after 24 hours of exposure (Fig. 20e). Therefore, a robust screen could not be set up with DU-145 cells.

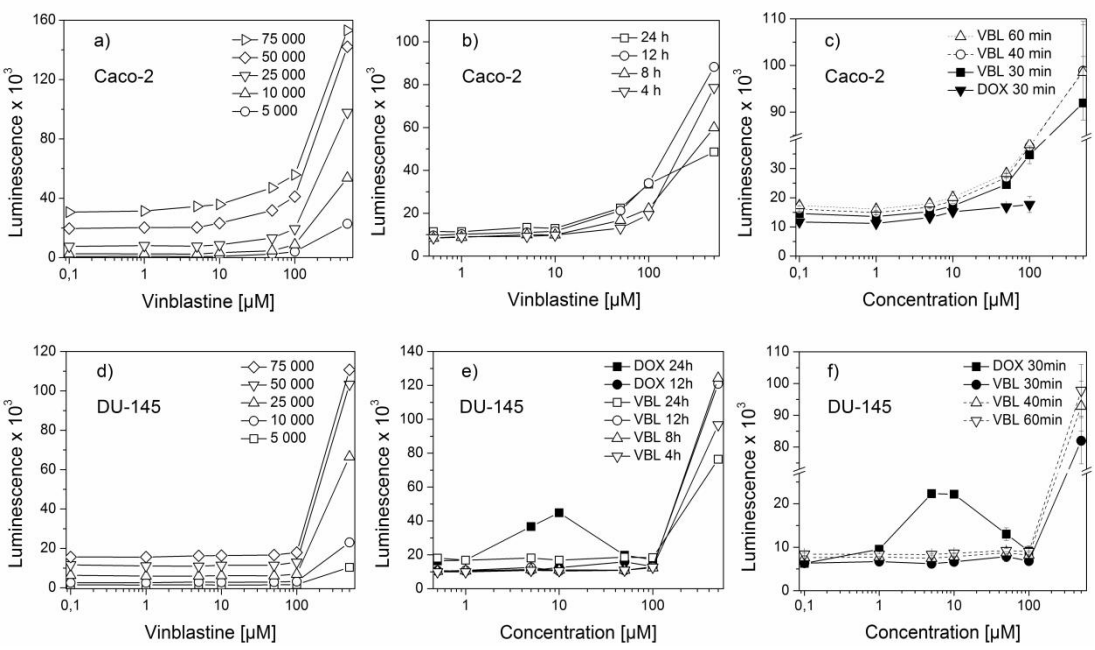

Figure 20. *Optimization of cell number (a,d), exposure time (b,e) and reagent incubation time of the automated Caspase-Glo® 3/7 assay on Caco-2 (a-c) and DU-145 (d-f) cell lines. For the standardization, dose-response curves were determined on both vinblastine (VBL) and doxorubicin (DOX) (c, f). Copyright © (2010) SAGE Publications. Reprinted with the permission.*

Sulforhodamine B assay

Optimization and standardization of the SRB assay was performed with both the cell lines. With the DU-145 cells, the linear increase in total protein up to 72 hours (Fig. 21a) and the sigmoidal dose-response profile with an S/B of 2.2 for vinblastine confirmed the choice of 10 000 cells per well as the appropriate cell number (Fig. 21b). Sigmoidal dose-response profiles were obtained for vinblastine, doxorubicin and 5-fluorouracil with GI50 values of 0.8 nM, 81 nM and 4.8 µM, respectively (Fig. 21c). Z´ factors for all the compounds were 0.4 or higher indicating successful cell-based assay (Falconer et al., 2002). Based on these data, the cell number of 10 000 cells per well and concentrations 1 nM (min) and 10 µM (max) were chosen for the screening with the DU-145 cells.

With Caco-2 cells, the optimization of SRB screen was not successful. Proliferation of the cells was not linear at the lowest cell numbers of 5 000 and 10 000, and no reliable dose-response correlations could be defined.

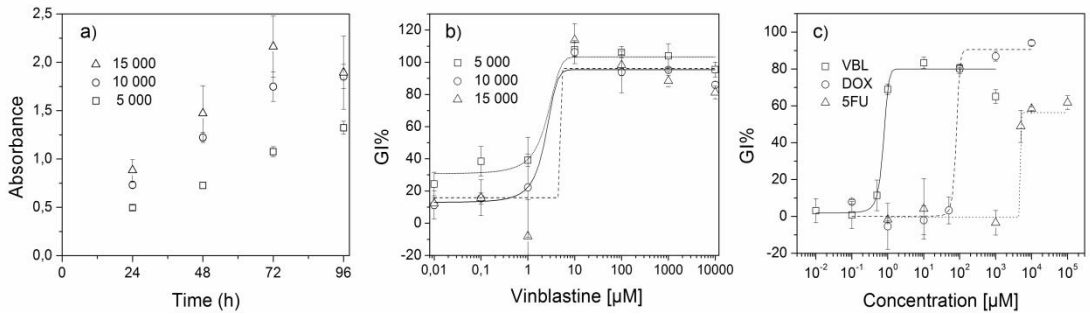

Figure 21. *Optimization and standardization of automated SRB assay on DU-145 cell line. a) Growth curves for the DU-145 cells and b) the sigmoidally fitted dose-response profiles for vinblastine on three different cell numbers. c) Dose-response profiles for vinblastine (VBL) (solid), doxorubicin (DOX) (dashed) and 5-fluorouracil (5-FU) (dotted) on the DU-145 cells. Copyright © (2010) SAGE Publications. Reprinted with the permission.*

Bidirectional Caco-2 permeability assay

Two automated protocols were set up for the bidirectional Caco-2 permeability experiments: the primary and secondary protocols with sampling intervals of 5 and 30 minutes without and with stirring, respectively. To reveal the significance of lacking stirring in the primary protocol, the high permeability compounds were evaluated using both protocols: the P_{app} values did not differ markedly between these two protocols (Fig. 22a).

The Caco-2 permeability experiments were standardized using both high and low permeability compounds and MDR1 efflux substrates. The high permeability compounds (metoprolol, propranolol, antipyrine, ketoprofen, carbamazepin) had P_{app} (A-B) values $>20^{x}10^{-6}$ cm/s (Fig. 22b), while the low permeability compounds (mannitol, atenolol, nadolol, hydrochlorthiazide, ranitidine) had P_{app} (A-B) values $<1^{x}10^{-6}$ cm/s. Hence, the difference was at least 20 fold resulting in a Z´ factor of 0.8

(nadolol vs. metoprolol). The efflux ratios for passively permeating compounds and MDR1 substrates (rhodamine 123, vinblastine and digoxin) were <3.5 and >7, respectively, which yields a Z´ factor of 0.5 (digoxin vs. nadolol).

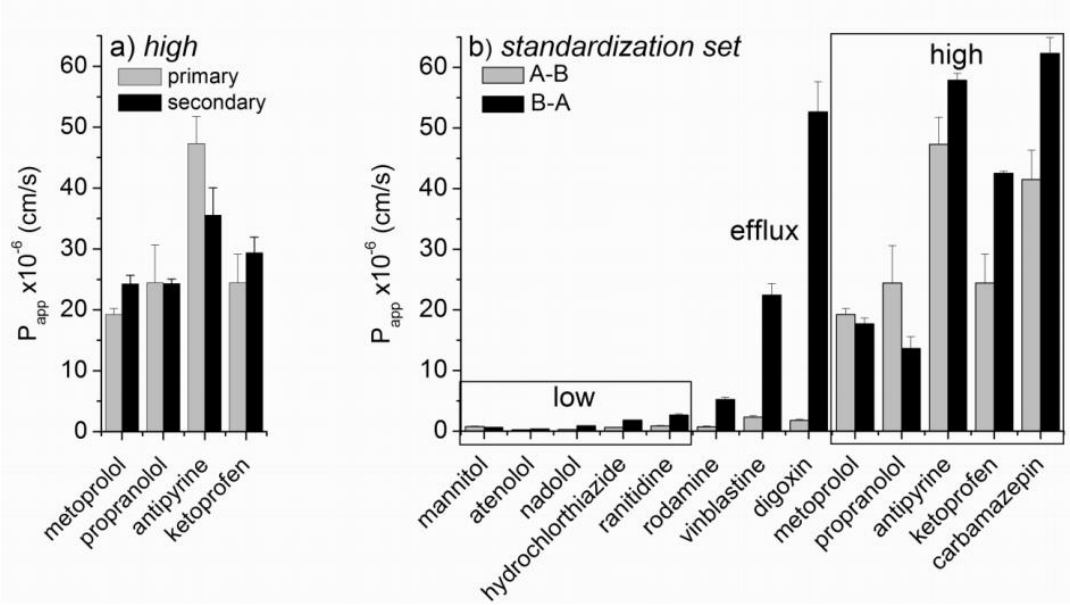

Figure 22. *Optimization and standardization of automated Caco-2 permeability experiments. a) P_{app} (A-B) values for the high permeability compounds were defined on both the automated primary and secondary permeability protocol to reveal the effect of lacking the stirring. b) The standardization of the automated bidirectional Caco-2 permeability experiments was done using the FDA recommended high and low permeability model compounds and the substrates of MDR1 efflux protein. Copyright © (2010) SAGE Publications. Reprinted with the permission.*

5.5 General discussion

During this thesis work, three automatable *in vitro* transport and metabolism assays were developed and/or utilized: a UGT1A6 screen (**I, II**), glucuronidation assays (**III**), and bidirectional Caco-2 permeability assay (**IV**). In addition, cytotoxicity assays sulforhodamine B (SRB) (**IV**) and Caspase-Glo® 3/7 (**IV**) were part of the studies. All the assays were transferred on a robotic workstation and run automated in the course of the studies, with the the exception of the glucuronidation assays (**III**).

The ease of implementing the assays on the robotic workstation was highly dependent on the amount of the liquid handling steps, properties of the liquids and sensitivity of the biological model system for mechanical stress. The developed UGT1A6 screen (**I, II**) and the commercial assay kit Caspase-Glo® 3/7 (**IV**) were easy to automate, whereas the SRB assay (**IV**) and the bidirectional Caco-2 transport assay (**IV**) were more challenging. Although the glucurodation assays were not automated in this study, they would be fairly easy to set up on a robotic workstation by slightly modifying the protocol used in the UGT1A6 screen.

The assays were automated on a Tecan Genesis RSP 150/8 workstation. This particular workstation was in the first place designed for the bidirectional transport assays in 24-well format, and was not optimal for the 96-well assays. In principle, the add-mix-measure type of assay does not require such a versatile robotic system, but the benefits of automation would be achieved already with a simple liquid dispenser, preferably equipped with a 96-tip head and connected to a plate storage system.

The overall throughput of an assay is not affected only by the time of the assay execution, but also by the time used in preparations before and after the actual assay, and in the analysis of the samples. It is always beneficial, if the biological model system can be prepared in advance at bigger batches, aliquoted, stored frozen and thawn on the assay day, as it was done with the recombinant enzyme preparations (**I, II, III**) and microsomes (**I, II**). In the cellular assays that is usually not possible, but the cell maintenance and culturing of the cells have to be coordinated to provide the cellular models at a defined timepoint. Depending on the desired properties of the cellular system, it may take from days to weeks to prepare the cells for the assays (**IV**). Obviously, also the fast plate reader-based analytical methods, which detect either the compound fluorescence (**I, II**), luminescence (**IV**) or absorbance (**IV**), are often preferred over the more time-consuming LC or LC-MS analysis (**III, IV**).

The throughput of an assay is an important determinant of its utilization potential for screening high number of compounds. The more complex, and thus the more laborious, assays often provide more *in vivo* relevant results. The results obtained in assays performed with model systems highly mimicking the *in vivo* intestinal wall, such as the bidirectional Caco-2 transport assays, are a sum of multiple processes, such as passive membrane permeability, passage via active uptake, and the impact of efflux transporters and intracellular metabolism. Although single transporters or enzymes separated from their natural cellular environment are useful in detailed mechanistic studies, they lack the other cellular components.

6 Conclusions

1. A new fluorescent HTS assay was developed based on 1-naphthol glucuronidation by UGT1A6 for the detecting of drug interactions with the human recombinant UGT1A6 (**I**).

2. The developed HTS assay for the UGT1A6 was succesfully used to provide a data set on compound interactions with the UGT1A6. The data was further used in developing a SVM classification method and 3-D QSAR models based on COMFA and COMSIA analysis (**I, II**).

3. The effect of pH on the interactions of diclofenac and indomethacin with human UDP-glucuronosyltransferases was found to be highly variable and enzyme specific (**III**).

4. Three different cellular assays were succesfully automated on a robotic workstation by optimizing the critical liquid handling parameters and experimental set-ups in each assay. The benefits gained by automation were dependent on the properties of the assay protocols and the instruments. The simplest assay was the most suitable for automation, but also the more challenging assays benefit from the automation (**IV**).

References

Abid A., Bouchon I., Siest G., Sabolovic N., 1995. Glucuronidation in the Caco-2 human intestinal cell line: Induction of UDP-glucuronosyltransferase 1*6. Biochem Pharmacol 50(4):557-561

Adachi Y., Suzuki H., Sugiyama Y., 2003. Quantitative evaluation of the function of small intestinal P-glycoprotein: Comparative studies between in situ and in vitro. Pharm Res 20(8):1163-1169

Ahmed F., Vyas V., Cornfield A., Goodin S., Ravikumar T. S., Rubin E. H., Gupta E., 1999. In vitro activation of irinotecan to SN-38 by human liver and intestine. Anticancer Res. 19(3A):2067-2071

Alsenz J., Haenel E., 2003. Development of a 7-day, 96-well Caco-2 permeability assay with high-throughput direct UV compound analysis. Pharm Res 20(12):1961-1969

An W. F., Tolliday N., 2010. Cell-based assays for high-throughput screening. Mol Biotechnol 45:180-186

Anderson C. M. H., Thwaites D. T., 2010. Hijacking solute carriers for proton-coupled drug transport. Physiology 25:364-377

Arrabito G., Pignataro B., 2010. Inkjet printing methodologies for drug screening. Anal Chem 82:3104-3107

Artursson P., Karlsson J., Ockling G., Schipper N., 1996a. Studying transport process in absorptive epithelia. In Epithelial cell culture –A practical approach, edited by Shaw A. J., Irl Press at Oxford University Press, Oxford, England, p. 111-133

Artursson P., Palm K., Luthman K., 1996b. Caco-2 monolayers in experimental and theoretical prediction of drug transport. Adv Drug Del Rev 22:67-84

Astle T. W., Akowitz A., 1996. Accuracy and tip carryover contamination in 96-well pipetting. J Biomol Screen 1(4):211-216

Augustijns P., F., Bradshaw T. P., Gan L.-S. L., Hendren R. W., Thakker D. R., 1993. Evidence for a polarized efflux system in Caco-2 cells capable of modulating cyclosporin A transport. Biochem Biophys Res Comm 197(2):360-365

Avdeef A., 2001. Physicochemical profiling (solubility, permeability and charge state). Curr Top Med Chem 1:277-351

Ayesh S., Shao Y-M., Stein W. D., 1996. Co-operative, competitive and non-competitive interactions between modulators of P-glycoprotein. Biochim Biophys Acta 1316:8-18

Bakos E., Evers R., Szakács G., Tusnády E., Welker E., Szabó K., de Haas M., van Deemter L., Borst P., Váradi A., Sarkadi B., 1998. Functional multidrug resistance protein (MRP1) lacking the N-terminal transmembrane domain. J Biol Chem 273(48):32167-32175

Balakrishnan A., Polli J. E., 2006. Apical sodium dependent bile acid transporter (ASBT, SLC10A2): A potential prodrug target. Mol Pharmaceutics 3(3):223-230

Ballatori N., Christian W. V., Lee J. Y., Dawson P. A., Soroka C. J., Boyer J. L., Madejczyk M. S., Li N., 2005. OSTα-OSTβ: A major basolateral bile acid and steroid transporter in human intestinal, renal, and biliary epithelia. Hepatology 42:1270-1279

Banks M., Binnie A., Fogarty S., 1997. High throughput screening using fully integrated robotic screening. J Biomol Screen 2(2):133-135

Bell L., Bickford S., Nguyen P. H., Wang J., He T., Zhang B., Friche Y., Zimmerlin A., Urban L., Bojanic D., 2008. Evaluation of fluorescence- and mass

spectrometry-based CYP inhibition assays for use in drug discovery. J Biomol Screen 13(5):343-353

Benoit-Biancamano M.-O., Connelly J., Villeneuve L., Caron P., Guillemette C., 2009. Deferiprone glucuronidation by human tissues and recombinant UDP glucuronosyltransferase 1A6: An in vitro investigation of genetic and splice variants. Drug Metab Dispos 37(2):322-329

Berg M., Undisz K., Thieriche K., Zimmermann P., Moore T., Posten C., 2001. Evaluation of liquid handling conditions in microplates. J Biomol Screen 6(1):47-56

Bjornsson T. D., Callaghan J. T., Einolf H. J., Fischer V., Gan L., Grim S., Kao J., King S. P., Miwa G., Ni L., Kumar G., McLeod J., Obach R. S., Robetrs S., Roe A., Shah A., Snikeris F., Sullivan J. T., Tweedie D., Vega J. M., Walsh J., Wrighton S. A., 2003. The conduct of in vitro and in vivo drug-drug interaction studies: A Pharmaceutical research and manufacturers of America (PhRMA) perspective. Drug Metab Dispos 31(7):815-832

Bock-Hennig B. S., Köhle C., Nill K., Bock K. W., 2002. Influence of *t*-butylhydroquinone and β-naphthoflavone on formation and transport of 4-methylumbelliferone glucuronide in Caco-2/TC-7 cell monolayers. Biol Pharmacol 63:123-128

Bonnefille P., Sezgin-Bayindir Z., Belkhelfa H., Arellano C., Gandia P., Woodley J., Houin G., 2011. The use of isolated enterocytes to study phase I intestinal drug metabolism: validation with rat and pig intestine. Fundam Clin Pharmacol 25:104-114

Borgnia M. J., Eytan G. D., Assaraf Y. G., 1996. Competition of hydrophobic peptides, cytotoxic drugs, and chemosensitizers on a common P-glycoprotein pharmacophore as revealed by its ATPase activity. J Biol Chem 271(6):3163-3171

Borst P., Elferink O. O., 2002. Mammalian ABC transporters in health and disease. Annu Rev Biochem 71:537-592

Brandsch M., Knütter I., Bosse-Doenecke E., 2008. Pharmaceutical and pharmacological importance of peptide transporters. J Pharm Pharmacol 60:543-585

Brimer C., Dalton J. T., Zhu Z., Schuetz J., Yasuda K., Vanin E., Ralling M. V., Lu Y., Schuetz E. G., Creation of polarized cells coexpressing CYP3A4, NADPH cytochrome P450 reductase and MDR1/P-glycoprotein. Pharm Res 17(7):803-810

Bronson D., Hentz N., Janzen W. P., Lister M. D., Menke K., Wegrzyn J., 2001. Basic considerations in designing high-throughput screening assays. In Handbook of drug screening, edited by Seethala R., Fernandes P. B., Marcel Decker, New York, USA, p. 5-30

Broudy M. I., Crespi C. L., Pattern C. J., 2001. A sensitive fluorometric high throughput inhibition assay for human UDP glucuronosyl transferase (UGT) 1A1. Poster presented at AAPS, Denver, CO, 2001

Bu H.-Z., Poglod M., Micetich R. G., Khan J. K., 2000. High-thoughput Caco-2 cell permeability screening by cassette dosing and sample pooling approaches using direct injection/on-line quard cartridge extraction/tandem mass spectrometry. Rapid Commun Mass Spectrom 14:523-528

Bucher K., Belli S., wunderli-Allenspach H., Krämer S. D., 2007. P-glycoprotein in proteoliposomes with low residual detergent: The effects of cholesterol. Pharm Res 24(11):1993-2004

Busby W. F. Jr, Ackermann J. M., Crespi C. L., 1999. Effect of methanol, ethanol, dimethyl sulfoxide, and acetonitrile on in vitro activities of cDNA-expressed human cytochromes P-450. Drug Metab Dispos 27(2):246-249

Buters J. T. M., Korzekwa K. R., Kunze K. L., Omata Y., Hardwick J. P., Gonzalez F. J., 1994. cDNA-directed expression of human cytochrome P450 CYP3A4 using baculovirus. Drug Metab Dispos 22(5):688-692

Cali J. J., Ma D., Sobol M., Simpson D. J., Frackman S., Good T. D., Daily W. J., Liu D., 2006. Luminogenic cytochrome P450 assays. Expert Opin Drug Metab Toxicol 2(4):629-645

Caro I., Boulenc X., Rousset M., Meunier V., Bourrié M., Julian B., Joyeux H., Roques C., Berger Y., Xweibaum A., Fabre G., 1995. Characterization of a newly isolated Caco-2 clone (TC-7), as a model of transport processes and biotransformation of drugs. Int J Pharm 116:147-158

Chan L. M. S., Lowes S., Hirst B. H., 2004. The ABCs of drug transport in intestine and liver: efflux proteins limiting drug absorption and bioavailability. Eur J Pharm Sci 21:25-51

Chang C.-C., Lin C.-J., 2011. LIBSVM: A library for support vector machines. ACM Trans Intell Syst Technol 2(3):1-27

Chang J. H., Yoo P., Lee T., Klopf W., Takao D., 2009. The role of pH in the glucuronidation of raloxifene, mycophenolic acid and ezemitibe. Mol Pharm 6(4):1216-1227

Chauret N., Tremblay N., Lackman R. L., Gauthier J.-Y., Silva J. M., Marois J., Yergey J. A., Nicoll-Griffith D. A., 1999. Description of a 96-well plate assay to measure cytochrome P4503A inhibition in human liver microsomes using a selective fluorescent probe. Anal Biochem 276:215-226

Chen G., Zhang D., Jing N., Yin S., Falany C. N., Radominska-Pandya A., 2003. Human gastrointestinal sulfotransferases: identification and distribution. Toxicol Appl Pharmacol 187:186-197

Cho M. J., Thompson D. P., Cramer C. T., Vidmar T. J., Scieszka J. F., 1989. The Madin Darby canine kidney (MDCK) epithelial cell monolayer as a model cellular transport barrier. Pharm Res 6(1):71-77

Cohen L. H., Remley M. J., Raunig D., Vaz A. D. N., 2003. In vitro drug interaction of cytochrome P450: An evaluation of fluoregenic to conventional substrates. Drug Metab Dispos 31(8):1005-1015

Coles B. F., Chen G., Kadlubar F. F., Radominska-Pandya A., 2002. Interindividual variation and organ-specific patterns of glutathione S-transferase alpha, mu, and pi expression in gastrointestinal tract mucosa of normal individuals. Arch Biochem Biophys 403:270-276

Collier A. C., Tingle M. D., Keelan J. A., Paxton J. W., Mitchell M. D., 2000. A highly sensitive fluorescent microplate method for the determination of UDP-glucuronosyltransferase activity in tissues and placental cells. Drug Metab Dispos 28(10):1184-1186

Copeland R. A., 2003. Mechanistic considereations in high-throughput screening. Anal Biochem 320:1-12

Cotreau M. M., von Moltke L. L., Beinfeld M. C., Greenblatt D. J., 2000. Methodologies to study the induction of rat hepatic and intestinal cytochrome P450 3A at the mRNA, protein, and catalytic activity. J Pharmacol Toxicol Methods 43:41-54

Covitz K-M. Y., Amidon G. L., Sadée W., 1996. Human peptide transporter, hPEPT1, stably transfected into Chinese ovary cells. Pharm Res 13(11):1631-1634

Crespi C. L., Miller V. P., 1999. The use of heterologously expressed drug metabolizing emzymes –state of the art and prospects for the future. Pharmacol Ther 84:121-131

Crespi C. L., Miller V. P., Penman B. W., 1997. Microtiter plate assay for inhibition of human drug-metabolizing cytochromes P450. Anal Biochem 248:188-190

Crespi C. L., Penman B. W., Hu M., 1996. Development of Caco-2 cells expressing high levels if cDNA-derived cytochrome P4503A4. Pharm Res 13(11):1635-1641

Crivori P., Reinach B., Pezzetta D., Poggesi I., 2006. Computational models for identifying P-glycoprotein substrates and inhibitors. Mol Pharm 3(1):33-44

Cubitt H. E., Houston J. B., Galetin A., 2009. Relative importance of intestinal and hepatic glucuronidation –Impact on the prediction of drug clearance. Pharm Res 26(5):1073-1083

de Montellano O., 1999. The cytochrom P450 oxidative system. In Handbook of Drug Metabolism, edited by Woolf T. F., Marcel Dekker, Inc., New York, USA, p. 109-130

Delaporte E., Slaughter D. E., Egan M. A., Gatto G. J., Santos A., Shelley J., Price E., Howells L., Dean D. C., Rodrigues A. D., 2001. The potential for CYP2D6 inhibition screening using a novel scintillation proximity assay-based approach. J Biomol Screen 6(4):225-231

Di L., Kerns E. H., Hong Y., Kleintop T. A., McConnel O. J., Huryn D. M., 2003. Optimization of a higher throughput microsomal stability screening assay for profiling drug discovery candidates. J Biomol Screen 8(4):453-462

Di Marco A., D´Antoni M., Attaccalite S., Carotenuto S., Laufer R., 2005. Determination of drug glucuronidation and UDP-glucuronosyltransferase selectivity using a 96-well radiometric assay. Drug Metab Dispos 33(6):812-819

Dong D., Wu B., 2012. In silico modeling of UDP-glucuronosyltransferase 1A10 substrates using the VolSurf approach. J Pharm Sci, doi 10.1002/jps

Eneroth A., Åström E., Hoogstraate J., Schrenk D., Conrad S., Kauffmann H-M., Gjellan K., 2001. Evaluation of a vincristine resistant Caco-2 cell line for use in a calcein AM extrusion screening assay for P-glycoprotein interaction. Eur J Pharm Sci 12:205-214

Ethell, B.T., Ekins, S., Wang, J., Burchell, B., 2002. Quantitative structure activity relationship for the glucuronidation of simple phenols by expressed human UGT1A6 and UGT1A9. Drug Metab Dispos 30:734-738

Evers R., Kool M., Van Deemter L., Janssen H., Calafat J., Oomen L. C. J. M., Paulusma C. C., Oude Elfering C. C., Baas F., Schinkel A. H., Borst P., 1998. Drug export activity of the human canicular multispecific organic anion transporter in polarized kidney MDCK cells expressing cMOAT (MRP2) cDNA. J Clin Invest 101:1310-1319

Fahrmayr C., König J., Fromm M.F., 2011. Identification of ezetimibe glucuronide as substrate of MRP2 using an OATP1B1-UGT1A1-MRP2 triple-transfected MDCKII cell line. Naunyn-Schmiedebergs Arch Pharmacol 383(Suppl. 1):S79

Falconer M., Smith F., Surah-Narwal S., Congrave G., Liu Z., Hayter P., Ciaramella G., Keithley W., Haddock P., Waldron G., Sewing A., 2002. High-throughput screening for ion channel modulators. J Biomol Screen 7:460-465

Fan J., Maeng H.-J., Du Y., Kwan D., Pang K. S., 2011. Transport of 5,5-diphenylbarbituric acid and its precursors and their effect on P-gp, MDR2 and CYP3A4 in Caco-2 and LS180 cells. Eur J Pharm Sci 42:19-29

Faria T. N., Timoszyk J. K., Stouch T. R., Vig B. S., Landowski C. P., Amidon G. L., Weaver C. D., Wall D. A., Smith R. L., 2004. A novel high-throughput PepT1 transporter assay differentiates between substrates and antagonists. Mol Pharm 1:67-76

FDA: Guidance for industry (Draft): Drug interaction studies –Study design, data analysis, and implications for dosing and labeling. Baltimore, USA, 2006.

Fine K. D., Santa Ana C. A., Porter J. L., Fordtran J. S., 1995. Effect of changing intestinal flow rate on a measurement of intestinal permeability. Gastroenterology 108:983-989

Fisher C.W., Claudle D. L., Martin-Wixtrom C., Quattrochi L.C., Tukey R.H., Waterman M. R., Estabrook R. W., 1992. High-level expression of functional human cytochrome P450 1A2 in Eschericia coli. FASEB J 6:759-764

Fisher M. B., VandenBrander M., Findlay K., Burchell B., Thummel K. E., Hall S. D., Wrighton S. A., 2000. Tissue distribution and interindividual variation in human UDP-glucuronosyltransferase activity: relationship between UGT1A1 promoter genotype and variability in a liver bank. Pharmacogenetics 10:727-739

Frégeau C. J., Yensen C., Elliot J., Fourney R. M., 2007. Optimized configuration of fixed-tip robotic liquid-handling stations for the elimination of biological sample cross-contamination. J Assoc Lab Autom 12:339-354

Fromm M. F., Kim R. B., Stein C. M., Wilkinson G. R., Roden D. M., 1999. Inhibition of P-glycoprotein-mediated drug transport: A unifying mechanism to explain the interaction between digoxin and quinidine. Circulation 99:552-557

Fujiwara R., Nakajima M., Yamanaka H., Katoh M., Yokoi T., 2008. Product inhibition of UDP-glucuronosyltransferase (UGT) enzymes by UDP obfuscates the inhibitory effects of UGT substrates. Drug Metab Dispos 36:361-367

Galetin A., Houston J. B., 2006. Intestinal and hepatic metabolic activity of five cytochrome P450 enzymes: Impact on prediction of first-pass metabolism. J Pharmacol Exp Ther 318:1220-1229

Galkin A., Pakkanen J., Vuorela P., 2008. Development of an automated 7-day 96-well Caco-2 cell culture model. Die Pharmazie 63:464-469

Ganapahty M. E., Brandsch M., Prasad P. D., Ganapathy V., Leipach F. H., 1995. Differential recognition of β-lactam antibiotics by intestinal and renal peptide transporters, PEPT1 and PEPT2. J Biol Chem 270(43):25672-25677

Ganapathy V., Leibach F. H., 1983. Role of pH gradient and membrane potential in dipeptide transport in intestinal and renal brush-border membrane vesicles from the rabbit. J Biol Chem 258(23):14189-14192

Gao H., Yao L., Mathieu H. W., Zhang Y., Maurer T. S., Troutman M. D., Scott D. O., Ruggeri R. B., Lin J., 2008. In silico modeling of nonspecific binding to human liver microsomes. Drug Metab Dispos 36(10):2130-2135

Garrigues A., Nugier J., Orlowski S., Ezan E., 2002. A high-throughput screening microplate test for the interaction of drugs with P-glycoprotein. Anal Biochem 305:106-114

Geertsma E. R., Mahmood N. A. B. N., Schuurman-Wolters G. K., Poolman B., 2008. Membrane reconstitution of ABC transporters and assays of translocator function. Nature Protocols 3(2):256-266

Gertz M., Harrison A., Houston J. B., Galetin A., 2010. Prediction of human intestinal first-pass metabolism of 25 CYP3A substrates from in vitro clearance and permeability data. Drg Metab Dispos 38:1147-1158

Gertz M., Houston J. B., Galetin A., 2011. Physiologically based pharmacokinetic modeling of intestinal first-pass metabolism of CYP3A substrates with hugh intestinal extraction. Drug Metab Dispos 39(9):1633-1642

Giacomini K. M., Huang S-M., Tweedie D. J., Benet L. Z., Brouwer K. L. R., Chu X., Dahlin A., Evers R., Fischer V., Hillgren K. M., Hoffmaster K. A., Ishikawa T., Keppler D., Kim R. B., Lee C. A., Niemi M., Polli J. W., Sugiyama Y., Swaan P. W., Ware J. A., Wright S. H., Yee S. W., Zamek-Gliszczynski M. J., Zhang L. (The International Transporter Consortium), 2010. Membrane transporters in drug development. Nature Rev Drug Discovery 9:215-236

Gibbs M. A., Thummel K. E., Shen D. D., Kunze K. L., 1999. Inhibition of cytochrome P-450 3A (CYP3A) in human intestinal and liver microsomes: Comparison of K_i values and impact of CYP3A5 expression. Drug Metab Dispos 27(2):180-187

Glaeser H., Drescher S., van der Kuip H., Behrens C., Geick A., Burk O., Dent J., Somogyi A., von Richter O., Griese E.-U., Eichelbaum M., Fromm M. F., 2002. Shed human enterocytes as a tool for the study of expression and function of intestinal drug-metabolizing enzymes and transporters. Clin Pharmacol Ther 71:131-140

Glavinas H., Kis E., Pál Á., Kovács R., Jani M., Vági E., Molnár É., Bándsághi S., Kele Z., Janáky T., Báthori G., von Richer O., Koomen G-J., Krajcsi P., 2007. ABCG2 (Breast cancer resistance protein/mitoxantrone resistance-associated protein) ATPase assay: A useful tool to detect drug-transporter interactions. Drug Metab Dispos 35:1533-1542

Gonzalez F. J., Korzekwa K. R., 1995. Cytochrores P450 expression systems. Annu Rev Pharmacol Toxicol 35:369-390

Gregory P. A., Lewinsky R. H., Gardner-Stephen D. A., Mackezie P. I., 2004. Regulation of UDP glucuronosyltransferases in the gastrointestinal track. Toxicol Appl Pharmacol 199:354-363

Gu H., Deng Y., 2007. Dilution effect in multichannel liquid-handling system equipped with fixed tips: Problems and solutions for bioanalytical sample preparation. J Assoc Lab Autom 12:355-362

Hakala K. S., Laitinen L., Kaukonen A. M., Hirvonen J., Kostiainen R., Kotiaho T., 2003. Development of LC/MS/MS methods for cocktail dosed Caco-2 samples using atmospheric pressure photoionization and electrospray ionization. Anal Chem 75:5969-5977

Hall S. D., Thummel K. E., Watkins P. B., Lown K. S., Benet L. Z., Paine M. F., Mayo R. R., Turgeon D. K., Bailey D. G., Fontana R. J., Wrighton S. A., 1999. Molecular and physical mechanisms of first-pass extraction. Drug Metab Dispos 27(2):161-166

Han H-k., Oh D-M., Amidon G., 1998. Cellular uptake mechanism of amino acid ester prodrugs in Caco-2/hPEPT1 cells overexpressing a human peptide transporter. Pharm Res 15(9):1382-1386

Hansen T., Borlak J., Bader A., 2000. Cytochorome P450 enzyme activity and protein expression in primary prochine enterocyte and hepatocyte cultures. Xenobiotoca 30(1):27-46

Harmsen S., Koster A. S., Beijnen J. H., Schellens J. H. M., Meijerman I., 2008. Comparison of two immortalized human cell lines to study nuclear receptor-mediated CYP3A4 induction. Drug Metab Dispos 36(6):1166-1171

Hartley D. P., Dai X., Yabut J., Chu X., Cheng O., Zhang T., He Y. D., Roberts C., Ulrich R., Evers R., Evans D. C., 2006. Identification of potential pharmacological and toxicological targets differentiating structural analogs by a combination of transcriptional profiling and promoter analysis in LS-180 and Caco-2 adenocarcinoma cell lines. Pharmacogenet Genomics 16(8):579-599

Hayeshi R., Hilgendorf C., Artursson P., Augustijns P., Brodin B., Dehertogh P., Fisher K., Fossati L., Hovenkamp E., Korjamo T., Masungi C., Maubon N., Mols R., Müllertz A., Mönkkönen J., O´Driscoll C., Oppers-Tiemissen H. M., Ragnarsson E. G. E., Rooseboom M., Ungell A-L., 2008. Comparison of drug transporter gene expression and functionality in Caco-2 cells from 10 different laboratories. Eur J Pharm Sci 35:383-396

Hegedüs C., Szakács G., Homolya L., Orbán T. I., Telbisz Á., Jani M., Sarkadi B., 2009. Ins and outs of the ABCG2 multidrug transporter: An update on in vitro functional assays. Adv Drug Deliv Rev 61:47-56

Henrich C. J., Bokesch H. R., Dean M., Bates S. E., Robey R. W., Goncharova E. R., Wilson J. A., McMahon J. B., 2006. A high-throughput cell-based assay for inhibitors of ABCG2 activity. J Biomol Screen 11(2):176-183

Hereley S. B., Marks B. D., Stafslien D. K., Singh U., Eliason H. C., Wolken J. K., Frazee W. J., 2007. Fluorescence-based biochemical assays for the study of pregnane X receptor and constitutive androstane receptor. Poster presented in ISSX 2007, Sendai, Japan

Hidalgo I., Raub T., Borchardt R., 1989. Characterization of the human colon carcinoma cell line (Caco-2) as a model system for intestinal epithelial permeability. Gastroenterology 96:736-749

Higgins C. F., 1992. ABC transporters: From microorganisms to man. Annu Rev Cell Biol 8:67-113

Hirouchi M., Suzuki H., Itoda M., Ozawa S., Sawada J-i., Ieiri I., Ohtsubo K., Sugiyma Y., 2004. Characterization of the cellular localization, expression level and function of SNP variants of MRP/ABCC2. Pharm Res 21(5):742-748

Holland M. L., Allen J. D., Arnold J. C., 2008. Interaction of plant cannabinoids with the multidrug transporter ABCC1 (MRP1). Eur J Pharmacol 591:128-131

Holló Z., Homolya L., Davis C. W., Sarkadi B., 1994. Calcein accumulation as a fluorometric functional assay of the multidrug transporter. Biochim Biophys Acta, Biomembr 1191(2):384-388

Hong J., Edel J. B., deMello A. J., 2009. Micro- and nanofluidic systems for high-throughout biological screening. Drug Discov Today 14(3/4):134-146

Horio M., Chin K.-V., Currier S. J., Goldenberg S., Williams C., Pastan I., Gottesman M. M., Handler J., 1989. Transepithelial transport of drugs by the multidrug transporter in cultured Madin-Darby Canine Kidney cell epithelia. J Biol Chem 264(25):14880-14884

Horio M., Gottesman M. M., Pastan I., 1988. ATP-dependent transport of vinblastine in vesicles from human multidrug-resistant cells. Proc Natl Acad Sci USA 85:3580-3584

Hubatsch I., Ragnarsson E. G. E., Artursson P., 2007. Determination of drug permeability and prediction of drug absorption in Caco-2 monolayers. Nature Prot 2(9):2011-2019

Hugger E. D., Cole C. J., Raub T. J., Burton P. S., Borchardt R. T., 2003. Automated analysis of polyethylene glycol-induced inhibition of p-glycoprotein activity in vitro. J Pharm Sci 91(1):21-26

Hunter J., Hirst B. H., Simmons N. L., 1993. Drug absorption limited by P-glycoprotein-mediated secretory drug transport in human intestinal epithelial Caco-2 cell layers. Pharm Res 10(5):743-749

Imai T., Imoto M., SakamotoH., Hashimoto M., 2005. Identification of esterases expressed in Caco-2 cells and effects of their hydrolyzing activity in predicting human intestinal absorption. Drug Metab Dispos 33:1185-1190

Imaoka S., Yamada T., Hiroi T., Hayashi K., Sakaki T., Uabusaki Y., Funae Y., 1996. Multiple forms of human P450 expressed in Saccharomyces cerevisiae: Systematic characterization and comparison with those of the rat. Biochem Pharmacol 51:1041-1050

Inui K.-I., Yamamoto M., Saito H., 1992. Transepithelial transport of oral cephalosporins by monolayers of intestinal epithelian cell line Caco-2: Specific transport systems in apical and basolateral membranes. J Pharmacol Exp Ther 621(1):195-201

Iversen P. W., Eastwood B. J., Sittampalam G. S., Cox K. L., 2006. A comparison of assay performance measures in screening assays: Signal window, Z´ factor and assay variability ratio. J Biomol Screen 11(3):247-252

Jacobs A., Emmert D., Wieschrath S., Hrycyna C. A., Wiese M., 2011. Recombinant synthesis of human ABCG2 expressed in the yeast Saccharomyces cerevisiae: An experimental methological study. Protein J 30:201-211

Jenkins K. M., Angels R., Quintos M. T., Xu R., Kassel D. B., Rourick R. A., 2004. Automated high throughput ADME assays for metabolic stability and cytochrome P450 profiling of combinatorial libraries. J Pharm Biomed Anal 34:989-1004

Jia L., Liu X., 2007. The conduct of drug metabolism studies considered good practice (II): *In vitro* experiments. Current Drug Metab 8:822-829

Jin H., Di L., 2008. Permeability –In vitro assays for assessing drug transporter activity. Current Drug Metab 9:911-920

Jonker J. W., Schinkel A. H., 2004. Pharmacological and physiological functions of the polyspecific organic cation transporters: OCT1, 2, and 3 (SLC22A1-3). J Pharmacol Exp Ther 308(1):2-9

Kalliokoski A., Niemi M., 2009. Impact of OATP transporters on pharmacokinetics. Br J Pharmacol 158:693-705

Kaminsky L. S., Zhang Q.-Y., 2003. The small intestine as a xenobiotic-metabolizing organ. Drug Metab Dispos 31:1520-1525

Kariv I., Fereshteh M. P., Oldenburg K. R., 2001. Development of a miniaturized 384-well high throughput screen for the detection of substrates of cytochrome P450 2D6 and 3A4 metabolism. J Biomol Screen 6(2):91-99

Kelety B., Diekert K., Tobien J., Watzke N., Dörner W., Obrdlik P., Fendler K., 2006. Transporter assays using solid supported membranes: A novel screening platforms for drug discovery. Assay Drug Dev Technol 4(5):575-582

Kemp D. C., Fan P. W., Stevens J. C., 2002. Characterization of raloxifene glucuronidation in vitro: Contribution of intestinal metabolism to presystemic clearance. Drug Metab Dispos 30(6):694-700

Kenworthy K. E., Bloomer J. C., Clarke S. E., Houston J. B., 1999. CYP3A4 drug interactions: correlation of 10 in vitro probe substrates. Br J Clin Pharmacol 48:716-727

Keogh J. P., Kunta J. R., 2006. Development, validation and utility of an in vitro technique for assessment of potential clinical drug-drug interactions involving P-glycoprotein. Eur J Pharm Sci 27:543-554

Kerns E., Di L. (editors), 2008. Chapter 27: Transporter methods, in Drug like properties: Concepts, structure design and methods from ADME to toxicity optimization, Academic Press, London, UK, p. 299-310

Kiang T. K. L., Ensom M. H. H., Chang T. K. H., 2005. UDP-glucuronosyltransferases and clinical drug-drug interactions. Pharmacol Ther 106:97-132

King C. D., Rios G. R., Green M. D., Tephly T. R., 2000. UDP-glucuronosyltransferases. Current Drug Metab 1:143-161

Klaassen C. D., Aleksunes L. M., 2010. Xenobiotic, bile acid, and cholesterol transporters: Function and regulation. Pharmacol Rev 62:1-96

Kleman-Leyer K. M., Klink T. A., Kopp A. L., Westermeyer T. A., Koeff M. D., Larson B. R., Worzella T. J., Pinchard C. A., van der Kar S. A. T., Zaman G. J. R., Hornberg J. J., Lowery R. G., 2009. Characterization and optimization of a red-shifted fluorescence polarization ADP detection assay. Assay Drug Dev Technol 7(1):56-67

Koljonen M., Hakala K. S., Ahtola-Sätilä T., Laitinen L., Kostiainen R., Kotiaho T., Kaukonen A. M., Hirvonen J., 2006. Evaluation of cocktail approach to standardize Caco-2 permeability experiments. Eur J Pharm Biopharm 64:379-387

Krämer S. D., Absorption prediction from physicochemical parameters. Pharm Sci Technol Today 2(9):373-380

Kronbach T., Mathys D., Umeno M., Gonzalez F. J., Meyer U. A., 1989. Oxidation of midazolam and triazolam by human liver cytocrome P450IIA3. Mol Pharmacol 36:89-96

Kumar V., Rock D. A., Warren C. J., Tracy T. S., Wahlstrom J. L., 2006. Enzyme source effects on CYP2C9 kinetics and inhibition. Drug Metab Dispos 34(11):1903-1908

Kurkela M., Carcía-Horsman A., Luukkanen L., Mörsky S., Taskinen J., Bauman M., Kostiainen R., Hirvonen J., Finel M., 2003. Expression and characterization of recombinant human UDP-glucuronosyltranferases (UGTs). J Biol Chem 278(6):3536-3544

Lahoz A., Gombau L., Donato M. T., Castell J. V., Gómez-Lechón M. J., 2006. In vitro ADME medium/high-throughput screening in drug preclinical development. Mini-Rev Med Chem 6:1053-1062

Laine R., 2008. Metabolic stability: Main enzymes involved and best tools to assess it. Current Drug Metab 9:921-927

Laitinen L., Kangas H., Kaukonen A. M., Hakala K., Kotiaho T., Kostiainen R., Hirvonen J., 2003. N-in-one permeability studies of heterogeneous sets of compounds across Caco-2 monolayers. Pharm Res 20(2):187-197

Larson B., Kelts J. L., Banks P., Cali J. J., 2011. Automation and miniaturization of the bioluminescent UGT-Glo assay for screening of UDP-glucuronosyltransferase inhibition by various compounds. J Assoc Lab Autom 16(1):38-46

Lechner C., Reichel V., Moennig U., Reichel A., Fricker G., 2010. Development of a fluorescence-based assay for drug interactions with human multidrug resistance related protein (MRP2; ABC2) in MDCKII-MRP2 membrane vesicles. Eur J Pharm Biopharm 75:284-290

Lennernäs H., 2007. Intestinal permeability and its relevance for absorption and elimination. Xenobiotica 37(10-11):1015-1051

Lenz K. A., Polli J. W., Wring S. A., Humpreys J. E., Polli J. E., 2000. Influence of passive permeability on apparent P-glycoprotein kinetics. Pharm Res 17(12):1456-1460

Lespine A., Dupuy J., Orlowski S., Nagy T., Glavinas H., Krajcsi P., Alvinerie M., 2006. Interaction of ivermectin with multidrug resistance proteins (MRP1, 2 and 3). Chem Biol Interact 159:169-179

Liang Y., wang G., Xie L., Sheng L., 2011. Recent development in liquid chromatography/mass spectrometry and emerging techniques for metabolite identification. Curr Drug Metab 12:329-344

Lin J. H., Chiba M., Baillie T. A., 1999. Is the role of the small intestine in the first-pass metabolism overemphasized? Pharmacol Rev 51(2):135-157

Lin Y., Schiavo S., Orjala J., Vouros P., Kautz R., 2008. Microscale LC-MS-NMR platform applied to the identification of active cyanobacterial metabolites. Anal Chem 80:8045-8054

Linnankoski J., Mäkelä J., Palmgren J., Mauriala T., Vedin C., Ungell A-L., Lazarova L., Partursson P., Urtti A., Yliperttula M., 2010. Paracellular porosity and pore size of the human intestinal epithelium in tissue and cell culture models. J Pharm Sci 99(4):2166-2175

Lipinski C. A., Lombardo F., Dominy B. W., Feeney P. J., 2001. Experimental and computational approached to estimate solubility and permeability in drug discovery and development settings. Adv Drug Delivery Rev 46:3-26

Litman T., Zeuthen T., Skovsgaard T., Stein W. D., 1997a. Structure-activity relationships of P-glycoprotein interacting drugs: kinetic characterization of their effects on ATPAse activity. Biochim Biophys Acta 1361:159-168

Litman T., Zeuthen T., Skovsgaard T., Stein W. D., 1997b. Competitive, non-competitive and cooperative interactions between substrates of P-glycoprotein as measured by its ATPase activity. Biochim Biophys Acta 1361:169-176

Litten B. A., Smith R., Banfield E., 2010. An automated 1536-well microplate format cytochrome P450 inhibition assay using a Tecan Freedom EVO workstation with integrated innovative Nanodrop II dispenser. J Assoc Lab Autom 15:58-64

Liu X., Jia L., 2007. The condict of drug metabolism studies considered good practice (I): Analytical systems and *in vivo* studies. Current Drug Metab 8:815-821

Liu Y.-T., Hao H.-P., 2007. Drugs as CYP3A probes, inducers, and inhibitors. Drug Metab Rev 39:699-721

Loe D. W., Almquist K. C., Deeley R. G., Cole S. P. C., 1996. Multidrug resistance protein (MRP)-mediated transport of leucotriene C_4 and chemotherapeutic agents in membrane vesicles: Demonstration of glutathione-dependent vincristine transport. J Biol Chem 271(16):9675-9682

Lohmann C.,Gelius B., Danielsson J., Skoging-Nyberg U., Hollnack E., Dudley A., Wahlberg J., Hoogstraate J., Gustavsson L., 2007. Scintillation proximity assay for measuring uptake by the human drug transporters hOCT1, hOAT3 and hOATP1B1. Anal Biochem 366:117-125

Lorenz M. G. O., 2004. Liquid handling robotic workstations for functional genomics. J Assoc Lab Autom 9:262-267

Lowes S., Simmons N. L., 2002. Multiple pathways for fluoroquinolone secration by human intestinal epithelial (Caco-2) cells. British J Pharmacol 135(5):1263-1275

Lu P., Liu R., Sharom F. J., 2001. Drug transport by reconstituted P-glycoprotein in proteoliposomes. Eur J Biochem 268:1687-1697

Luukkanen L., Taskinen J., Kurkela M., Kostiainen R., Hirvonen J., Finel M., 2005. Kinetic characterization of the 1A subfamily of recombinant human UDP-glucuronosyltransferases. Drug Metab Dispos 33:1017-1026

Ma D., Cali J. J., 2007. Identify P-glycoprotein substrates and inhibitors with the rapid, HTS P-gp-Glo^{TM} assay system. Promega Notes 96:11-14

Maddox C. B., Rasmussen L., White E. L., 2008. Adapting cell-based assays to the high-throughput screening platform: Problems encountered and lessons learned. J Assoc Lab Autom 13:168-173

Manevski N., Moreolo P. S., Yli-Kauhaluoma J., Finel M., 2011. Bovine serum albumin decreases K_m values of human UDP-glucuronosyltransferases 1A9 and 2B7 and increases V_{max} values of UGT1A9. Drug Metab Dispos 39(11):2117-2129

Martin C., Berridge G., Higgins C. F., Mistry P., Charlton P., Callaghan R., 2000. Communication between multiple drug binding sites on P-glycoprotein. Mol Pharmacol 58:624-632

Matsson P., Pedersen J. M., Norinder U., Bergström C. A. S., Artursson P., 2009. Indentification of nocel specific and general inhibitors of the three major human ATP-binding cassette transporters P-gp, BCRP and MRP2 among registered drugs. Pharm Res 26(8):1816-1831

Mazur C. S., Kenneke J. F., Hess-Wilson J. K., Lipscomb J. C., 2010. Differencies between human and rat intestinal and hepatic bisphenol A glucunidation and the influence of alamethicin on in vitro kinetic measurements. Drug Metab Dispos 38:2232-2238

McNaney C. A., Dexler D. M., Hnatyshyn S. Y., Zvyaga T. A., Knipe J. O., Belcastro J. V., Sanders M., 2008. An automated liquid chromatography-mass spectrometry process to determine metabolic stability half-life and intrinsic clearance of drug candidates by substrate depletion. Assay Drug Dev Technol 6(1):121-129

Meier P. L., Sztul E. S., Reuben A., Boyer J. L., 1984. Structural and functional polarity of canalicular and basolateral plasma membrane vesicles isolated in hibh yield from rat liver. J Cell Biol 98:991-1000

Meinl W., Ebert B., Glatt H., Lampen A., 2008. Sulfotransferase forms expressed in human intestinal Caco-2 and TC7 cells at varying stages of differentiation and role in benzo[a]pyrene metabolism. Drug Metab Dispos 36:276-283

MeisenheimerP. L., Uyeda H. T., Ma D., Sobol M., McDougall M. G., Corona C., Simpson D., Klaubert D. H., Cali J., 2011. Proluciferin acetals as bioluminescent substrates for cytochrome P450 activity and probes for CYP3A inhibition. Drug Metab Dispos 39(12):2403-2410

Miller V., 2011. High-throughput in vitro ADME analysis with Agilent RapidFire/MS systems: Cytochrome P450 inhibition. Application Note, Agilent Technologies

Miners J. O., Mackenzie P. I., Knights K. M., 2010. The prediction of drug-glucuronidation parameters in humans: UDP-glucuronosyltransferase enzyme-selective substrate and inhibitor probes for reaction phenotyping and in vitro-in vivo extrapolation of drug clearance and drug-drug interaction potential. Drug Metab Dispos 42(1):196-208

Miret S., Abrahamse L., de Groene E., 2004. Comparison of in vitro models for the prediction of compound absorpition across the human intestinal mucosa. J Biochem Screen 9:598-606

Mitre E., Schulze M., Cumme G. A., Röbler F., Rausch T., Rhode H., 2007. Turbo-mixing in microplates. J Biomol Screen 12(3):361-369

Moody G. C., Griffin S. J., Mather A. N., McGinity D. F., Riley R. J., 1999. Fully automated analysis of acitivities catalyzed by the major human liver cytochrome P450 (CYP) enzymes: assessment of human CYP inhibition potential. Xenobiotica 29(1):53-75

Murer H., Hopfer U., Kinne-Safran E., Kinne R., 1974. Glucose transport in isolated brush-border and lateral-basal plasma membrane vesicles from intestinal epithelial cells. Biochim Biophys Acta 345:170-179

Nebert D. W., Gonzales F. J., 1987. P450 genes: Structure, evolution, and regulation. Ann Rev Biochem 56:945-993

Newman M. J., Wilson T. H., 1980. Solubilization and reconstitution of lactose transport systems from Escherihia coli. J Biol Chem 255(22):10583-10586

Nguyen N., Tukey R. H., 1997. Baculovirus-directed expression of rapid UDP-glucuronosyltransferases in spodoptera frugiperda cells. Drug Metab Dispos 25(6):745-749

Nies A. T., Herrmann E., Brom M., Keppler D., 2008. Vectrorial transport of the plant alkaloid berberine by double-transfected cells expressing the human organic cation transporter 1 (OCT1, SLC22A1) and the efflux pump MDR1 P-glycoprotein (ABCB1). Naunyn-Schmiedeberg´s Arch Pharmacol 376:449-461

Nishimura M., Naito S., 2006. Tissue-specific mRNA profiles of human phase I metabolizing enxymes except for cytochrome P450 and phase II metabolizing enzymes. Drug Metab Pharmacokinet. 21(5):357-374

O´Brien M. A., Daily W. J., Hesselberth P. E., Moravec R. A., Scurria M. A., Klaubert D. H., Bulleit R. F., Wood K. V., 2005. Homogenous, bioluminescent protease assays: Caspase-3 as a model. J Biomol Screen 10:137-148

Obach R. S., Zhang Q.-Y., Dunbar D., Kaminsky L. S., 2001. Metabolic characterization of the major human small intestinal cytochrome P450s. Drug Metab Dispos 29(3):347-352

Ohno S., Nakajin S., 2009. Determination of mRNA exression of human UDP-glucuronosyltransferses and application for localization in various human tissues by real-time reverse transcriptase-polymerase chain reaction. Drug Metab Dispos 37:32-40

Oldenburg K., Pooler D., Scudder K., Lipinski C. H., Kelly M., 2005. High throughput sonication: evaluation for compound solubilization. Com Chem High Throughput Screen 8:449-512

Oostendorp R. L., Beijnen J. H., Schellens J. H. M., 2009. The biological and clinical role of drug transporters at the intestinal barrier. Cancer Treat Rev 35:137-147

Osborne R., Joel S., Trew D., Sevin M., 1990. Morphine and metabolite behavior after different routes of morphine administration: Demonstration of the importance of the active metabolite morphine-6-glucuronide. Clin Pharmacol Ther 47:12-19

Ozawa N., Shimizu T., Morita R., Yokono Y., Ochiai T., Munesada K., Ohashi A., Aida Y., Hama Y., Taki K.,… 2004. Transporter data-base, TP-search: a web-accessible comprehensive database for research in pharmacokinetics of drugs. Pharm Res 21:2133-2134

Paine M. F., Hart H. L., Ludington S. S., Haining R. L., Rettie A. E., Zeldin D. C., 2006. The human intestinal cytochrome P450 “pie”. Drug Metab Dispos 34:880-886

Paine M. F., Khalighi M., Fisher J. M., Shen D. D., Kunze K. L., Marsh C. L., Perkins J. D., Thummel K. E., 1997. Characterization of interintestinal and intraintestinal variations in human CYP3A-dependent metabolism. J Pharmacol Exp Ther 283(3):1552-1562

Palmer J. L., Scott R. J., Gibson A., Dickins M., Pleasance S., 2001. An interaction between the cytochrome P450 probe substrates chlorzoxazone (CYP2E1) and midazolam (CYP3A). Br J Clin Pharmacol 52:555-561

Parkinson A., Kazmi F., Buckley D. B., Yerino P., Ogilvie B. W., Paris B. L., 2010. System-dependent outcomes during the evaluation of drug candidates as inhibitors of cytochrome P450 (CYP) and uridine diphosphate glucuronosyltransferase (UGT) enzymes: Human hepatocytes versus liver microsomes versus recombinant enzymes. Drug Metab Pharmacokinet 25(1):16-27

Patil A. H., D´Souza R., Dixit N., Damre A., 2011. Validation of quinidine as a probe substrate for the in vitro P-gp inhibition assay in Caco-2 cell monolayers. Eur J Drug Metab Pharmacokinet 36:115-119

Perloff M. D., Störmer E., von Moltke L. L., Greenblatt D. J., 2003. Rapid assessment of P-glycoprotein inhibition and induction in vitro. Pharm Res 20(8):1177-1183

Peters W. H. M., Kock L., Nagengast F. M., Kremers P. G., 1991. Biotransformation enzymes in human intestine: critical low levels in the colon? Gut 32:408-412

Peters W. H. M., Roelofs H. M. J., 1989. Time-dependent activity and expression of glutathione S-transferases in the human colon adenocarcinoma cell line Caco-2. Biochem J 264:613-616

Pfrunder A., Gutmann H., Beglinger C., Drewe J., 2003. Gene expression of CYP3A4, ABC-transporters (MDR1 and MRP1-5) and hPXR in three different human colon carcinoma cell lines. J Pharm Pharmacol 55:59-66

Pinto M., Robine-Leon S., Appay M-D., Kedinger M., Triadou N., Dussaulx E., Lacroix B., Simon-Assman P., Haffen K., Fogh J., Zweibaum A., 1983.

Enterocyte-like differentiation and polarization of the human colon carcinoma cell line Caco-2 in culture. Biol Cell 47:323-330

Polli J. W., Wring S. A., Humphreys J. E., Huang L., Morgan J. B., Webster L. O., Sebarjit-Singh C. S., 2001. Rational use of in vitro P-glycoprotein assays in drug discovery. J Pharmacol Exp Ther 299(2):620-628

Polson C., Sarkar P., Incledon B., Raguvaran V., Grant R., 2003. Optimization of protein precipitation based upon effectiveness of protein removal and ionization effect in liquind chromatography-tandem mass spectrometry. J Chromatograph B 785:263-275

Putnam W. S., Pan L., Tsutsui K., Takahashi L., Benet L. Z., 2002. Comparison of bidirectional cephalexin transport across MDCK and Caco-2 cell monolayers: Interactions with peptide transporters. Pharm Res 19(1):27-33

Radominska-Pandya A., Bratton S., Little J. M., 2005. A historical overview of the heterologous expression of mammalian UDP-glucuronosyltransferase isoforms over the past twenty years. Current Drug Metab 6:141-160

Rautio J., Humphreys J. E., Webster L. O., Balakrishnan A., Keogh J. P., Kunta J. R., Serabjit-Singh C. J., Polli J. W., 2006. In vitro P-glycoprotein inhibition assays for assessment of clinical drug interaction potential of new drug candidates: A recommendation for probe substrates. Drug Metab Dispos 34(5):786-792

Riches Z., Stanley E. L., Bloomer J. C., Coughtrie M. W. H., 2009. Quantitative evaluation of the expression and activity of five major sulfotransferases (SULTs) in human tissue: The SULT “Pie”. Drug Metab Dipos 37:2255-2261

Rodrigues A. D., Mulford D. J., Lee R. D., Surber B. W., Kukulka M. J., Ferrero J. L., Thomas S. B., Shet M. S., Estabrook R. W., 1995. In vitro metabolism of terfenadine by a purified recombinant fusion protein containing cytochrome P4503A4 and NADPH-P450 reductase. Drug Metab Dispos 23(7):765-775

Rowland A., Knights K. M., Mackenzie P. I., Miners J. O., 2008. The “albumin effect” and drug glucuronidation: Bovine serum album and fatty acid-free human serum albumin enhance the glucuronidation of UDP-glucuronosyltransferase (UGT) 1A9 substrates but not UGT1A1 and UGT1A6 activities. Drug Metab Dispos 36(6):1056-1062

Sabolovic N., Heydel J.-M., Li X., Little J. M., Humbert A.-C., Radominska-Pandya A., Magdalou J., 2004. Carboxyl non steroidal anti-inflammatory drugs are efficiently glucuronidated by microsomes of the human gastrointestinal tract. Biochim Biophys Acta 1675:120-129

Saha S., New L. S., Ho H. K., Chui W. K., Chan E. C. Y., 2010. Direct toxicity effects of sulfo-conjugated troglitazone on human hepatocytes. Tox Letters 195:135-141

Sarkadi B., Price E. M., Boucher R. C., German U. A., Scarborough G. A., 1992. Expression of the human multidrug resistance cDNA in insect cells generates a high activity drug-stimulated membrane ATPase. J Biol Chem 267(7):4854-4858

Saunders K. C., 2004. Automation and robotics in ADME screening. Drug Discov Today Technol 1(4):373-380

Schwab D., Fischer H., Tabatabaei A., Poli S., Huwyler J., 2003. Comparison of in vitro P-glycoprotein screening assays: recommendations for their use in drug discovery. J Med Chem 46:1716-1725

Scow J. S., Madhavan S., Chaudhry R. M., Zheng Y., Duenes J. A., Sarr M. G., 2011. Diffentiating passive from transporter-mediated uptake by PepT1: A comparison and evaluation of four methods. J Surgical Res 170:17-23

Seithel A., Karlsson J., Hilgendorf C., Björquist A., Ungell A-L., 2006. Variability in mRNA expression of ABC- and SLC-transporters in human intestinal cells:

Comparison between human segments and Caco-2 cells. Eur J Pharm Sci 28:291-299

Shapiro A. B., Ling V., 1997. Positively cooperative sites for drug transport by P-glycoprotein with distinct drug specificities. Eur J Biochem 250:130-137

Shapiro A. B., Walkup G. K., Keating T. A., 2009. Correlation for interference by test samples in high-throughput assays. J Biomol Screen 14:1008-1016

Shaw P. M., Hosea N. A., Thompson D. V., Lenius J. M., Guengerich F. P., 1997. Reconstitution premixes for assays using purified recombinant human cytochrome p450, NADPH-cytochrome P450 reductase, and cytochrome b_5. Arch Biochem Biophys 348(1):107-115

Shirasaka Y., Onishi Y., Sakurai A., Nakagawa H., Iskikawa T., Yamashita S., 2006. Evaluation of human P-glycoprotein (MDR1/ABCB1) ATPase acitivty assay method by comparing with in vitro transport measurements: Michaelis-Menten kinetic analysis to estimate the affinity of P-glycoprotein to drugs. Biol Pharm Bull 29(12):2465-2471

Shou M., Grogan J., Mancewicz J. A., Krausz K. W., Gonzalez F. J., Gelboin H. V., Korzekwa K. R., 1994. Activation of CYP3A4: Evidence for the simultaneous binding of two substrates in a cytochrome P450 active site. Biochemistry 33:6450-6455

Shou W. Z., Magis L., Li A. C., Naidong W., Bryant M. S., 2005. A novel approach to perform metabolite screening during quantitative LC-MS/MS analyses of in vitro metabolic stability samples using a hybrid triple-quadrupole linear ion trap mass spectrometer. J Mass Spectrom 40:1347-1356

Shukla S. J., Nguyen D-T., MacArthur R., Simeonov A., Frazee W. J., Hallis T. M., Marks B. D., Singh U., Eliason H. C., Printen J., Austin C. P., Inglese J., Auld D. S., 2009. Indentification of pregnane X reseptor ligards using time-resolved fluorescence resonance energy transfer and quantitative high-throughput screening. Assay and Drug Dev Technol 7(2):143-169

Siissalo S., Hannukainen J., Kolehmainen J., Hirvonen J., Kaukonen A. M., 2009. A Caco-2 cell based screening method for compounds interacting with MRP2 efflux protein. Eur J Pharm Sci 71:332-338

Siissalo S., Zhang H., Stilgenbauer E., Kaukonen A. M., Hirvonen J., Finel M., 2008. The expression of the most UDP-glucuronosyltransferases (UGTs) is increased significantly during Caco-2 cell differentiation, whereas UGT1A6 is highly expressed also in undifferentiated cells. Drug Metab Dispos 36(11):2331-2336

Sils M. A., 1997. Integrated robotics vs. task-oriented automation. J Biomol Screen 2(3):137-138

Simeonov A., Jadhav A., Thomas C. J., Wang Y., Huang R., Southall N. T., Shinn P., Smith J., Austin C. P., Auld D. S., Inglese J., 2008. Fluorescence spectroscopic profiling of compound libraries. J Med Chem 51:2363-2371

Skehan P., Storeng P., Scudiero D., Monks A., McMahon J., Vistica D., Warren J. T., Bokesch H., Kenney S., Boyd M. R., 1990. New colorimetric cytotoxicity assay for anticancer-drug screening. J Nat Cancer Inst 82:1107-1119

Skopelitou K., Labrou N. E., 2010. A new colorimetric assay for glutathione transferase-catalyzed halogen ion release for high-throughput screening. Anal Biochem 405:201-206

Soars M. G., Burchell B., Riley R. J., 2002. In vitro analysis of human drug glucuronidation and prediction of in viv metabolic clearance. J Pharmacol Exp Ther 301:382-390

Sohlenius-Sternbeck A.-K., Orzechowski A., 2004. Characterization of the rates of testosterone metabolism to various products and of glutathione transferase and sulfotransferase activities in rat intestine and comparison to the corresponding

hepatic and renal drug-metabolizing enzymes. Chem Biol Interact 148(1-2):49-56

Sorich, M.J., Miners, J.O., McKinnon, R.A., Winkler, D.A., Burden, F.R., Smith, P.A., 2003. Comparison of linear and nonlinear classification algorithms for the prediction of drug and chemical metabolism by human UDP-glucuronosyltransferase isoforms. J Chem Inf Comput Sci 43:2019-2024

Spahn-Langguth H., Benet L. Z., 1992. Acyl-glucuronides revisited: is the glucuronidation process a toxification as well as a detoxification mechanism? Drug Metab Rev 24:5-47

Steck T. L., Weinstein R. S., Straus J. H., Wallach D. F. H., 1970. Inside-out red cell membrane vesicles: preparation and purification. Science 168: 255-257

Stresser D. M., Blanchard A. P., Turner S. D., Erve J. C., Dandeneau A. A., Miller V. P., Crespi C. L., 2000. Substrate-dependent modulation of CYP3A4 catalytic activity: Analysis of 27 test compounds with four fluorometric substrates. Drug Metab Dispos 28(12):1440-1448

Stresser D. M., Turner S. D., Blanchard A. P., Miller V. P., Crespi C. L., 2002. Cytochrome P450 fluorometric substrates: Identification of isoform-selective probes for rat CYP2D2 and CYP3A4. Drug Metab Dispos 30:845-852

Sun D., Lennernäs H., Welage L. S., Barnett J. L., Landowski C. P., Foster D., Fliesher D., Lee K-D., Amidon G. L., 2002. Comparison of human duodenum and Caco-2 gene expression profiles for 12,000 gene sequences tags and correlation with permeability if 26 drugs. Pharm Res 19(10):1400-1416

Suzuki H., Sugiyama Y., 2000. Role of metabolic enzymes and efflux transporters in the absorption of drugs from the small intestine. Eur J Pharm Sci 12:3-12

Szakács G., Váradi A., Özvegy-Laczka C., Sarkadi B., 2008. The role of ABC transporters in drug absorption, distribution, metabolism, excretion and toxicity (ADME-Tox). Drug Discovery Today 13(9/10):379-393

Tabas L. B., Dantzig A. H., 2002. A high-throughput assay for measurement of multidrug resistance protein-mediated transport of leukotriene C_4 into membrane vesicles. Anal Biochem 310:61-66

Taipalensuu J., Törnblom H., Lindberg G., Einarsson C., Sjöqvist F., Melhus H., Garbert P., Sjöström B., Lundgren B., Artursson P., 2001. Correlation of gene expression of ten drug efflux proteins of the ATP-binding cassette transporter family in normal human jejunum and in human intestinal epithelial Caco-2 cell monolayers. J Pharmacol Exp Ther 299:164-170

Tamai I., Sai Y., Ono A., Kido Y., Yabuuchi H., Takanaga H., Satoh E., Ogihara T., Amano O., Izeki S., Tsuji A., 1999. Immunohistochemical and functional characterization of pH-dependent intestinal absorption of weak organic acids by the monocarboxylic acid transporter MCT1. J Pharm Pharmacol 51:1113-1121

Tang F., Horie K., Borchardt R. T., 2002. Are MDCK cells transfected with the human MDR1 gene a good model of the human intestinal mucosa? Pharm Res 19(6):765-772

Tang F., Ouyang H., Yang J. Z., Borchardt R. T., 2004. Bidirectional transport of rhodamine 123 and Hoecst 33342, fluorescence probes of the binding sites on P-glycoprotein, across MDCK-MDR1 cell monolayers. J Pharm Sci 93(5):1185-1194

Tang W., Wang R. W., Lu A. Y. H., 2005. Utility of recombinant cytochrome P450 enzymes: A drug metabolism perspective. Current Drug Metab 6:503-517

Taub M. E., Podila L., Ely D., Almeida I., 2005. Functional assessment of multiple p-glycoprotein (P-gp) probe substrates: Influence of cell line and modulator concentration on P-gp activity. Drug Metab Dispos 33(11):1679-1687

Taylor P. B., Ashman S., Baddeley S. M., Bartram S. L., Battle C. D., Bond B. C., Clemets Y. M., Gaul N. J., McAllister W. E., Mostacero J. A., Ramon F., Wilson J. M., Hertzberg R. P., Pope A. J., Macarron R., 2002. A standard operating procedure for assessing liquid handler performance in high-throughput screening. J Biomol Screen 7(6):554-569

TECAN, 2007. L-10 Liquid handling training for Genesis pipetting platforms (course material).

Thelen K., Dressman J. B., 2009. Cytochrome P450-mediated metabolism in the human gut wall. J Pharm Pharmacol 61:541-558

Thummel K. E., O´Shea D., Paine M., Shen D. D., Kunze K. L., Perkins J. D., Wilkonson G. R., 1996. Oral first-pass elimination of midazolam involves both gastrointestinal and hepatic CYP3A-mediated metabolism. Clin Pharmacol Ther 59(5):491-502

Thummel K. E., Shen D. D., Podoll T. D., Kunze K. L., Trager W. F., hartwell P. S., Raisys V. A., Marsh C. L., McVicar J. P., barr D. M., Perkins J. D., Carithers R. L. Jr., 1994. Use of midazolam as a human cytocrome P450 probe: I. *In vitro-in vivo* correlations in liver transplant patients. J Pharmacol Exp Ther 271(1):549-556

Tolonen A., Turpeinen M., Pelkonen O., 2009. Liquid chromatography-mass spectrosmetry in in vitro drug metabolism screening. Drug Discovery Today 14(3/4):120-133

Troutman M. D., Thakker D. R., 2003. Rhodamine 123 requires carrier-mediated influx for its activity as a P-glycoprotein substrate in Caco-2 cells. Pharm Res 20(8):1192-1199

Trubeskoy O. V., Finel M., Kurkela M., Fitzgerald M., Peters N. R., Hoffman F- M., Trubetskoy V. S., 2007. High throughput screening assays for UDP-glucuronosyltransferases 1A1 glucuronidation profiling. Assay and Drug Dev Technol 5(3):343-354

Trubetskoy O. V., Gibson J. R., Marks B. D., 2005. Highly miniaturized formats for in vitro drug metabolism assays using Vivid® fluorescent substrates and recombinant human cytochrome P450 enzymes. J Biomol Screen 10(1):56-66

Trubetskoy O. V., Shaw P., 1999. A fluorescent assay amenable to measuring production of β-D-glucuronides produced from recombinant UDP-glycosyl transferase enzymes. Drug Metab Dispos 27(5):555-557

Tucker G. T., Houston J. B., Huang S.-M., 2001. Optimizing drug development: Strategies to assess drug metabolism/transporter interaction potential –Towards a consensus. Pharm Res 18(8):1071-1080

Uchaipichat V., Galetin A., Houston J. B., Macknzie P. I., Williams J. A., Miners J. O., 2008. Kinetic modeling of the interactionds between 4-methylumbelliferone, 1-naphthol, and zidovudine glucuronidation by UDP-glucuronosyltransferase 2B7 (UGT2B7) proves evidence for multiple substrate binding and effector sites. Mol Pharmacol 74(4):1152-1162

Uchaipichat V., Mackenzie P. I., Guo X.-H., Gardner-Stephen D., Galetin A., Houston J. B., Miners O., 2004. Human UDP-glucuronosyltransferases: Isoform selectivity and kinetics of 4-methylumbelliferone and 1-naphthol glucuronidation, effects of organic solvents , and inhibition by diclofenac and probenesid. Drug Metab Dispos 32(4):413-423

Ueng Y.-F., Kuwabara T., Chun Y.-J., Guengerich F. P., 1997. Cooperativity in oxidations catalyzed by cytochrome P450 3A4. Biochemistry 36:307-381

V&P Scientific Inc. Allicator microplate tumble stirrer. Retrieved 21.3.2012 from: http://www.vp-scientific.com/tumble_stirrer_alligator.php

Vaidyanathan J. B., Walle T., 2003. Cellular uptake and efflux of the tea flavonoid (–)-epicatechin-3-gallate in the human intestinal cell line Caco-2. J Pharmacol Exp Ther 307:745-752

van de Kerkhof E. G., de Graaf I. A. M., Groothuis G. M. M., 2007. In vitro methods to study intestinal drug metabolism. Current Drug Metab 8:658-675

van der Sandt I. C. J., Blom-Roosemalen M. C. M., de Boer A. G., Breimer D. D., 2000. Specificity of doxorubicin versus rhodamine-123 in assessing P-glycoprotein functionality in the LLC-PK1, LLC-PK1:MDR1 and Caco-2 cell lines. Eur J Pharm Sci 11:207-214

VandenBrink B. M., Foti R. S., Rock D. A., Wienkers L. C., Wahlstrom J. L., 2012. Prediction of CYP2D6 drug interactions from in vitro data: Evidence for substrate-dependent inhibition. Drug Metab Dispos 40(1):47-53

Varma M. V., Amber C. A., Ullah M., Rotter C. J., Sun H., Litchfield J., Fenner K. S., El-Kattan A. F., 2010. Targeting intestinal transporters for optimizing oral drug absorption. Current Drug Metab 11:730-742

Vichai V., Kirtikara K., 2006. Sulforhodamine B colorimetric assay for cytotoxicity screening. Nat Prot 1:1112-1116

Vig B. S., Stouch T. R., Timoszyk J. K., Quan Y., Wall D. A., Smith R. L., Faria T. N., 2006. Human PEPT1 pharmacophore distinquishes between dipeptide transport and binding. J Med Chem 49:3636-3644

Volpe D. A., 2008. Variability in Caco-2 and MDCK cell-based intestinal permeability assays. J Pharm Sci 97(2):712-725

Wang H., Li H., Moore L. B., Johnson M. D. L., Maglich J. M., Goodwin B., Ittoop O. R. R., Wisely B., Creech K., Parks D. J., Collins J. L., Willson T. M., Kalpana G. V., Venkatesh M., Xie W., Cho S. Y., Roboz J., Redinbo M., Moore J. T., Mani S., 2008. The phytoestrogen coumesterol is a naturally accuring antagonist of the human pregnane X receptor. Mol Endocrinol 22(4):838-857

Wang Q., Strab R., Karlos P., Ferguson C., Li J., Owen A., Hidalgo H. I., 2008. Application and limitation of inhibitors in drug transporter interactions studies. Int J Pharm 356:12-18

Wang R. W., Newton D. J., Liu N., Atkins W. M., Lu A. Y. H., 2000. Human cytochrome P-450 3A3: In vitro drug-drug interaction patterns are substrate dependent. Drug Metab Dispos 28(3):360-366

Washington N., Washington C., Wilson C. G. (editors), 2001. Drug absorption from the small intestine. In Physiological pharmaceutics: Barriers to drug absorption, 2nd edition, Taylor and Francis Group, London, England, p. 109-142

Weiser M., 1973. Intestinal epithelial cell surface membrane clycosynthesis. I. An indicator of cellular differentiation. J Biol Chem 248(7):2536-2541

Williams A. M., Worral S., de Jersey J., Dickinson R. D., 1992. Studies on the reactivity of acyl glucuronides-III: Glucuronide-derived adducts of valproic acid and plasma protein and antiadduct antibodies in humans. Biochem Pharmacol 43:745-755

Worboys P. D., Carlile D. J., 2001. Implications and consequences of enzyme induction on preclinical and clinical drug development. Xenobiotica 31(8/9):539-556

Xia C. Q., Liu N., Yang D., Miwa G., Gan L.-S., 2005. Expression. localization. and functional characteristics of breast cancer resistance protein in Caco-2 cells. Drug Metab Dispos 33:637-643

Xiao Y., Davisdon R., Smith A., Pereira D., Zhao S., Soglia J., Gebhard D., de Morais S., Duignan D. B., 2005. A 96-well efflux assay to identify ABCG2 substrates using a stably transfected MDCK II cell line. Mol Pharm 3(1):45-54

Yamashita S., Konishi K., Yamazaki Y., Taki Y., Sakane T., Sezaki H., Furuyama Y., 2001. New and better protocols for a short-term Caco-2 cell culture system. J Pharm Sci 91(3):669-679

Yan Y.-D., Kim H.-K., Sco K.-H., Lee W. S., Lee G.-S., Woo J.-S., Yong C.-S., Choi H.-G., 2010. The physicochemical properties, in vitro metabolism and pharmacokinetics of a novel ester prodrug EXP3174. Mol Pharm 7(6):2132-2140

Yang J., Jamei M., Rowland-Yeo K., Tucker G. T., Rostami-Hodjegan A., 2007. Prediction of intestinal first-pass drug metabolism. Curr Drug Metab 8:676-684

Yasgar A., Shultz J., Zhou W., Wang H., Huang F., Murphy N., Abel E. L., DiGiovanni J., Inglese J., Simeonov A., 2010. A high-throughput 1,536-well luminescence assay for glutathione S-transferase activity. Assay and Drug Dev Technol 8(2):200-211

Yuan R., Madani S., Wei X.-X., Reynolds K., Huang S.-M., 2002. Evaluation of cytochrome P450 probe substrates commonly used by the pharmaceutical industry to study in vitro drug interactions. Drug Metab Dispos 30(12):1311-1319

Zhang E. Y., Knipp G. T., Ekins S., Swaan P. W., 2002. Structural biology and function of solute transporters: implication for identification and designing substrates. Drug Metab Rev 34(4):709-750

Zhang H., Tolonen A., Rousu T., Hirvonen J., Finel M., 2011. Effects of cell differentiation and assay conditions on the UDP-glucuronosyltransferase activity in Caco-2 cells. Drug Metab Dispos 39:456-464

Zhang J.-H., Chung T. D. Y., Oldenburg K. R., 1999a. A simple statistical parameter for use in evaluation and validation of high throughput assays. J Biomol Screen 4(2):67-73

Zhang L., Lin G., Kovács B., Jani M., Kajcsi P., Zuo Z., 2007. Mechanistic study on the intestinal absorption and disposition of baicalein. Eur J Pharm Sci 31:221-231

Zhang L., Strong J. M., Qui W., Lesko L. J., Huang S.-M., 2006. Scientific perspective on drug transporters and their role in drug interactions. Mol Pharm 3(1):62-69

Zhang Q.-Y., Dunbar D., Ostrowska A., Zeisloft S., Yang J., Kaminsky L. S., 1999b. Characterization of human small intestinal cytochromes P-450. Drug Metab Dispos 27(7):804-809

Zhang Z.-Y., Wong Y. N., 2005. Enzyme kinetics for clinically relevant CYP inhibition. Curr Drug Metab 6:241-257